Institute of Nuclear Sciences „Vinča”
Materials Science Laboratory
University of Belgrade

Annual Report (2011)

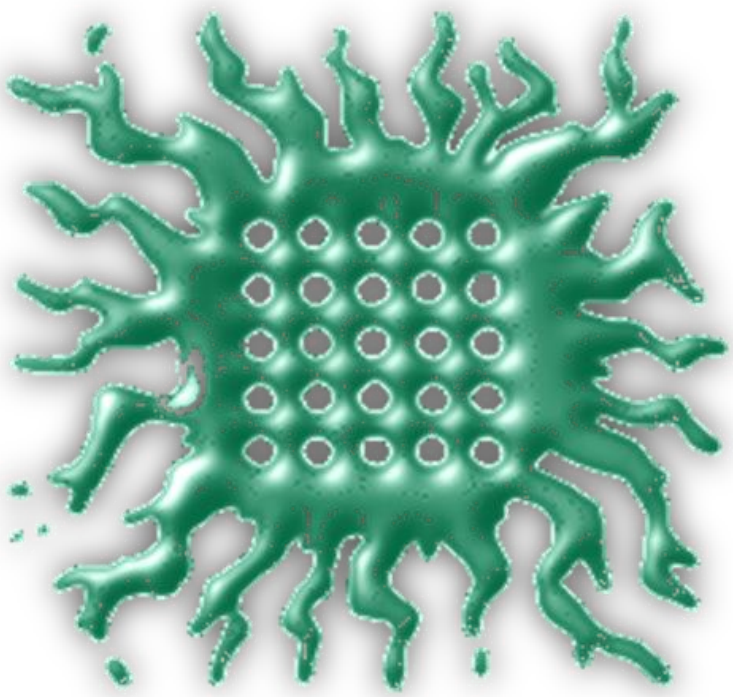

Belgrade, 2014.

Publication of the Materials Science Laboratory

Series: ANNUAL REPORT

Publisher
Institute of Nuclear Sciences „Vinča“
Materials Science Laboratory
University of Belgrade, P.O. Box 522, 11001 Belgrade, Serbia
Phone: (381-11) 3408-224

For the Publisher
Dr. Rer. Nat. Branko Matović, Director of the Laboratory

ISSN
Institute of Nuclear Sciences „Vinča“

Associate Editors
Scientific board

Editors
Dr. Vesna Maksimović
Dr. Branko Matović

Layout
Dipl.ing. Jelena Pantić

Printed by
Printing office of the Institute of Nuclear Sciences „Vinča“ in 20 copies
July 2014

Research topics

Metallic materials

Energy

Biomaterials

Carbon materials

Enviromental protection

Advanced ceramics

Raw materials and heritage

Functional ceramics

Ceramic composites

Doctoral dissertations

Table of Contents:

1. Metallic materials 1
2. Energy 15
3. Biomaterials 24
4. Carbon materials 34
5. Enviromental protection 41
6. Advanced ceramics 47
7. Raw materials and heritage 59
8. Functional ceramics 66
9. Ceramic composites 73
10. Doctoral dissertations 80
11. Domestic collaborations 85
12. International collaborations 89

Metallic materials

Synthesis and properties of a Cu–Ti–TiB_2 composite hardened by multiple mechanisms

D. Božić, J. Stašić, J. Ružić, M. Vilotijević, V. Rajković

Institute of Nuclear Sciences Vinča, University of Belgrade, P.O.B. 522, 11001 Belgrade, Serbia

Multiple hardening mechanisms of a copper matrix have been presented and discussed. The gas atomized Cu–0.6 wt.%Ti–2.5 wt.%TiB_2 (Cu–Ti–TiB_2) powders were used as starting materials. Dispersoid particles TiB_2 were formed in situ in the copper matrix during gas atomization. The powders have been consolidated by hot isostatic pressing (HIP). Optical microscopy, transmission electron microscopy (TEM), and X-ray diffraction (XRD) analysis were performed for microstructural characterization of powders and composite compacts. High hardening of the Cu–Ti–TiB_2 composite achieved by aging is a consequence of the simultaneous influence of the following factors: the development of modulated structure with metastable $Cu_4Ti_{(m)}$ particles and in situ formed TiB_2 dispersoid particles.

Keywords:composites, hardness measurement, hardening, powder metallurgy, thermomechanical processing, electron microscopy.

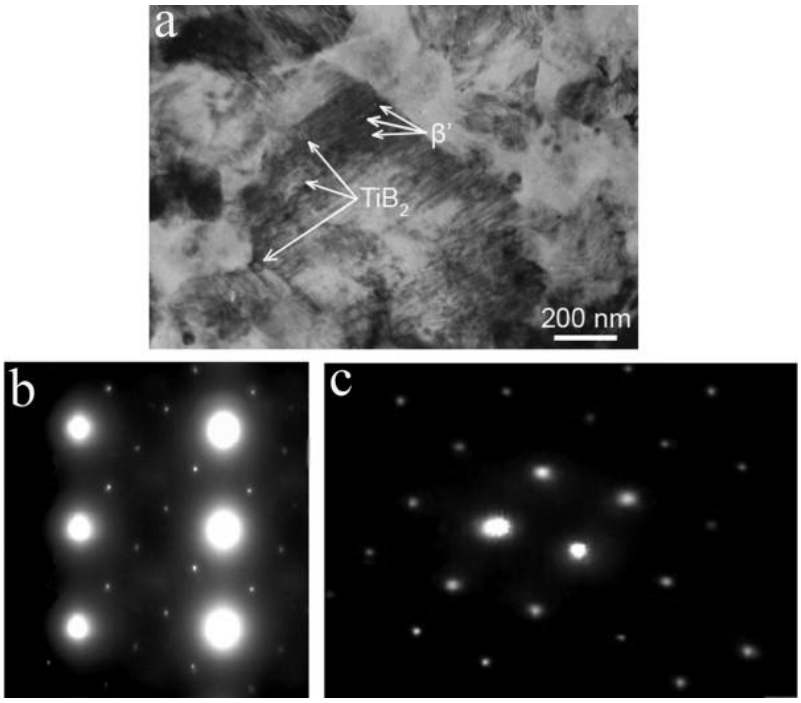

Figure: TEM micrograph of the Cu–Ti–TiB_2 composite for a peak-aged condition: T = 500 °C, t = 30 min, showing the metastable Cu_4Ti (β′-phase) and the dispersoid TiB_2, particles in copper matrix (a) SAD pattern of metastable Cu_4Ti (b) and TiB_2, (c) in copper matrix.

***Materials Science and Engineering: A*, 528 (2011) 8139–8144.**

Microstructures and mechanical properties of ZA27-Al_2O_3 composites obtained by powder metallurgy process

D. Božić, J. Stašić, V. Rajković

Institute of Nuclear Sciences Vinča, University of Belgrade, 11001 Belgrade, Serbia

This paper describes a study of the microstructures and mechanical properties of Zn matrix composites reinforced by 10 wt.% Al_2O_3 particles of 0.7 μm average size. Commercial Zn-Al-Cu (ZA27) alloy was gas atomized and the resulting powder was mixed with an Al_2O_3 powder, and then hot pressed into cylindrical pellets. Metal powder and powder mixtures were pressed at 230°C, for 45 min under the pressure of 150 MPa. The compressive strength testing was performed in the temperature range from 20°C to 160°C, with a deformation rate of $2.4\times10^{-3}s^{-1}$. The microstructures and the fracture surface of the samples were investigated by optical and scanning electron microscopy.

Keywords: composite materials, powder metallurgy, microstructure, mechanical properties, Scanning Electron Microscopy (SEM).

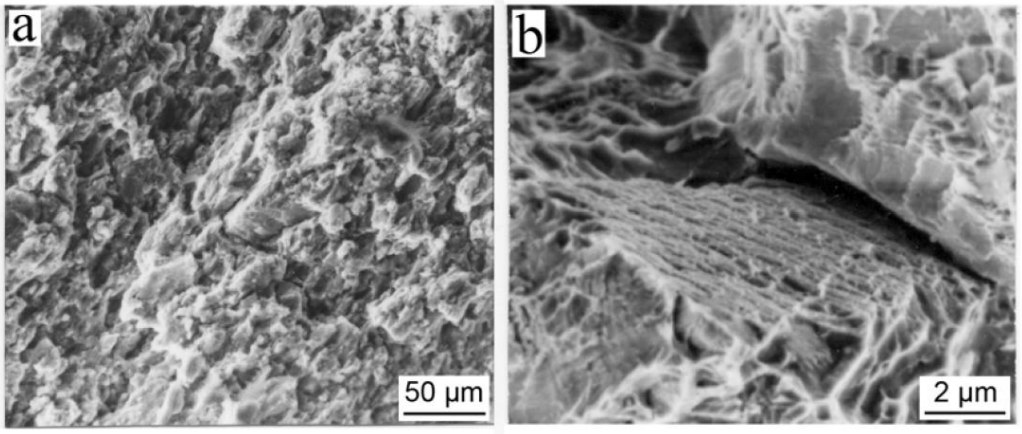

Figure: SEM. Fracture surface of ZA27 alloy: decohesion of alloy particles.

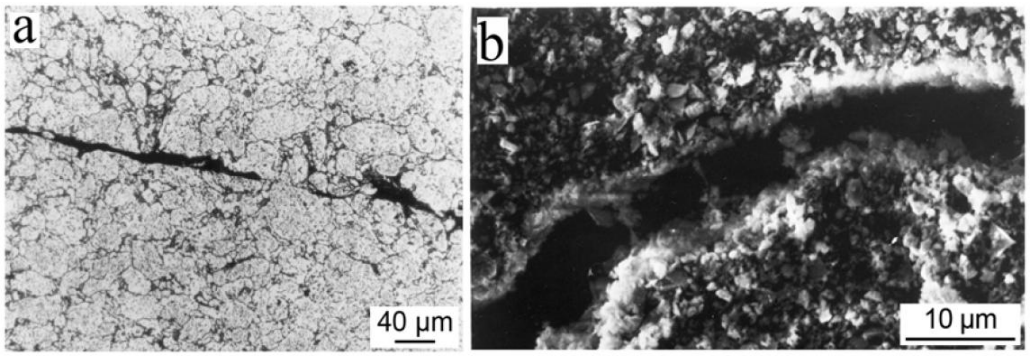

Figure: Fracture surface of ZA27-Al_2O_3 composite: a. OM. Crack propagation, b. SEM. Al_2O_3 agglomerate.

***Science of Sintering*, 43(2011) 63-70.**

Multiple strengthening mechanisms in nanoparticle-reinforced copper matrix composites

Dušan Božić, Jelena Stašić, Biljana Dimčić, MiroljubVilotijević, Višeslava Rajković

Institute of Nuclear Sciences Vinča, University of Belgrade, 11001 Belgrade, Serbia

The multiple hardening mechanisms of a copper matrix have been presented and discussed. The pre-alloyed ball milled Cu–3 wt.%Al and the atomized Cu–0·6 wt.%Ti–2·5 wt.%TiB_2 powders have been used as starting materials. Dispersoid particles Al_2O_3 and TiB_2were formed *in situ*. The powders have been hot consolidated. Optical microscopy, SEM, TEM, and X-ray diffraction analysis were performed for microstructural characterization. Increase in microhardness of Cu–3 wt.%Al compacts is a consequence of the crystallite size refinement and the presence of Al_2O_3 particles. High hardening of Cu–0·6 wt.%Ti–2·5 wt.%TiB_2 is a consequence of the presence of modular structure, $Cu_4Ti_{(m)}$, and TiB_2 particles.

Keywords: Metal–matrix composites (MMCs), nanoparticles, hardness testing, microstructural characterization.

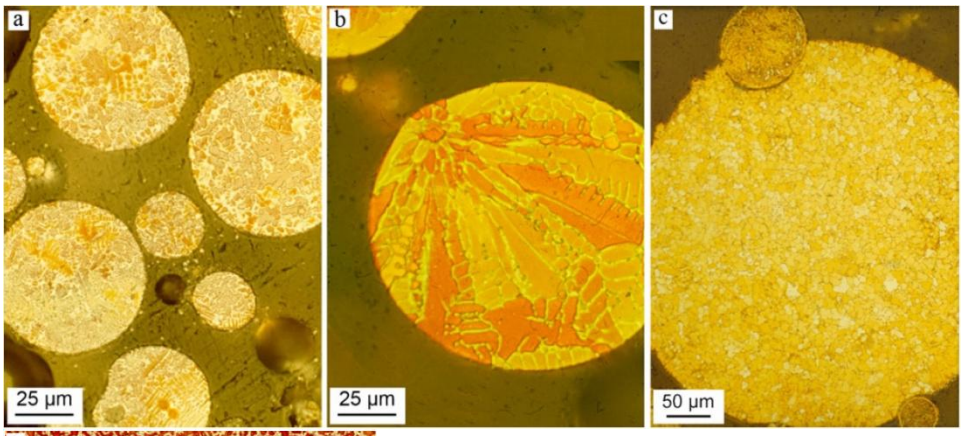

Figure: OM micrographs showing microstructure of different as-atomized Cu–0·6Ti–2·5TiB_2 (wt.%) alloy powder sieving fractions:**a.** d <80 μm, **b.** 80 μm< d <150 μm, and **c.** 200 μm< d <500 μm.

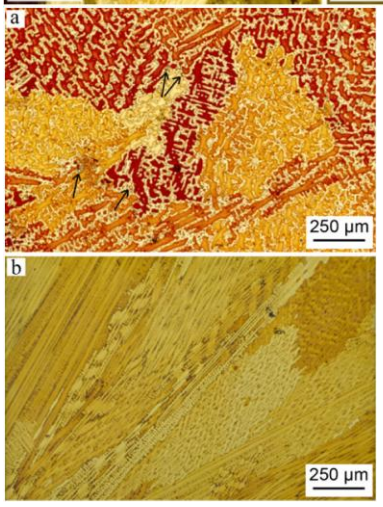

Figure: OM micrographs showing microstructure of as cast: **a.** Cu–3·8Ti (wt.%) and **b.** Cu–1·2B (wt.%) master alloys.

***Bulletin of Materials Science*, 34 (2011) 217-226.**

Synthesis and properties of discontinuously reinforced aluminum matrix composites

Dušan Božić, Biljana Dimčić

Institute of Nuclear sciences Vinča, University of Belgrade, 11001 Belgrade, Serbia

In the last two decades there was an intense development of one class of composites with aluminum alloy matrix best known as the discontinuously reinforced aluminum materials (DRA). These materials consist of aluminum alloy matrix reinforced by ceramic particles. Although, DRA composites can be produced in many ways, powder metallurgy technique offers the best results.

This article presents results of both fundamental and development studies of sintered composite materials with the Al-Zn-Mg-Cu matrix and the SiC reinforcing phase, conducted in last couple of years. As this is the composite which is already commercially applied or on the verge of being applied, all gathered results are thoroughly analyzed from the aspects of its synthesis, microstructure and several mechanical and fracture properties.

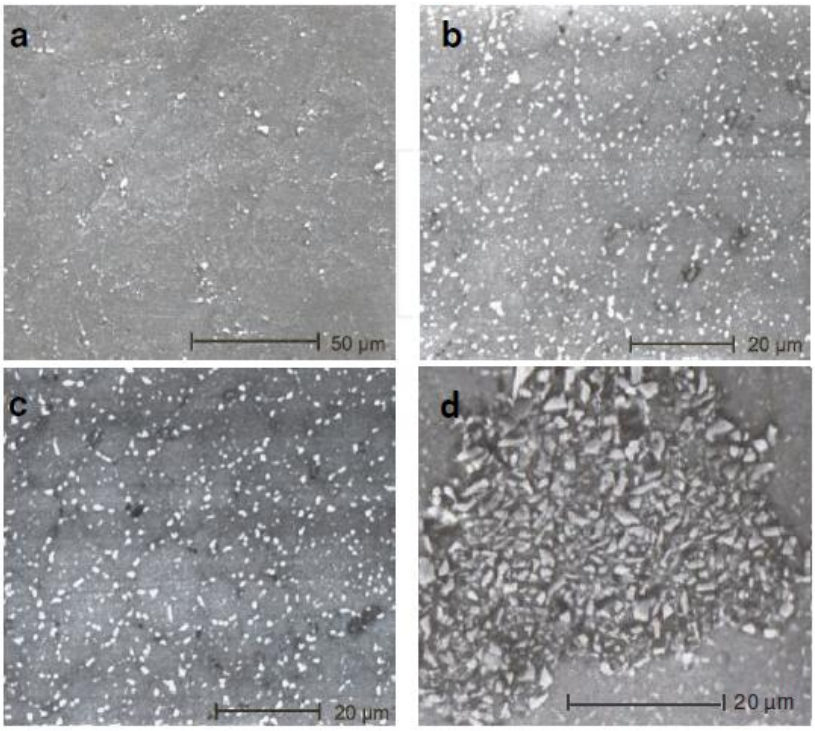

Figure: SEM. Composite microstructure (d_{SiC}=0.7 µm)-optimal homogeneity. a) 5 vol. % SiC, b) 10 vol. % SiC, c) 15 vol. % SiC, and example of prolonged mixing time effect, d) 15 vol. % SiC, 150 min mixing time.

Chapter 8 in *Nanocomposites with Unique Properties and Applications in Medicine and Industry*, ISBN 978-953-307-351-4, edited by John Cuppoletti, publisher InTech, Rijeka, Croatia (2011) pp. 151-174.

Surface texturing of the carbon steel AISI 1045 using femtosecond laser in single pulse and scanning regime

J. Stašić[1], B. Gaković[1], W. Perrie[2], K. Watkins[2], S. Petrović[1], M. Trtica[1]

[1]Institute of Nuclear Sciences Vinča, University of Belgrade, 11001 Belgrade, Serbia
[2]Department of Engineering, University of Liverpool, Liverpool L69 3GH, UK

Surface texturing of the metals, including steels, gained a new dimension with the appearance of femtosecond lasers. These laser systems enable highly precise modifications, which are very important for numerous applications of metals. The effects of a Ti:sapphire femtosecond laser with the pulse duration of 160 fs, operating at 775 nm wavelength and in two operational regimes – single pulse (SP) and scanning mode, on a high quality AISI 1045 carbon steel were studied. The estimated surface damage threshold was 0.22 J/cm^2 (SP). Surface modification was studied for the laser fluences of 0.66, 1.48 and 2.37 J/cm^2. The fluence of 0.66 J/cm^2, in both working regimes, induced texturing of the material, i.e. formation of periodic surface structures (PSS). Their periodicity was in accordance with the used laser wavelength. Finally, changes in the surface oxygen content caused by ultrashort laser pulses were recorded.

Keywords: steel; femtosecond laser; laser processing; periodic surface structures.

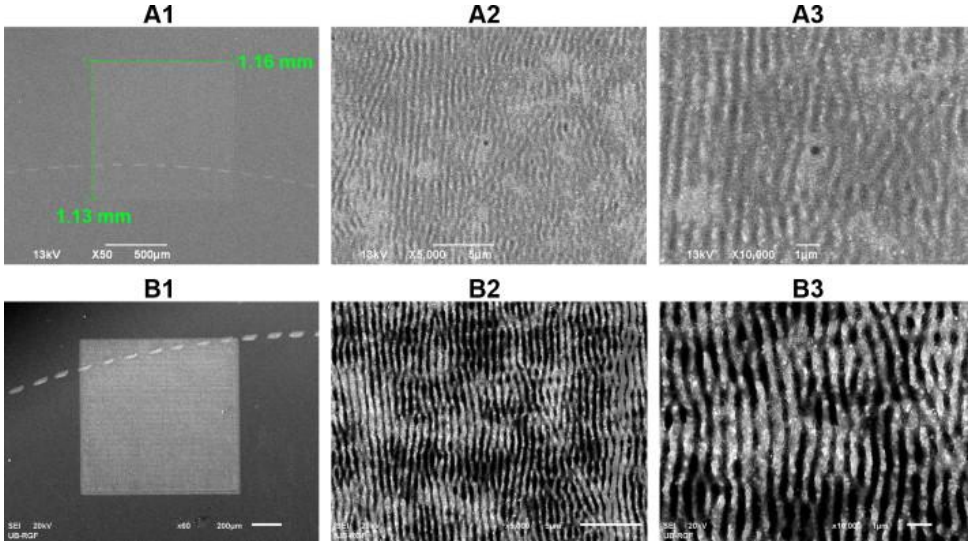

Figure: SEM micrographs of the AISI 1045 steel surface after scanning with femtosecond laser at λ = 775 nm; Φ_3 = 0.66 J/cm^2; pulse repetition 1 kHz; scanning rate 10 mm/s. A – after single scanning, B – after triple scanning. (A2, A3, B2, B3 – central zone of the damage.)

***Applied Surface Science*, 258 (2011) 290–296.**

Hydrogenation properties of Hf-Ni intermetallics - Experimental and theoretical investigation

Dragica Lj. Stojić[a], Katarina D. Ćirić[b], Božidar Đ. Cekić[b], Vasil J. Koteski[b], Slavica P. Zec[c], Žarko D. Bogdanov[d]

[a]Department of Physical Chemistry, Vinča Institute of Nuclear Sciences, University of Belgrade, 11000 Belgrade, Serbia
[b]Department of Nuclear and Plasma Physics, Vinča Institute of Nuclear Sciences, University of Belgrade, 11000 Belgrade, Serbia
[c]Department of Material Sciences, Vinča Institute of Nuclear Sciences, University of Belgrade, 11000 Belgrade, Serbia
[d]Department of Atomic Physics, Vinča Institute of Nuclear Sciences, University of Belgrade, 11000 Belgrade, Serbia

The hydrogenation properties of HfNi and Hf_2Ni_7 intermetallics were investigated at the constant pressure of 1 bar and in the temperature ranges 373-573 K for HfNi and 323-473 K for Hf_2Ni_7. The kinetic parameters, rate constants and activation energies of the absorption processes were determined. Maximal hydrogen absorption, i.e., number of hydrogen atoms absorbed per metal atom, H/M, are 1.05 and 0.04 achieved at 373 K for HfNi and Hf_2Ni_7, respectively. Multiple hydriding/dehydriding was found to influence the improvement of the kinetic parameters. XRD and SEM methods were used to investigate the structural and morphological changes of the samples due to hydrogen absorption. The thermodynamic parameters of hydriding together with the structural properties of the intermetallics and their hydrides, calculated using the full-potential linearized augmented plane waves (FP-LAPW) code based on the density functional theory (DFT), were utilized for the sake of explaining the experimental investigations.

Keywords: HfNi, Hf_2Ni_7, hydrogen absorption kinetic, hydriding capacity, activation energy, FP-LAPW calculations

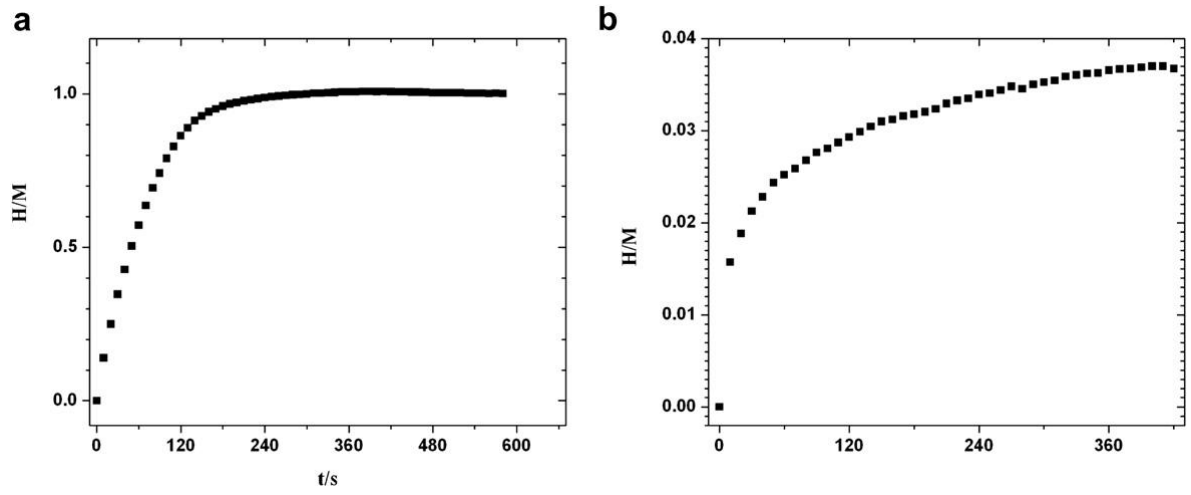

Figure: Hydrogen absorption isotherms at 373 K for HfNi (a) and Hf_2Ni_7 (b).

***International Journal of Hydrogen Energy*, 36 (2011) 10771- 10778.**

Synthesis of ZrO_2 Particles Reinforced ZA25 Alloy Composites by Compocasting Process

Z. Acimović-Pavlović[a], K. T. Raić[a], I. Bobić[b], B. Bobić[c]

[a]Faculty of Technology and Metallurgy, University of Belgrade, Belgrade, Serbia
[b]Vinca Institute of Nuclear Sciences, University of Belgrade, Belgrade, Serbia
[c]IHIS Research and Development Center, Belgrade, Serbia

Microstructures and compressive properties of Zn25Al3Cu/ZrO_2 particulate composites were studied. The composites were obtained by compocasting process through infiltration of 1 and 3 wt% ZrO_2 particles of different size into the semi-solid melt of the base alloy. The influence of reinforcing particles' size and quantity on microstructure and mechanical properties of the composites was examined. The composites have shown significant improvement of mechanical properties with respect to the base alloy. Increase in hardness and compressive yield strength of the composites was more expressed in the composites with coarse ZrO_2 particles.

Keywords: Metal matrix composites, ZA25 alloy, ZrO_2 strengthener, compocasting process, mechanical properties.

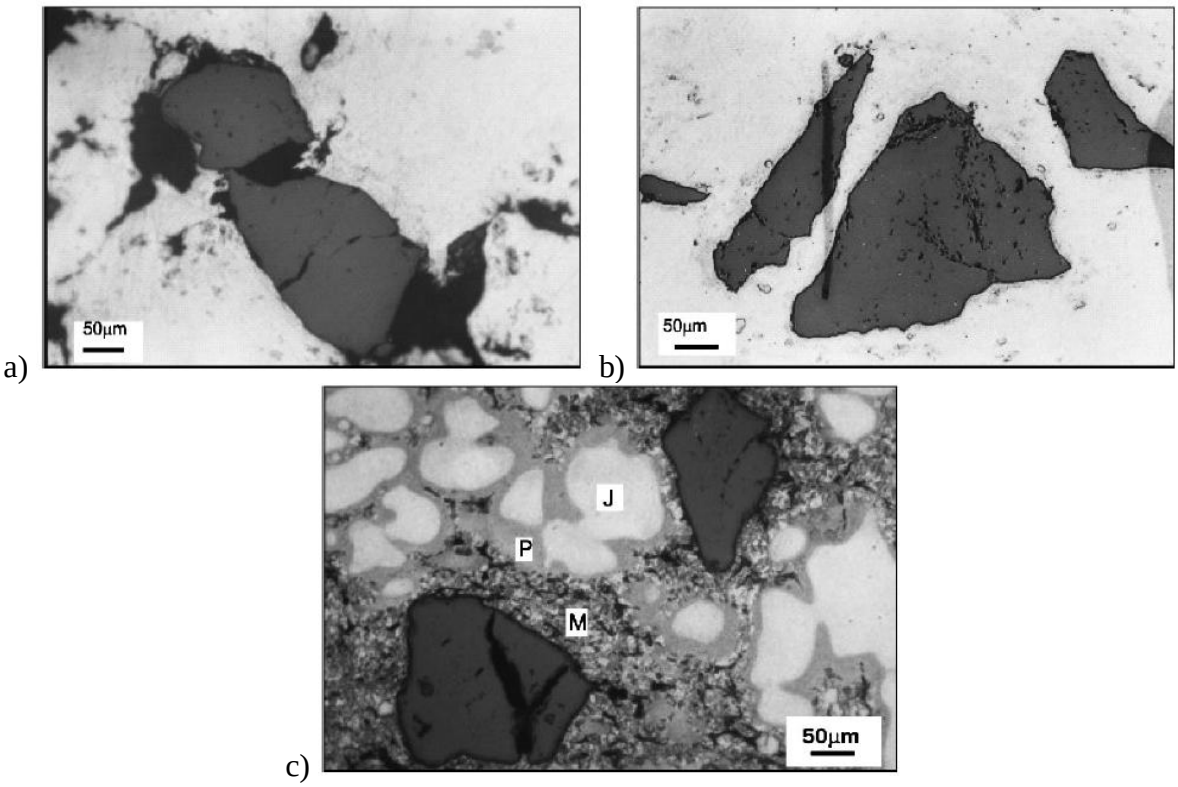

Figure: Microstructure of ZA25/ZrO_2 composite. OM, polished. Sample C: 3 wt% ZrO_2, 100 μm particle size. (a) As-cast, (b) after hot-pressing, c) Microstructure of ZA25/ZrO_2 composite after hot-pressing. OM, etched. Sample C: 3 wt% ZrO_2, 100 μm particle size.

***Advanced Composite Materials,* 20 (2011) 375–384.**

The effect of T4 heat treatment on the microstructure and corrosion behaviour of Zn27Al1.5Cu0.02Mg alloy

Biljana Bobic[a], Jelena Bajat[b], Zagorka Acimovic-Pavlovic[b], Marko Rakin[b], Ilija Bobic[c]

[a]IHIS R&D Center, Batajnicki put 23, 11080 Zemun, Serbia
[b]Faculty of Technology and Metallurgy, Karnegijeva 4, 11120 Belgrade, Serbia
[c]INN Vinca, University of Belgrade, Mike Petrovica Alasa 12-14, 11001 Belgrade, Serbia

The effect of heat treatment on the microstructure and corrosion behaviour of Zn27Al1.5Cu0.02Mg alloy was examined. The alloy was prepared by melting and casting route and then thermally processed (T4 regime). Corrosion behaviour of the as-cast and heat treated alloy was studied in 3.5 wt.% NaCl solution using immersion method and electrochemical polarization measurements. The applied heat treatment affected the alloy microstructure and resulted in increased ductility and higher corrosion resistance of the heat treated alloy. Electrochemical measurements of the corrosion rate at the free corrosion potential are in agreement with the results obtained using the weight loss method.

Keywords: Zinc, Alloy, Weight loss, Polarization, SEM.

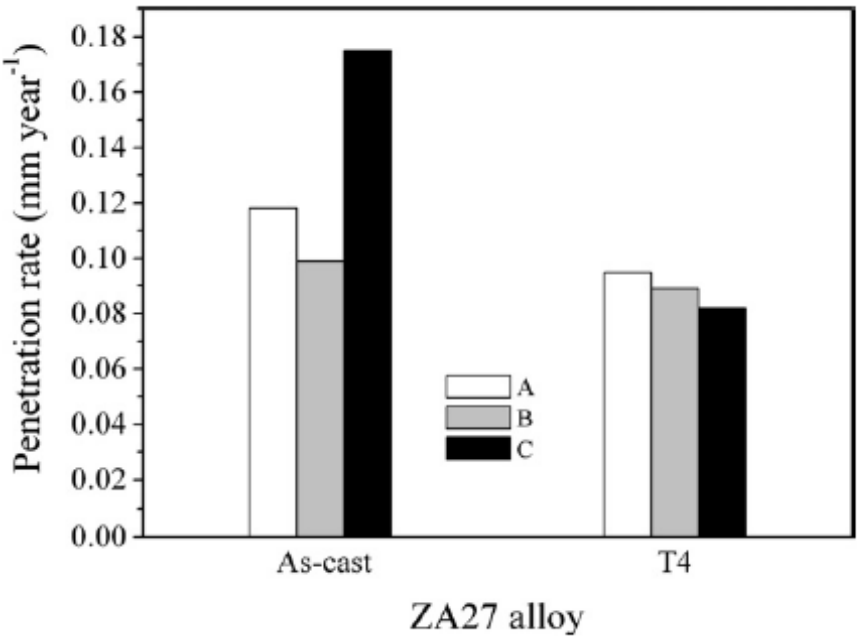

Figure: Corrosion rates of ZA27 alloy. (A) weight loss method, (B) linear polarization resistance test, (C) Tafel plots.

***Corrosion Science*, 53 (2011) 409–417.**

Modeling the flow of fresh and deep frozen calibrated fruit by rotating sizing machines

Dragan Marković[1], Milan Veljić[1], Vojislav Simonović[1], Maria Čebela[2]

[1]Faculty of Mechanical Engineering, 11000 Beograd, Kraljice Marije 16, Serbia
[2]Institute of Nuclear Sciences Vinča, University of Belgrade, PO Box 522, 11001 Belgrade, Serbia

The principle of rotating sizing machines based on a division of the fruits of various geometrical characteristics of the gaps of the same dimensions are typical for any given class separately. The classes are deployed from the smallest to the largest in the direction of rotation of the disk, and arc sizing board can be mixed performance, as slope metering gape and step metering gape. This paper discusses the movement of fruit in relation of their speed, and analyzes the model for determining the capacity of rotating sizing machines for different kinds of fresh fruit and deep-frozen raspberries. Mass flow calibrator or capacity for fruits tested in this paper are similar to those obtained in some other known methods. Calibrated mass flow is proportional to the weight of fruit and fruit in inverse proportion to the diameter of treated fruit.

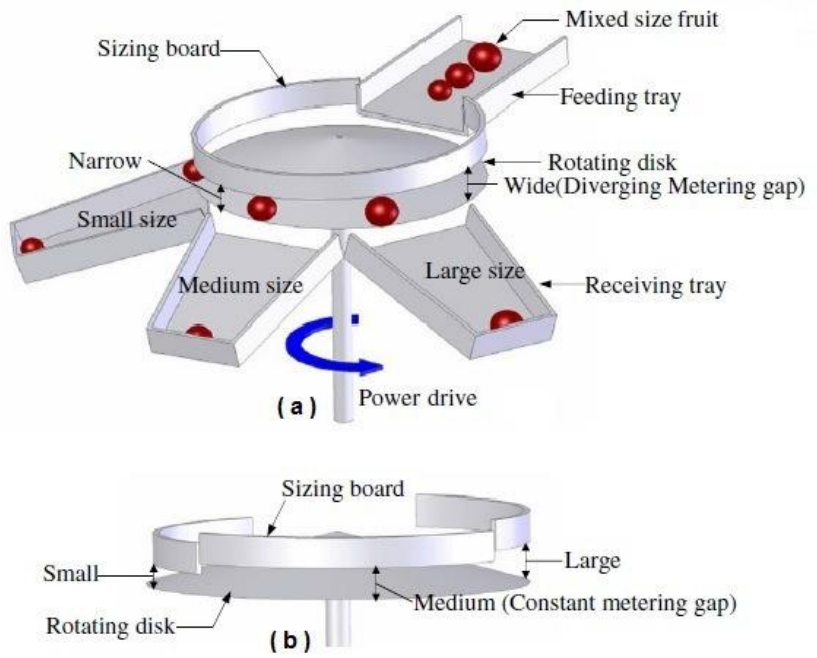

Figure: Model of rotating disc fruit sizing machine. (a) Slope metering gape and (b) step metering gape.

***Journal on Processing and Energy in Agriculture,* 15 (2011) 67-70.**

Electrodeposition of Cobalt Powders with Novel Three-Dimenstional Structure

V.M.Maksimović[1], U.Č.Lačnjevac[2], V.D.Jović[2], B.M.Jović[2], M.G.Pavlović[3]

[1]Institute of Nuclear Sciences Vinča, University of Belgrade, P.O. Box 522, 11001 Belgrade, Serbia
[2]Institute for Multidisciplinary Research, University of Belgrade, P.O. Box 33, 11030 Belgrade, Serbia
[3]ICTM – Institute of Electrochemistry, University of Belgrade, Njegoševa 12, P.O. Box 473, 11001 Belgrade

Novel three-dimensional cobalt powder structures were successfully prepared by electrodeposition. Electrodeposited cobalt powder were characterized by scanning electron microscopy (SEM) and light microscopy. It was possible to control the morphology and structure of cobalt particles by adjusting process parameters of electrodeposition such as current density and type of working electrode. The morphology and structure of cobalt powders were investigated and the formation mechanism of agglomerate was also discussed.

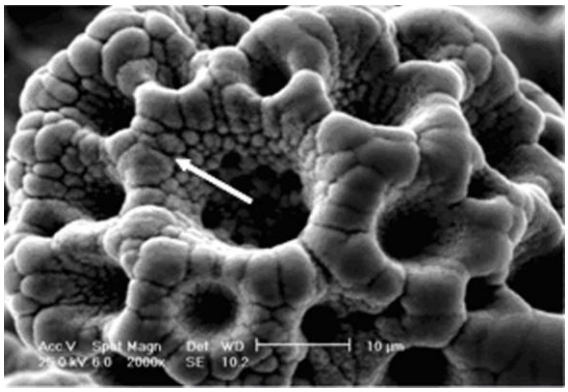

a b

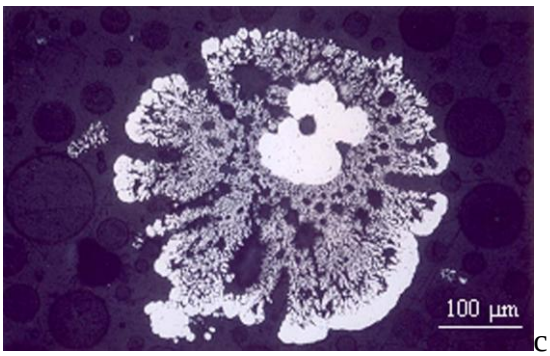

c

Figure: SEM photographs of cobalt powder particles deposeted at $j_{L(Co)}$ = 770 mAcm^{-2} onto (a) nickel electrode; (b) cobalt electrode; (c) Light microscope microphotograph of cross-section ball-like agglomerate in cobalt powder electrodeposited at j_{Co} = 500 mA cm^{-2}.

***Metalurgija-MJoM,* 17 (2011) 103-110.**

Effect of the anodic current density on copper electrodeposition in the hydrogen co-deposition range by the reversing current (RC) regime

N.D. Nikolić[1], G. Branković[2], V.M. Maksimović[3]

[1]ICTM – Institute of Electrochemistry, University of Belgrade, Njegoševa 12, P.O. Box 473, 11001 Belgrade
[2]Institute for Multidisciplinary Research, University of Belgrade, P.O. Box 33, 11030 Belgrade, Serbia
[3]Institute of Nuclear Sciences Vinča, University of Belgrade, P.O. Box 522, 11001 Belgrade, Serbia

In this study, the effect of the anodic current density in the regime of reversing current (RC) on the quantity of evolved hydrogen and morphology of copper deposits was considered. The quantity of evolved hydrogen was quantified by the determination of the average current efficiency for hydrogen evolution reaction, while morphology and internal structures of electrodeposited copper were analyzed using scanning electron (SEM) and optical microscopy techniques, respectively. In all RC experiments, the cathodic current density of 440 mA/cm^2, cathodic pulse of 10 ms and anodic pulse of 5 ms were applied, while the analyzed anodic current densities were: 40, 240, 440 and 640 mA/cm^2. The number, size and shape of holes formed of detached hydrogen bubbles strongly depended on the selected parameters of square waves RC. Due to the decrease of the quantity of evolved hydrogen with the increasing anodic current density, the change of morphology of copper deposits formed around holes from cauliflower-like agglomerates of copper grains to dendrites was observed. Honeycomb-like structures were formed with the anodic current density values up to 440 mA/cm^2. The compactness of the honeycomb-like structures increased with the increase of the anodic current density. The improvement of structural characteristics of the honeycomb-like electrodes was achieved by the application of the RC regime in comparison with both the pulsating current (PC) and constant galvanostatic regimes. It was found that the regime of reversing current is superior in the production of the honeycomb-like electrodes in relation to other current regimes of electrolysis.

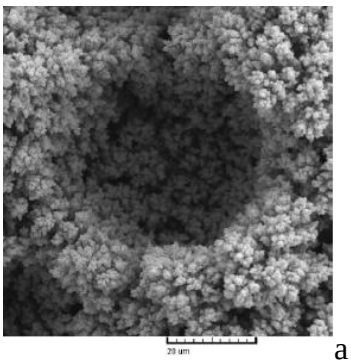

a

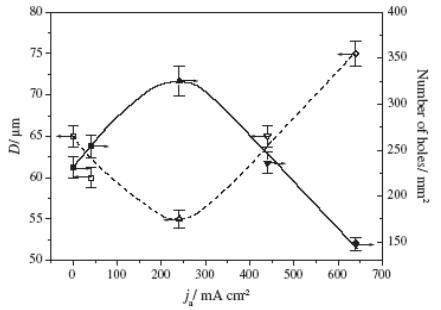

b

Figure: (a) non-coalesced hole obtained by the RC regime with j_a = 440 mA/cm^2; (b) the dependences of the average diameter, D and the number of holes per mm^2 surface area of copper electrodes on the anodic current density value.

***Journal of Electroanalytical Chemistry*, 661 (2011) 309-316.**

Effect of alloy purity on fracture behaviour of overaged 7000 alloy plates

Z. Cvijović[1], M. Vratnica[2], I. Cvijović-Alagić[3]

[1]Faculty of Technology and Metallurgy, University of Belgrade, Karnegijeva 4, 11120 Belgrade, Serbia
[2]Faculty of Metallurgy and Technology, University of Montenegro,Cetinjski put b.b., 81000 Podgorica, Montenegro
[3]Institute of Nuclear Sciences Vinča, P.O. Box 522, 11001 Belgrade, Serbia

The paper deals with the relations between microstructural parameters, microscopic fracture mechanisms and resultant plane-strain fracture toughness, K_{Ic}, of hot-forged 7000 alloy plates in overaged condition. Three industrially produced alloys with the (Zn+Mg+Cu) content of ~ 11.5 mass% and different contents of (Fe+Si) impurities (from 0.23 to 0.37 mass%) were used. The variation in alloy purity generated differences in the geometric characteristics of coarse intermetallic phase (IMP) particles, exerting significant effect on fracture behaviour of these alloys. To evaluate the fracture mechanism, characterization of the broken K_{Ic} test specimen surfaces was performed using scanning electron microscopy (SEM).
Three micromechanisms governing fracture process were identified. The extent of primary voiding at coarse IMP particles increases systematically with the increase of (Fe+Si) level, while the extent of intergranular/transgranular fracture decreases. This observation was confirmed by a quantitative description of fractures by means of a profilometric method. It was found that morphological parameters of the fracture profiles clearly differentiate between different fracture modes and offer conclusive proof that coarse voiding at fractured IMP particles dominates fracture at low alloy purity. A higher fraction of coarse voiding is shown to result in an overall reduction of fracture toughness.

Keywords: 7000 alloys; Microstructure; Failure modes; Fracture toughness; Fractography

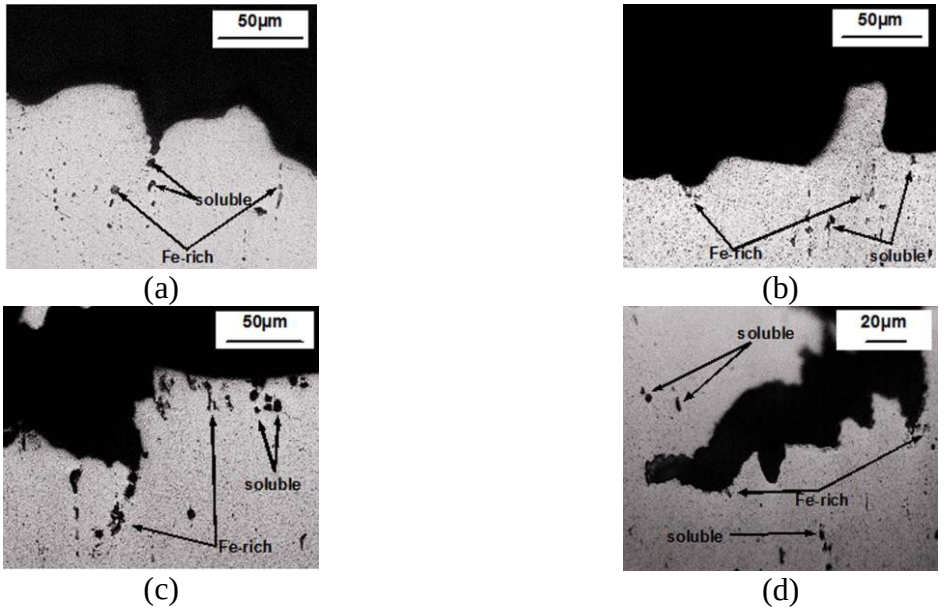

Figure: Characteristic fragments of fracture surfaces: (a) alloy 1, (b) alloy 2 and (c), (d) alloy. 3.

***International Journal of Damage Mechanics*, 20 (2011) 179-193.**

Morphology and composition of Ni-Co electrodeposited powders

V.M. Maksimović[1], U.Č. Lačnjevac[2], M.M. Stoiljković[1], M.G. Pavlović[3], V.D. Jović[2]

[1]Institute of Nuclear Sciences Vinča, University of Belgrade, P.O. Box 522, 11001 Belgrade, Serbia
[2]Institute for Multidisciplinary Research, University of Belgrade, P.O. Box 33, 11030 Belgrade, Serbia
[3]ICTM – Institute of Electrochemistry, University of Belgrade, Njegoševa 12, P.O. Box 473, 11001 Belgrade,

The morphology, phase and chemical composition of Ni–Co alloy powders electrodeposited from an ammonium sulfate-boric acid containing electrolyte with different ratio of Ni/Co ions were investigated. The ratios of Ni/Co ions were 1/1, 1/2 and 1/3. The morphology, chemical composition and phase composition of the electrodeposited alloy powders were investigated using AES, SEM, EDS and XRD analysis. Composition of the electrolyte, i.e. the ratio of Ni/Co concentrations was found to influence both, the alloy phase composition and the morphology of Ni–Co alloy powders. At the highest ratio of Ni/Co=1/1 concentrations typical 2D fern-like dendritic particles were obtained. With a decrease of Ni/Co ions ratio among 2D fern-like dendrites, 3D dendrites and different agglomerates were obtained. X-ray diffraction studies showed that the alloy powders mainly consisted of the face centered cubic α-nickel phase and hexagonal close-packed ε-cobalt phase and minor proportions of face-centered cubic α-cobalt phase. The occurrence of the latter phase was observed only in the alloy powder with the higher cobalt concentration in electrolyte. The electrodeposition of Ni–Co powders occurred in an anomalous manner.

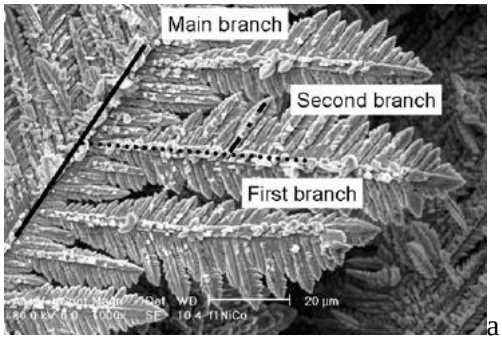

a

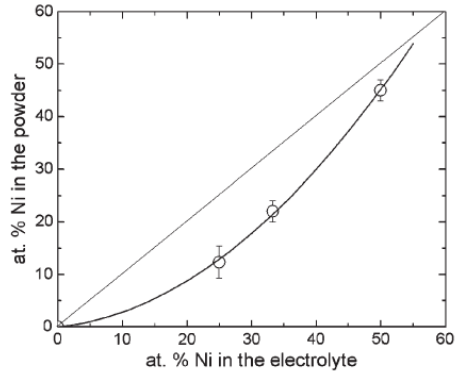

b

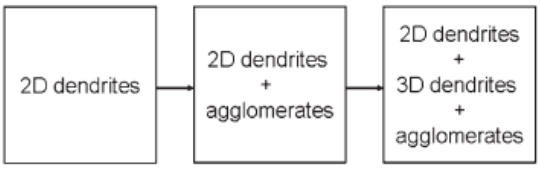

Figure: (a) SEM microphotograph of Ni–Co powder particles electrodeposited from electrolyte with Ni/Co=1/1 ions ratio;
(b) Atomic percentage of nickel in the alloy powder as a function of the atomic percentage of nickel in the electrolyte;
Scheme of the morphological change as a function of Co^{2+} ions concentration in electrolyte (Ni/Co ions ratio 1/1→1/2→1/3).

***Materials Characterization*, 62 (2011) 1173-1179.**

Energy

Changes of hydrogen storage properties of MgH_2 induced by boron ion irradiation

Sandra Kurko[a], Ljiljana Matovic[a], Nikola Novakovic[b], Branko Matovic[a], Zoran Jovanovic[c], Bojana Paskas Mamula[b], Jasmina Grbovic Novakovic[a]

[a]Laboratory of Material Science, Vinca Institute of Nuclear Sciences, PO Box 522, 11001 Belgrade, Serbia
[b]Laboratory for Nuclear and Plasma Physics, Vinca Institute of Nuclear Sciences, PO Box 522, 11001 Belgrade, Serbia
[c]Laboratory of Physics, Vinca Institute of Nuclear Sciences, PO Box 522, 11001 Belgrade, Serbia

MgH_2 powder samples have been irradiated with 45 keV B^{3+} ions with different ion fluencies ranging from 10^{12} to 10^{16}ions/cm^2. Irradiation effects have been estimated by SRIM calculations. To characterize induced modifications and its influence on the hydrogen desorption behavior of MgH_2, X-ray diffraction (XRD) analysis, particle size analysis and temperature programmed desorption (TPD) have been used. Changes of TPD spectra with irradiation conditions suggest that there are several mechanisms involved in desorption process which depend on defect concentration and their interaction and ordering. It has been demonstrated that the changes in near-surface area play the crucial role in hydrogen desorption kinetics. The results also confirm that there is possibility to control the thermodynamic parameters by controlling vacancies concentration in the systems.

Keywords: Magnesium hydride, Ion irradiation, Sorption, Desorption, Structural analysis, Recoil

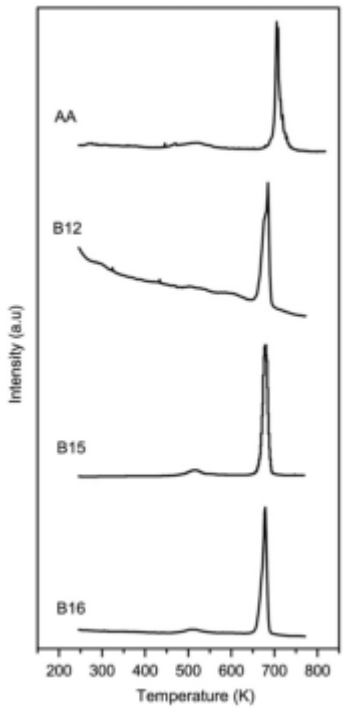

Figure: Results of TPD measurements, obtained at a constant heating rate of 5 K/min, in the temperature range from RT to 973 K, under the starting vacuum of 3 x 10^{-6}mbar, commercial (AA) MgH_2 powder, and samples irradiated using 45 keV B^{3+} ions, with ion fluencies of 1012(B12), 1015(B15) to 1016(B16) ions/cm.

International Journal of Hydrogen Energy **, 36 (2011) 1184-1189.**

Hydrogen storage properties of MgH_2 mechanically milled with α and β SiC

Sandra Kurko[a], Željka Rašković[a], Nikola Novaković[a], Bojana Paskaš Mamula[a], Zoran Jovanovic[a], Zvezdana Baščaravić[b], Jasmina Grbović Novaković[a], Ljiljana Matovic[a]

[a]Vinca Institute of Nuclear Sciences, University of Belgrade, PO Box 522, 11001 Belgrade, Serbia
[i]Institute for Multidisciplinary Research, Kneza Viseslava 1, 11030 Belgrade, Serbia

To understand the influence of various crystallographic phases on hydrogen storage properties, ball milling of MgH_2 with hexagonal (α) and cubic (β) SiC have been performed. Structural characterization of all samples has been done by X-ray diffraction (XRD) analysis, particle size analysis and scanning electron microscopy (SEM). Investigation of hydrogen desorption properties of prepared nanocomposites has been done using temperature programmed desorption (TPD) technique. Despite the results of structural and morphological characterization of obtained nanocomposites are very similar, TPD spectra show significant differences regarding existence of intermediate temperature peak. In the sample milled with hexagonal SiC this peak originates both from H_2 and H_2O, while in the sample milled with cubic phase it only comes from H_2O. Both samples exhibit low temperature H peak at 385 K.

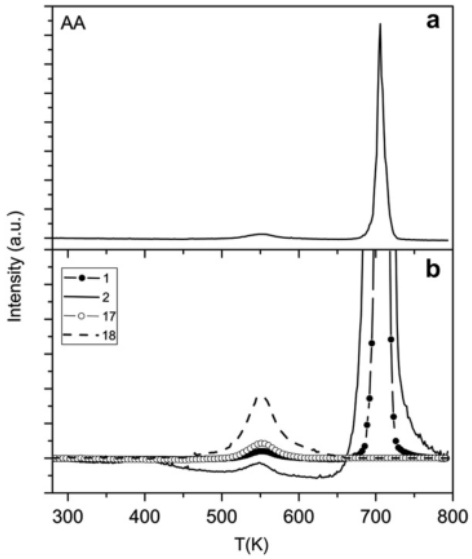

Figure: Results of TPD measurements, obtained at constant heating rate of 5 K/min, in the temperature range from RT to 973 K, under the starting vacuum of3 x10^{-6}mbar of commercial MgH_2 powder (AA): a) total signal of all desorption products, b) separate signals of desorption product: 1(H^+), 2 (H), 17 (OH^-) and 18 (H_2O)

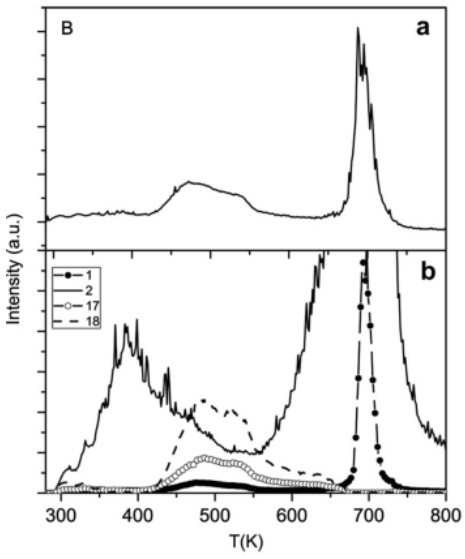

Figure: Results of TPD measurements, obtained at constant heating rate of 5 K/min, in the temperature range from RT to 973 K, under the starting vacuum of 3 x10^{-6}mbar of MgH_2/β-SiC powder: a) total signal of all desorption products, b) separate signals of desorption product: : 1(H^+), 2 (H), 17 (OH^-) and 18 (H_2O)

***International Journal of Hydrogen Energy* , 36 (2011) 549-554.**

The Influence of Boron Doping Concentration on MgH_2 Electronic Structure

S. Kurko[1], B. Paskaš-Mamula[1], Lj. Matovic[2], J. Grbovic Novakovic[2], N. Novakovic[1]

[1]University of Belgrade, Vinca Institute of Nuclear Sciences, Laboratory for Nuclear and Plasma Physics, P.O. Box 522, 11001 Belgrade, Serbia
[2]University of Belgrade, Vinca Institute of Nuclear Sciences, Laboratory for Material Sciences P.O. Box 522, 11001 Belgrade, Serbia

We have performed ab initio electronic structure calculations of $Mg_{1-x}B_xH$ compounds with different boron concentrations, ranging from x =0.0625 to 0.5. Full structural relaxation was performed in order to properly describe influence of dopant on host matrix. Results showed that there is a strong influence of boron concentration on structural and thermodynamic stability of compound. B-H bond length is substantially shorter then in Mg-H coordination polyhedron. Boron significantly contributes to density of states at Fermi level within energy gap. The width of boron electronic states heavily depends on boron concentration, causing reduction of energy gap of host MgH_2, and leading to metallic nature of compound with highest boron concentration. The predicted thermodynamic instability of compounds with higher boron concentration is in agreement with experimental findings that under similar stoichiometry, boron with magnesium forms only complex hydride, $Mg(BH_4)_2$. It is also shown that existence of stable hydrides with MgH_2 rutile structure and small concentration of boron ispossible in principle and that boron can be used to further destabilize MgH_2 in order to enhance its hydrogen sorption-desorption kinetics.
PACS: 31.15.A–, 88.80.F–, 88.30.R–

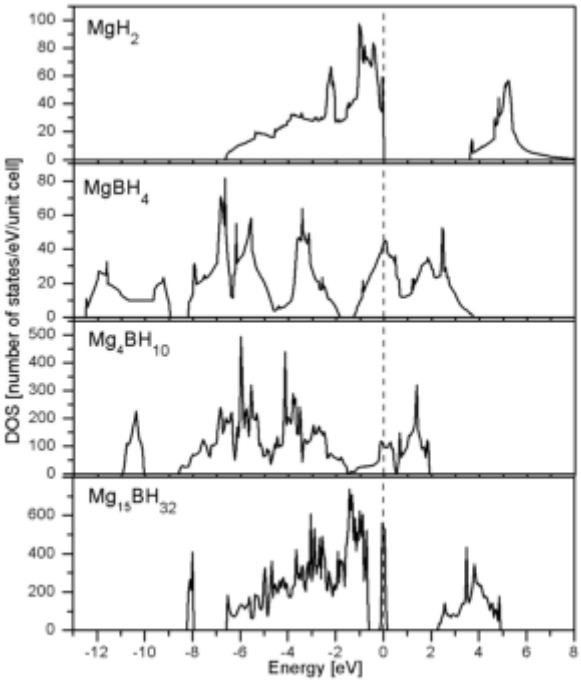

Figure: Total densities of states for all four investigated systems. Fermi level is marked with vertical dashed line.

***Acta physica polonica A,* 120 [2] (2011) 238-2.**

Microstructure and hydrogen storage properties of MgH_2-TiB_2 composites

S. Milošević[1], Ž. Rašković-Lovre[1], I. Milanović[1], S. Kurko[1], R. Vujasin[1], Z. Baščarević[2], Lj. Matović[1], J. Grbović Novaković[1]

[1]Laboratory for Materials Science, Vinča Institute of Nuclear Sciences, PO Box 522, Belgrade, 11000, Serbia
[2]Institute of Multidisciplinary Research, Kneza Višeslava 1, Belgrade, 11000, Serbia

Although hydrogen is an ideal energy carrier, there are still substantial technological challenges, which hinder its use as a fuel. One of the major tasks for a future hydrogen technology for both mobile and stationary applications is the development of a safe, non-expensive and lightweight storage facility. Several methods for storing hydrogen have been proposed and tested but none of them fulfills all the necessary requirements. Hydrogen storage in lightweight metals or compounds is being considered as a most promising method for solid-state storage. The solid state bonding of hydrogen in metals provides several advantages: the density of hydrogen is high, which is ideal for transportation, there is no risk of leakage or explosion, and finally, the hydrogen retained by this method has high purity, which is essential for its utilization in fuel cells. Among the metal hydrides, magnesium hydride exhibits a high gravimetric density of hydrogen up to 7.6 wt % and therefore, magnesium has been proposed for hydrogen storage. However, slow sorption reaction rate is severe problem and to solve it, two methods have been proposed: a decrease of crystallite size of magnesium to nanoscale size through high-energy ball milling and the use of suitable catalysts. We have investigated combined influence of both mechanical milling and addition of TiB_2 to MgH_2 on its desorption properties.

Milling process was performed under argon atmosphere for 10 h in Turbula Type 2TC Mixer using hardened steel vial and balls with BPR fixed at 10:1. Microstructural and morphological analysis was done by XRD and laser scattering particle size analysis (PSD). The calculation of crystallite size and strain was obtained by means of Cauchy/Gaussian approximation. A VEGA TS 5130MM Tescan Brno SEM equipped with EDS detector was used to obtain the phase distribution, the material homogeneity and the morphology of the powder particles. Malvern 2000SM Mastersizer laser scattering particle size analysis system was used to obtain the quantitative particle size distributions. The specified resolution range of the system was sub-mm to 2 mm. 2-propanol was used as suspension media. All samples were ultrasonicated for 15 min prior to measurements. All measurements were performed in the same stirring speed and obscuration level. Desorption properties of obtained MgH_2-TiB_2 composite were followed by DTA/TGA analysis using SDT 2960 Instrument at a constant heating rate of 15 K/min, starting from room temperature to 600K.

The results show that there is considerable improvement of desorption properties in the examined system.

***Proceedings of 10th Multinational Congress of Microscopy*, Urbino 4-9.09.2011, Italy, pp. 495.**

Mechanochemical synthesis of MgH_2-TiB_2 composites for hydrogen storage

I. Milanović, R. Vujasin, S. Milošević, Ž. Rašković-Lovre, S. Kurko, Lj. Matović, J. Grbović Novaković

Vinca Insitute of Nuclear Sciences, University of Belgrade, Belgrade, Serbia

Hydrogen storage is a key enabling technology for the development of hydrogen and fuel cell power technologies in transportation, stationary and portable applications. On-board hydrogen storage is considered to be the most challenging aspect for the successful transition to a hydrogen economy. Modified nanostructure materials offer promise for superior hydrogen storage due to short diffusion distances, new phases with better capacity, reduced heats of adsorption/desorption, faster kinetics. High energy mechanical milling was used to synthesize MgH_2 (90 wt.%) + TiB_2 (10 wt.%) composite as possible solution for hydrogen storage. XRD and SEM analysis was used to determine microstructure and morphology while the DSC analysis was used to resolve the hydrogen desorption properties. It has been shown that use of nanostructurated TiB_2 decrease the MgH_2 desorption temperature.

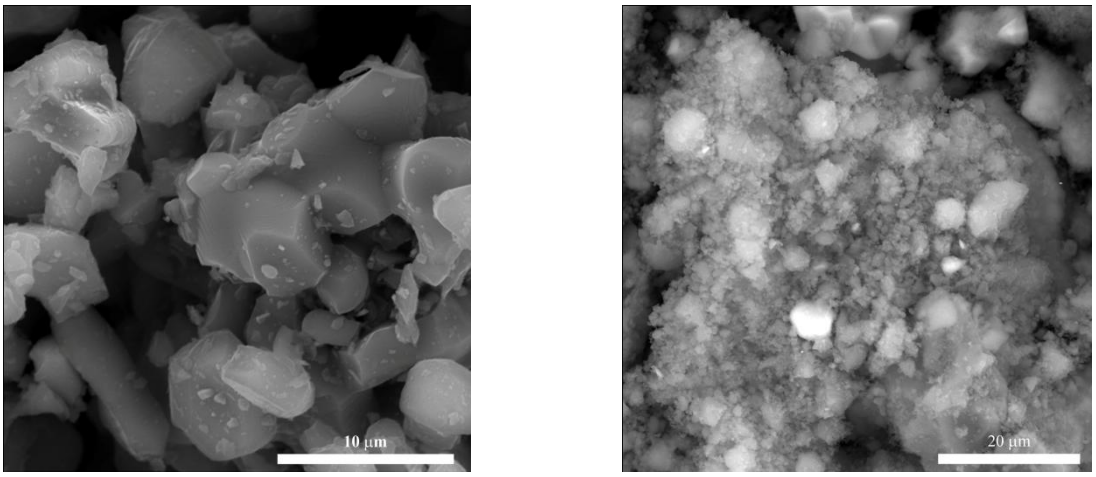

Figure: SEM images of pure TiB_2 (left) and composite material with MgH_2.

***VII International Conference on Mechanochemistry and Mechanical Alloying INCOME 2011*, Herceg Novi, August 31-September 3, 2011, pp. 5**

Mechanical milling of magnesium based composites for hydrogen storage

I. Milanović[1], R. Vujasin[1], S. Milošević[1], Ž. Rašković[1], S. Kurko[1], Lj. Matović[1], J. Grbović Novaković[1], A. Aurora[2], A. Montone[2]

[1]Vinca Insitute of Nuclear Sciences, University of Belgrade, Belgrade, Serbia
[2]ENEA, UTTMAT Research Centre of Casaccia, Rome, Italy

High-energy ball milling (HEBM) provides mechanical activation to metal hydrides to increase the rates of adsorption, desorption and chemical reactions. This is the main nanotechnology top–down approach for the synthesis of nanoparticles suitable for hydrogen storage since the applied force is sufficient to disperse the material into fine nanometric particulates or agglomerates. We have shown that HEBM of MgH_2 with additives such as metals (Fe, Co) metal oxides (VO_2,Nb_2O_5 etc), ceramics SiC,TiB_2 destroy the thin chemically passive surface coatings (e.g., surface oxides) and form fresh, clean chemically active MgH_2 surface. We have also demonstrated that such milling introduces the defects into solid compounds, which is extremely important for suitable hydrogen storage materials. Reactive milling in hydrogen atmosphere and non reactive milling in inert atmosphere to produce materials for hydrogen storage were performed.

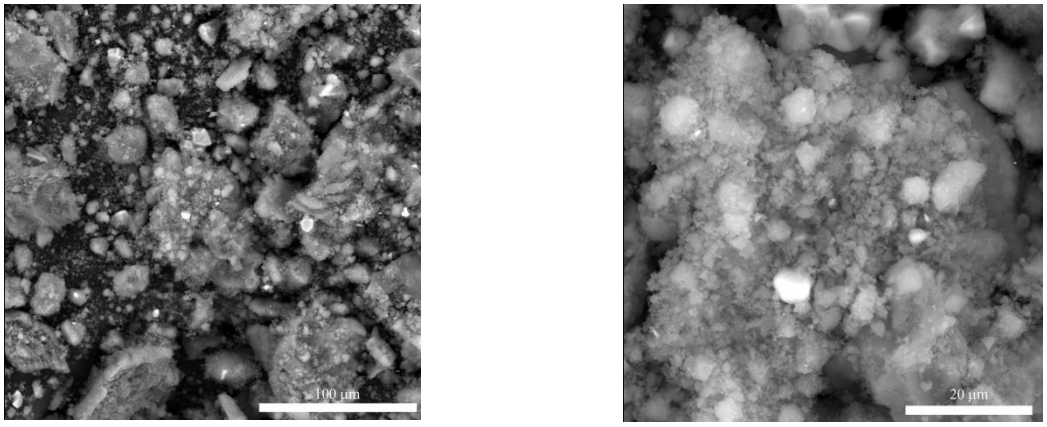

Figure: Composite material before and after mechanochemical treatment.

***VII International Conference on Mechanochemistry and Mechanical Alloying INCOME 2011*, Herceg Novi, August 31-September 3, 2011, pp. 76.**

Mechanical synthesys of magnesium based nanocomposites

I. Milanović, R. Vujasin, S. Milošević, Ž. Rašković-Lovre, S. Kurko, Lj. Matović, J. Grbović Novaković

Vinča Institute of Nuclear Sciences, University of Belgrade, Belgrade, Serbia

The solid state bonding of hydrogen in metals provides several advantages: the density of hydrogen is high, which is ideal for transportation, there is no risk of leakage or explosion, and finally, the hydrogen retained by this method has high purity, which is essential for its utilization in fuel cells. Among the metal hydrides, magnesium hydride has been considered as solution for energy storage since exhibits a high gravimetric density of hydrogen. Anyhow the slow sorption kinetics give rise to several problems that has to be solved before hydrogen enter to the economy. To solve this problem, two methods have been proposed: a decrease of crystallite size of magnesium to nanoscale size through high-energy ball milling and the use of suitable catalysts. We have investigated combined influence of both mechanical milling and addition of TiB_2 and SiC additive to MgH_2 on its desorption properties. Microstructural and morphological properties has been correlated to the desorption properties. The considerable improvement is desorption properties has been achieved.

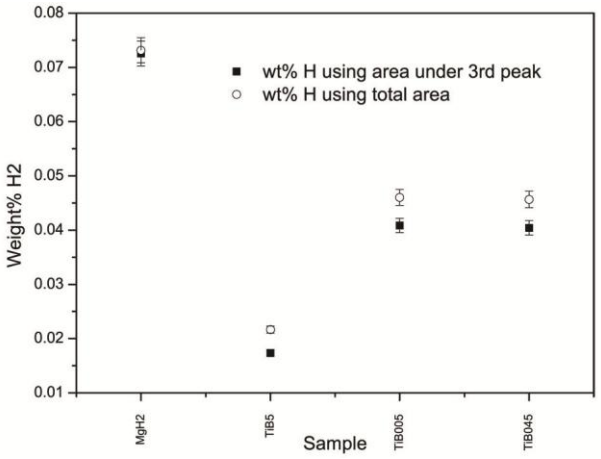

Figure: Mass of desorbed hydrogen from the composites.

***Thirteenth annual conference yucomat 2011*, Herceg Novi, September 5-9, 2011, Montenegro, pp. 150.**

Microstuctural evaluation in MgH_2-CeO_2 composites during high energy mechanical milling

Željka Rašković, Jelena Gulicovski, Sandra Kurko, Bojana Paskaš Mamula, Ljiljana Matović, Slobodan Milonjić

Vinča Institute of Nuclear Sciences, University of Belgrade, Belgrade, Serbia

The way of safely storage at the high volumetric and gravimetric density is not completely assessed. MgH_2 that contain 7.6 mass% of H is one of the solution. But its formation is extremely slow, and in thermodynamic equilibrium a plateau pressure of 1 bar requires 300 °C. The powder is often processed by high-energy ball milling, since, in this way, in a single process it is possible to introduce a high density of defects and a fine dispersion of metal particles having catalytic properties. Surprisingly, transition metal oxides have shown remarkably higher catalytic effects than the pure metals. Milling process under Ar atmosphere for 10 h in Turbula Type 2TC Mixer using hardened steel vial and balls with BPR fixed at 10:1. Morphological and microanalytical characterization of obtained composites was carried out by VEGA TS 5130MM, Tescan Brno SEM equipped with EDS detector and TEM SAGFGAGAR. Malvern 2000SM Mastersizer laser scattering particle size analysis system was used to obtain the quantitative MgH_2 particle size distributions.

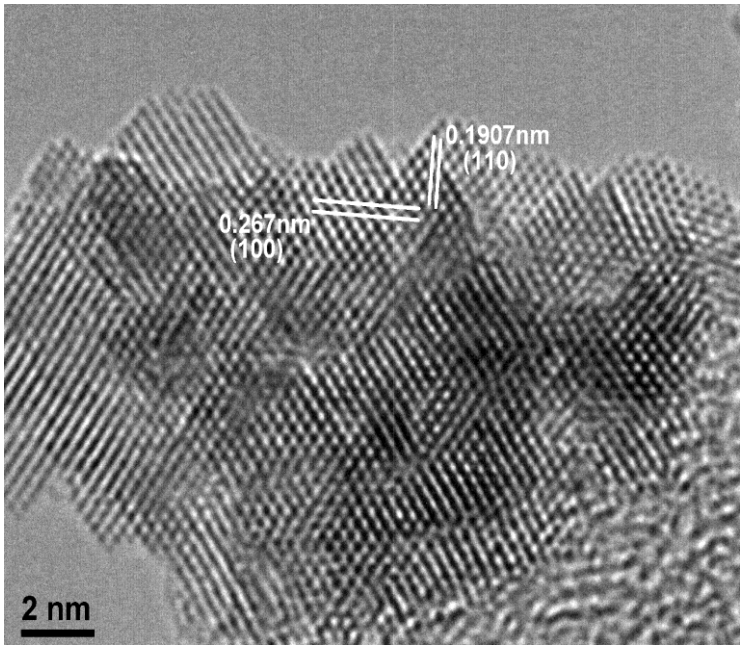

Figure: TEM of CeO_2

Proceedings of *10th Multinational Cogress of Microscopy*, Urbino 4-9.09.2011, Italy, pp. 507.

Biomaterials

Synthesis and modification of nanomaterials: Changes in characteristics of brushite depending on the particle size

Miljana Miljević[1], Anja Došen[1], Aleksandra Rosić[2]

[1]Institute of Nuclear Science Vinca, University of Belgrade, 11001 Belgrade, Serbia
[2]Faculty of Mining and Geology, University of Belgrade, 11000 Belgrade, Serbia

Brushite, $CaHPO_4 \cdot 2H_2O$, a calcium phosphate mineral, crystallizes in the monoclinic crystal system, space group *Ia*. Brushite has layered structure, in which the layers are held by the water molecules *via* hydrogen bonds. In nature, brushite can be found in caves, phosphate deposits and soils. Brushite has wide range of applications. It is the major component of toothpaste due to its abrasive properties. It is also used as remediation media and in waste water treatment. The main objective of this preliminary study was to determine the properties of brushite regards to its grain size. Characterization was preformed on samples obtained by precipitation from the solution, and further characterization of modified nanomaterials prepared by grinding in the vibrating mill. Material preparation was preformed by titration of the solution $(CH_3COO)_2Ca \cdot H_2O$ with the solution $NaH_2PO_4 \cdot H_2O$, under constant stirring, with an initial pH = 5 and temperature around 60 °C. Material was analyzed by X-ray powder diffraction and Raman spectroscopy. Crystallite size was modified by grinding in vibrating mill. The sample was ground five times for 2,5 minutes and analyzed by X-ray powder diffraction each time between grinding. Crystallite size was determined from the X-ray powder diffraction method using Scherer equation. Milling in the vibrating mill leads to increase in temperature and reduction in particle size. Due to a temperature increase, there is a phase transformation of brushite to monetite ($CaHPO_4$) after 5 minutes of grinding.

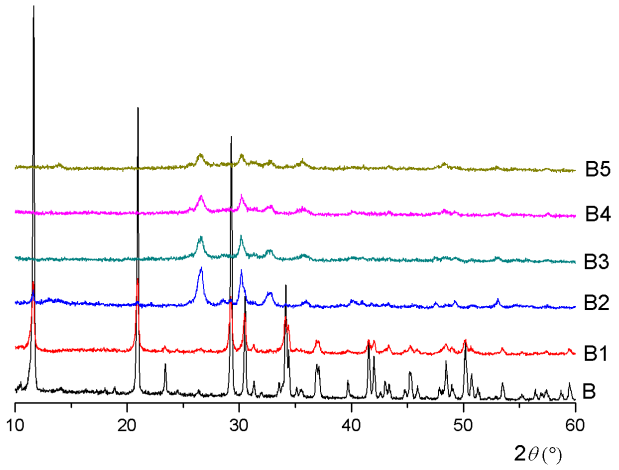

Figure: XRPD patterns of synthesized and treated materials: B – synthesized sample, B1 – sample treated in vibrating mill for 2.5 minutes, B2 – sample treated for 5 minutes, B3 – sample treated for 7.5 minutes, B4 – sample treated for 10 minutes, B5 – sample treated for 12.5 minutes.

***XVIII Conference of the Serbian crystallographic society,* June 02-04.2011. Andrevlje, Fruška gora, The Book of Abstracts, pp. 52.**

Synthesis and characterization of bio-calcium phosphates

Miljana Miljević, Anja Došen

Institute of Nuclear Science Vinca, University of Belgrade, 11001 Belgrade, Serbia

Calcium phosphates (CaP) such as octacalcium phosphate (OCP, $Ca_8H_2(PO_4)_6 \cdot 5H_2O$), hydroxyapatite (HAP, $Ca_{10}(PO_4)_6(OH)_2$), brushite ($CaHPO_4 \cdot 2H_2O$) and monetite $CaHPO_4$ are of great scientific interest in the field of biomaterials. HAP is the main constituent of bone, dental calculi and enamel. OCP is structurally similar to HAP, and is a precursor for formation of HAP in bone, also it has very good biodegradabile and osteoconductive characteristics. Brushite is a biological mineral that occurs in bones and teeth and as transitional phase in the crystalization of HAP. It is also used as a CaP cement, and as an abrasive in a toothpaste. When brushite loses its structural water it transforms to monetite. The preliminary objective of this study is synthesis and characterization of these CaP phases. Materials were obtained by titration of the solution $(CH_3COO)_2Ca \cdot H_2O$ with the solution $NaH_2PO_4 \cdot H_2O$ in different molar ratios, under constant stirring, and temperature around 60 °C. Brushite forms at pH around 5, and at pH around 7 OCP and HAP are formed. This was confirmed by XRD and Raman spectroscopy. Pure brushite nanomaterial was obtained, and crystallite size was modified by grinding in vibrating mill. The sample was ground five times for 2.5 minutes and analyzed by XRD between grinding. Particle sizes were determined from the XRD patterns using Scherer equation. After about 5 min of grinding an increase in temperature causes a phase transformation from brushite to monetite. BET method indicates that synthesized brushite have micro porosity. After 5 minutes of milling have mezzo porosity, these results were confirmed by SEM analysis. Using this method can be very difficult to synthesize pure HAP and OCP. Ritveld refinement showed that we did not get pure OCP.

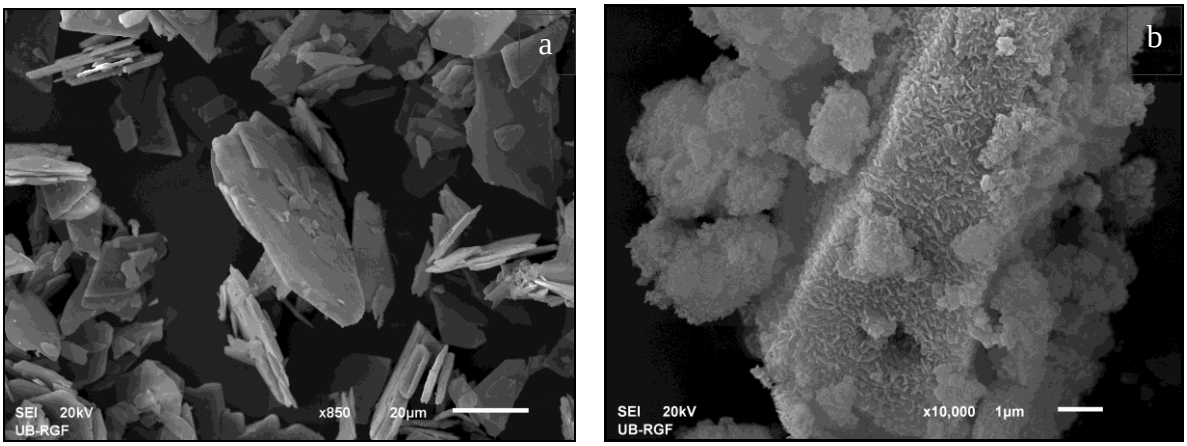

Figure: a) plate like brushite grains b) monetite grain with agregates.

The Ninth Student's Meeting, SM – 2011, **November 16-18, 2011. Novi Sad, Serbia, The Book of Abstracts, pp. 65.**

Influence of retained hydride particles and microstructure on mechanical properties of PM produced Ti–6Al–4V alloy

D. Božić, V. Rajković, M. T. Jovanović, B. Dimčić

Institute of Nuclear Sciences Vinča, University of Belgrade, 11001 Belgrade, Serbia

Compacts of Ti–6Al–4V alloy were produced via the powder metallurgy technique applying the hydride–dehydride process and hot isostatic pressing. The conditions of reversible hydride–dehydride process were controlled by chemical and X-ray diffraction analysis and scanning electron microscopy. Powders were pressed above and below the α→β transus temperature. The presence of titanium hydrides and morphology of the microstructure have the direct influence on the tensile properties and fracture toughness of the Ti–6Al–4V alloy, but the effect of microstructure is more pronounced.

Keywords: Ti-6Al-4V chips, hydride dehydride process, hot isostatic pressing, microstructure, mechanical properties, fractography.

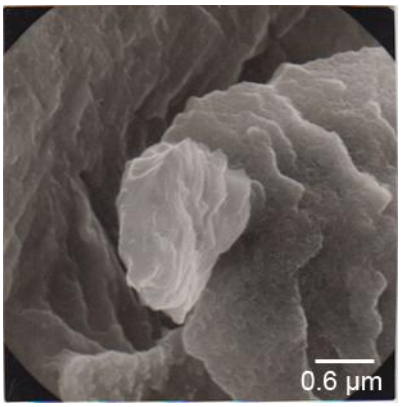

Figure: SEM. Precipitated titanium hydride particles.

***Powder Metallurgy*, 54 (2011) 40-45.**

Phase and demographic statistical analysis of urinary stones

Miljana Miljević[1], Aleksandra Rosić[2]

[1]Institute of Nuclear Science Vinca, University of Belgrade, 11001 Belgrade, Serbia
[2]Faculty of Mining and Geology, University of Belgrade, 11000 Belgrade, Serbia

The idea of this paper is to investigate the phase composition and demographic distribution of urinary stones from Serbian patients of both sexes. To determinate the phase characteristics, we use a method of X-ray diffraction analysis. X-ray diffraction analysis indicate the presence of the following phases: Whewellite ($CaC_2O_4 \cdot H_2O$) and Weddelite ($CaC_2O_4 \cdot 2H_2O$) from oxalate, Apatite ($Ca_5(PO_4)_3X$), Brushite ($CaHPO_4 \cdot 2H_2O$) and Struvite ($MgNH_4PO_4 \cdot 6H_2O$) from phosphate group, as well as Uricite ($C_5H_4N_4O_3$) and L-cystine ($C_6H_{12}N_2O_4S_2$). The SEM analysis confirmed the obtained structures.

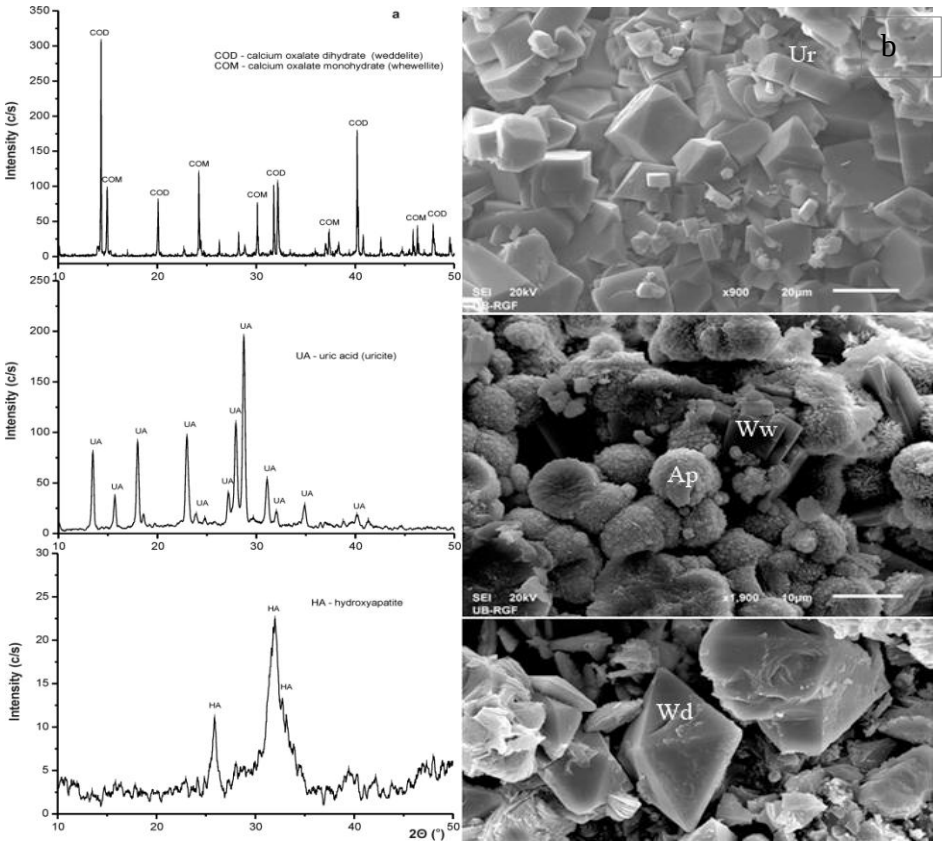

Figure: a) XRPD patterns of Whewellite and Weddelite, Uricite, Apatite (Hydroxyapatite) b) SEM micrographs of Uricite (Ur), Apatite (Ap) and Whewellite (Ww) and Weddellite (Wd).

***1st Conference of the Serbian Ceramic Society*, March 17-18.2011. Belgrade, Serbia, The Book of Abstracts, pp. 48.**

The effect of recasting on structure and microhardness of high gold dental alloy

V.M. Maksimović[1], A.D. Čairović[2], I. Cvijović-Alagić[1]

[1]Institute of Nuclear Sciences Vinča, University of Belgrade, P.O. Box 522, 11001 Belgrade, Serbia
[2]School of Dental Medicine, University of Belgrade, Rankeova 4, Belgrade, Serbia

Noble and semi-noble dental casting alloys are often reused by recasting. Recasting may change the composition and structure of these alloys and thus effects alloy mechanical properties and castability, as well as the alloy corrosion resistance degradation. Literature data, regarding the effect of recasting on changes in elemental composition and microstructure of high gold dental alloy, are very rare.
Recasting procedure changes the microstructure and microhardness of the high gold dental alloy and such a procedure should be avoided in the dental practice. This type of high gold dental alloy can be safely recast only a small number of times.

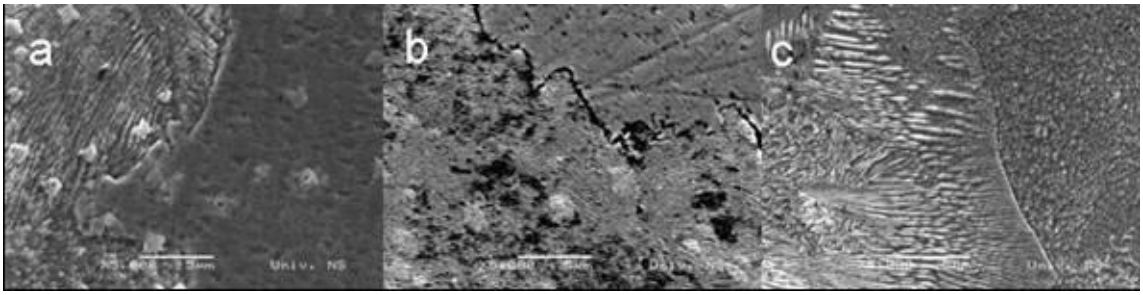

Figure: SEM micrographs. Microstructure of high gold dental alloy of grain bounders; (a) first, (b) fourth and (c) eighth cast.

***10th Multinacional Congres on Microscopy*, September 4-9 2011 Urbino, Italy, pp. 617.**

Wear Behaviour of Ti6Al4V Alloy against Al_2O_3 under Linear Reciprocating Sliding

F. Živić[1], M. Babić[1], I. Cvijović-Alagić[2], S. Mitrović[1], A.Vencl[3]

[1]Tribology Laboratory, Faculty of Mechanical Engineering, University of Kragujevac, Sestre Janjić 6, 34000 Kragujevac, Serbia
[2]Institute of Nuclear Sciences Vinča, University of Belgrade, Mike Petrovića Alasa 12-14, 11001 Belgrade, Serbia
[3]Tribology Laboratory, Faculty of Mechanical Engineering, University of Belgrade, 11000 Belgrade, Serbia

Tribological behaviour of four different heat-treated Ti6AI4V alloys, during linear reciprocating sliding against alumina, on the microscale, was investigated. Experiments were carried out for dry sliding and in the Ringer solution, over a range of loads (100-1000 mN) and speeds (4-12 mm/s). The wear mechanisms were investigated based on observations of worn surfaces. Specific wear rates for tested Ti6Al4V alloy were of order of 10^{-7}-10^{-4} mm^3/Nm. The lowest wear factor (order of 10^{-7} mm^3/Nm) was observed for the Ti6AI4V annealed for 1h at 750^{o}C in Ar atmosphere and then cooled down to room temperature in the furnace, tested in the Ringer solution. Load dependence of the wear factor exhibited transition characteristics. Wear mechanism has changed with change of load. The Ringer solution lowered wear factor for all tested conditions.

Keywords: Ti6AI4V, alumina, wear mechanism

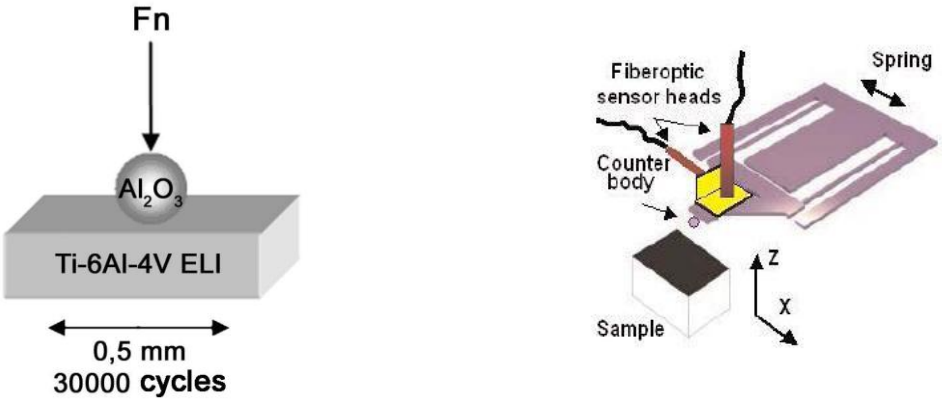

Figure: Scheme of the contact pair geometry and nanotribometer contact geometry.

Nano-Scale Tribological Investigation of Ti-6Al-4V Alloy for Orthopedic Applications

I. Cvijović-Alagić[1], Z. Cvijović[2], F. Živić[3], K. Gerić[4], M. Rakin[2]

[1]Institute of Nuclear Sciences Vinča, University of Belgrade, P.O.Box 522, 11001 Belgrade, Serbia
[2]Faculty of Technology and Metallurgy, University of Belgrade, Karnegijeva 4, 11120 Belgrade, Serbia
[3]Faculty of Mechanical Engineering, University of Kragujevac, Sestre Janjić 6, 34000 Kragujevac, Serbia
[4]Faculty of Technical Sciences, University of Novi Sad, Trg Dositeja Obradovića 6, 21000 Novi Sad, Serbia

Ti-6Al-4V alloy is widely used for orthopedic implants manufacture due to its excellent corrosion resistance and mechanical properties. Friction and wear, however, play an important role in determining the performance of orthopedic prosthesis. Standard Ti-6Al-4V alloy is reported to possess a low friction wear resistance. This calls for the tailored design of Ti-6Al-4V alloy to optimize the tribological properties. Because of that a detailed knowledge of microstructural effects on its tribological behavior is required. In this study, linear reciprocating nanotribometer is applied to measure friction coefficient of Ti-6Al-4V alloy available in four different microstructural conditions produced by heat treatment variations. The friction tests were conducted in simulated body fluid at room temperature with a load of 250-1000mN and sliding speed of 4-12mm/s.

It was observed that tribological performance of heat treated Ti-6Al-4V alloy strongly dependent on its microstructure. The mixed alpha+beta phase microstructures exhibit substantial friction reduction. The friction coefficients are lower than those of martensitic microstructure. Microstructure with coarse equiaxed alpha provides lowest friction coefficients at loads 250, 500 and 750mN, irrespective of sliding speed. At highest load, the friction coefficients of lamellar alpha+beta microstructure are lowest. For all microstructural conditions, the friction coefficient varies with applied load and speed. It decreases initially as the load is increased to 500mN and further remains more or less the same. At loads ranging from 500 to 1000mN, however, it increases with increasing sliding speed. At lowest load, the friction coefficient of two phase microstructures and martensitic one follows two distinct trends. The friction coefficients of former microstructures tend to decrease gradually as speed increased, while of martensitic microstructure increase to highest value. The worn surfaces examination reveals that observed behavior is due to the change in the wear mechanism.

Keywords: Nano-Scale Tribology, Ti alloys, Orthopedic Implants

***Euro BioMat 2011 - European Symposium on Biomaterials and Related Areas*, April 13th-14th 2011, Jena, Germany, The Book of Abstracts.**

Hydroxyapatite coatings prepared by a high power laminar plasma jet

Miroljub Vilotijević[a], Petar Marković[a], Slavica Zec[b], Slobodan Marinković[b], Vukoman Jokanović[b]

[a]Plasma Jet Co, Branicevska 29, 11000 Belgrade, Serbia
[b]VINCA Institute of Nuclear Sciences, Mike Petrovica Alasa 12-14 Belgrade, Serbia

For two hydroxyapatite (HA) powders, containing particles differing in mass by a factor of 20, a set of optimum deposition parameters was defined, leading to the coatings with high crystallinity (80–90%), high adhesion strength (60 and 40 MPa for the coating thicknesses of 120 μm and 350 μm, respectively) and excellent microstructure (coatings were without micro- or macro-cracks, without delaminating on substrate-coating surface contact, and possess low porosity, 1–2%). It was shown that higher plasma power (52 kW) did not necessarily lead to a higher HA decomposition.

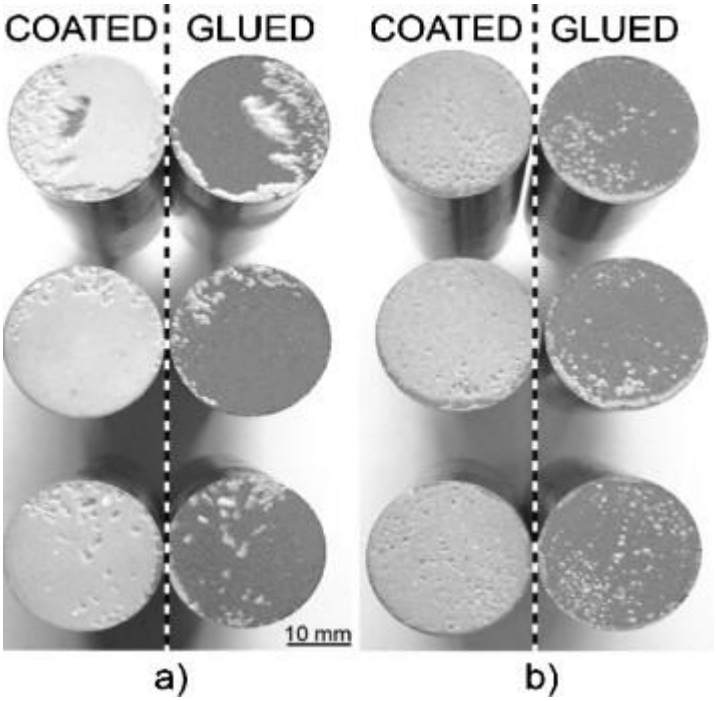

Figures: Fractographs of specimens, SOD = 80 mm, T_s = 200 °C. (a) Finer powder, coating surface flattened, coating thickness 280 ± 14 μm. (b) Coarser powder, as-deposited coating surface, coating thickness 260–290 μm.

***Journal of Materials Processing Technology*, 211 [6] (2011) 996–1004**

Wear and corrosion behaviour of Ti-13Nb-13Zr and Ti-6Al-4V alloys in simulated physiological solution

I. Cvijović-Alagić[1], Z. Cvijović[2], S. Mitrović[3], V. Panić[4], M. Rakin[2]

[1]Institute of Nuclear Sciences Vinča, University of Belgrade, P.O.Box 522, 11001 Belgrade, Serbia
[2]Faculty of Technology and Metallurgy, University of Belgrade, Karnegijeva 4, 11120 Belgrade, Serbia
[3]Faculty of Mechanical Engineering, University of Kragujevac, Sestre Janjić 6, 34000 Kragujevac, Serbia
[4]ICTM - Center of Electrochemistry, Njegoševa 12, 11000 Belgrade, Serbia

Wear and corrosion behaviour of cold-rolled Ti-13Nb-13Zr alloy, with martensitic microstructure, and Ti-6Al-4V ELI alloy, in martensitic and two-phase (α+β) microstructural conditions, was studied in a Ringer's solution. The wear experiments were performed at room temperature with a normal load of 40 N and sliding speeds 0.26, 0.5 and 1.0 m/s. The corrosion behaviour was studied at 37 ^{o}C using open circuit potential-time measurements and potentiodynamic polarization. It was found that Ti-13Nb-13Zr alloy has a substantially lower wear resistance than Ti-6Al-4V ELI alloy in both microstructural conditions. Surface damage extent increases with sliding speed increase and is always smallest for martensitic Ti-6Al-4V ELI alloy with highest hardness. Both alloys exhibit spontaneous passivity in Ringer's solution. Corrosion potential values are similar for all three materials. However, Ti-13Nb-13Zr and martensitic Ti-6Al-4V ELI alloys show improved corrosion resistance comparatively to Ti-6Al-4V ELI alloy with (α+β) microstructure. Martensitic Ti-6Al-4V ELI alloy possesses the best combination of both corrosion and wear resistance, although its corrosion resistance is found to be slightly higher than that of the Ti-13Nb-13Zr alloy.

Keywords: Ti orthopaedic alloys; Microstructures; Wear rate; Corrosion resistance; Ringer's solution

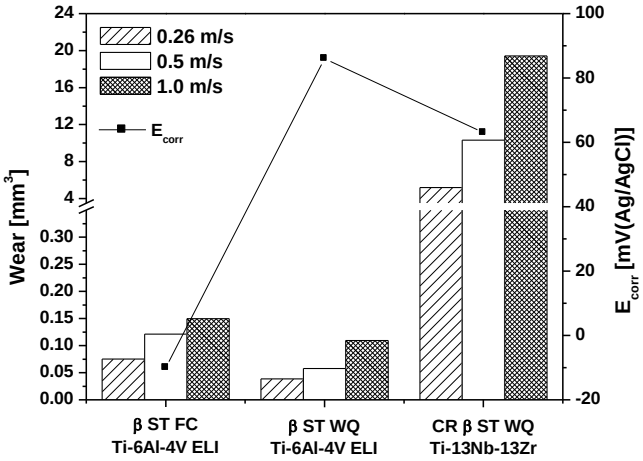

Figure: Relation between wear volume and corrosion potential for investigated materials.

***Corrosion Science*, 53 [2] (2011) 796-808.**

Carbon materials

Synthesis and characterization of carbon cryogel/zeolite composites

Biljana Babić, Maja Kokunešoski, Jelena Gulicovski, Marija Prekajski, Jelena Pantić, Ana Radosavljević-Mihajlović, Branko Matović

Institute for Nuclear Sciences Vinca, University of Belgrade, P.O. Box 522, 11001 Belgrade, Serbia

A novel method for synthesis of carbon cryogel/zeolite composites was obtained. Method considers forming of carbon cryogel from the sol-gel polycondenzation of resorcinol and formaldehyde, followed by freeze drying, and subsequent pyrolysis in presence of different amount of zeolite. Characterization of composite materials by nitrogen adsorption shows that samples are micro- and mesoporous and that specific surface area decrease with increasing the amount of zeolite in samples. XRD method confirms amorphous structure of carbon cryogel and crystalline structure of zeolite, i.e. structure of zeolite has not been destroyed by carbonization process. SEM and EDX analyses reveal homogenous distribution of zeolite through out carbon cryogel and corresponding composition.

Keywords: composite materials, sol-gel process, characterization.

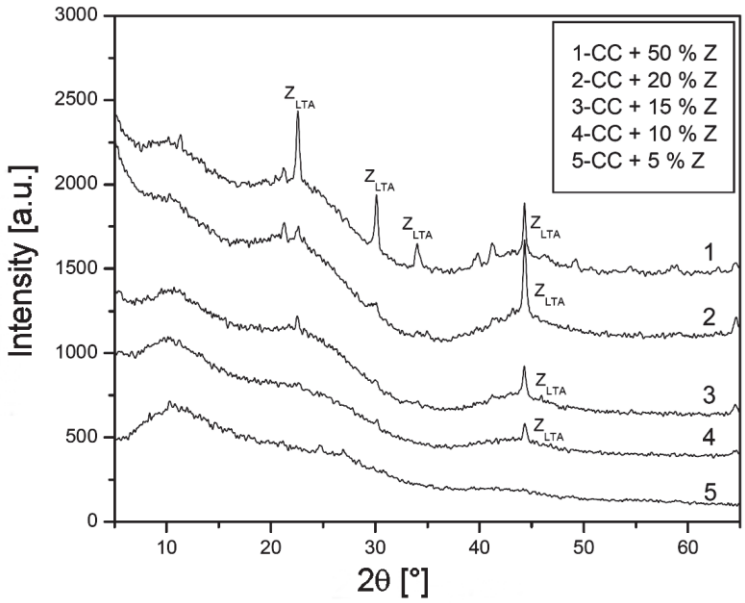

Figure: XRD patterns of carbon cryogel samples with different amount of zeolite.

***Processing and Application of Ceramics,* 5 [2] (2011) 91–96.**

Influence of chemical agents on the surface of active area and porosity carbon hollow fibers

Kljajević Ljiljana M.[1], Jovanović Vladislava M.[2], Stevanović Sanja I.[2], Bogdanov Žarko D.[1], Kaluđerović Branka V.[1]

[1]Institute of Nuclear Science Vinca, University of Belgrade, 11001 Belgrade, Serbia
[2]ICTM –Department of electrochemistry, P.O.Box 473, Belgrade, Serbia

Active carbon hollow fibers were prepared with regenerated polysulfone hollow fibers by chemical activation using: disodium hydrogen phosphate 2-hydrate, di-sodium tetraborate 10-hydrate, hydrogen peroxide, and diammonium hydrogen phosphate. The adsorption characteristics of obtained carbons were studied by nitrogen adsorption–desorption isotherms at 77 K, while the structures were examined with scanning electron microscopy and X-ray diffraction. The activation process increases the adsorption properties of fibers being more pronounced for active carbone fibers obtained with di-sodium tetraborate 10-hydrate and hydrogen peroxide as activator. The obtained active hollow carbons are microporous with different pore size distribution. Chemical activation with phosphates produces active carbon material with small surface area with but with both mesopores and micropores. X-ray diffraction shows that besides turbostratic structure typical for carbon materials, there are some peaks which indicate some intermediate reaction products when sodium salts were used as activating agent. Based on data from the electrochemical measurements the activity and porosity of the active fibers depend strongly on the oxidizing agent applied.

Key words: carbon hollow fibers, chemical activation, adsorption, cyclic voltammetry

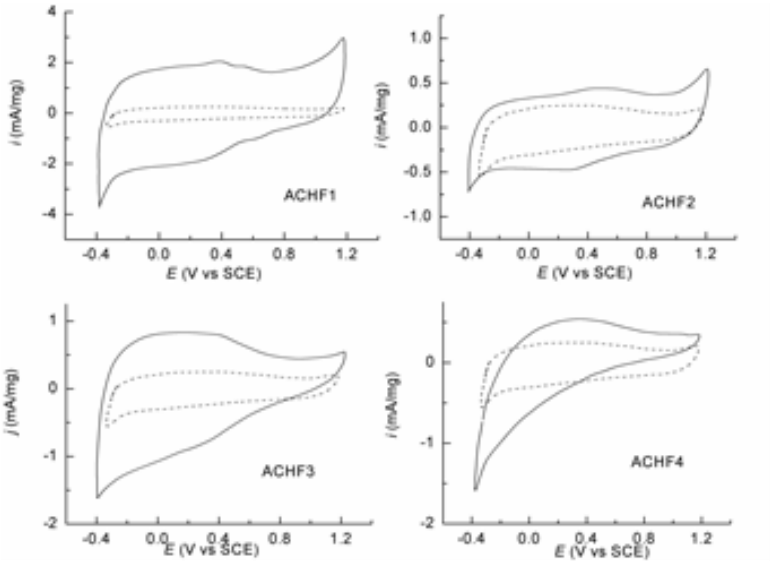

Figure: Cyclic voltamograms for carbon hollow fibers (CHF) - dash line; and activated with different agents – straight line

***Journal of Serbian Chemical Society,* 76 (2011) 1283-1294.**

Properties of SBA-15/carbon cryogel nanocomposites as a function of synthesis conditions

M. Kokunešoski, B. Matović, B. Babić

Institute of Nuclear Sciences Vinča, P. O. Box 522, 11000 Belgrade, Serbia

Ordered mesoporous silica SBA-15 materials were synthesized by using Pluronic P123 (non-ionic triblock copolymer, $EO_{20}PO_{70}EO_{20}$) as a template, under acidic condition. SBA-15/carbon cryogel composites were obtained by the sol-gel polycondenzation of resorcinol and formaldehyde, in the presence of different amount of SBA-15, followed by freeze drying, and subsequent pyrolysis. These materials were characterized by nitrogen adsorption-desorption measurements, X-ray diffraction and scanning electron microscopy. Samples have high specific surface area (350-520 m^2g^{-1}) developed meso- and microporosity and can be controlled by concentration of starting solution.

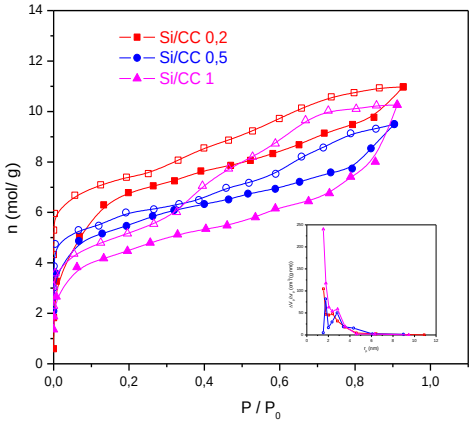

Figure: Nitrogen adsorption-desorption isotherms and BJH-PSD curves (inset) of composites Si/CC x (x = 0.2, 0.5, 1).

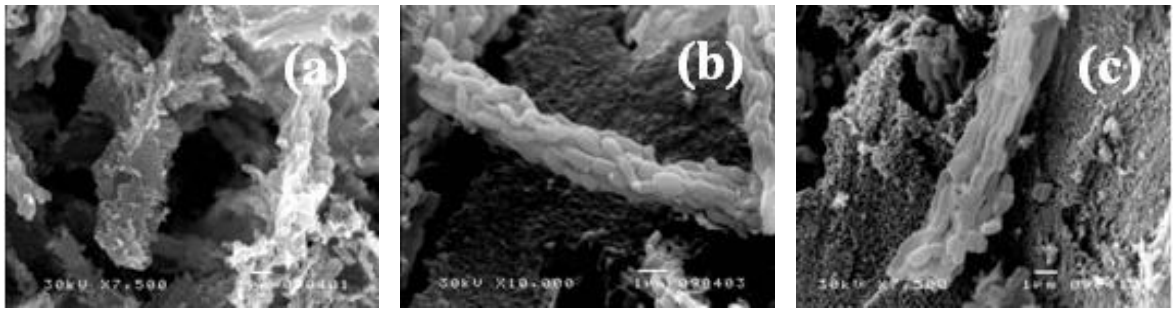

Figure: SEM images of composites Si/CC 0.2 (a), Si/CC 0.5 (b), and Si/CC 1 (c).

***1CSCS-2011*, March 17-18, 2011. Belgrade, Serbia, The Book of Abstracts pp. 41.**

Analysis of the interaction of pulsed laser with nanoporous activated carbon cloth

B. V. Kaludjerović,[1] M.S. Trtica,[2] B.B. Radak,[2] J. M. Stašić,[1] S. S. Krstić Mušović,[1] V.M. Dodevski[1]

[1]Laboratory of Material Science, Vinča, Institute for Nuclear Sciences, University of Belgrade, P.O. Box 522, 11001, Serbia
[2]Laboratory of Physical Chemistry, Vinča, Institute for Nuclear Sciences, University of Belgrade, P.O. Box 522, 11001, Serbia

Interaction of pulsed transversely excited atmospheric (TEA) CO_2-laser radiation at 10.6 mm with nanoporous activated carbon cloth was investigated. Activated carbon cloth of different adsorption characteristics was used. Activated carbon cloth modifications were initiated by laser pulse intensities from 0.5 MW/cm^2 to 28 MW/cm^2, depending on the cloth adsorption characteristics. CO_2 laser radiation is effectively absorbed by the used activated carbon cloth and largely converted into thermal energy. The type of modification depended on laser power density, number of pulses, but mostly on material characteristics such as specific surface area. The higher surface area of activated carbon cloth the higher damage threshold is.

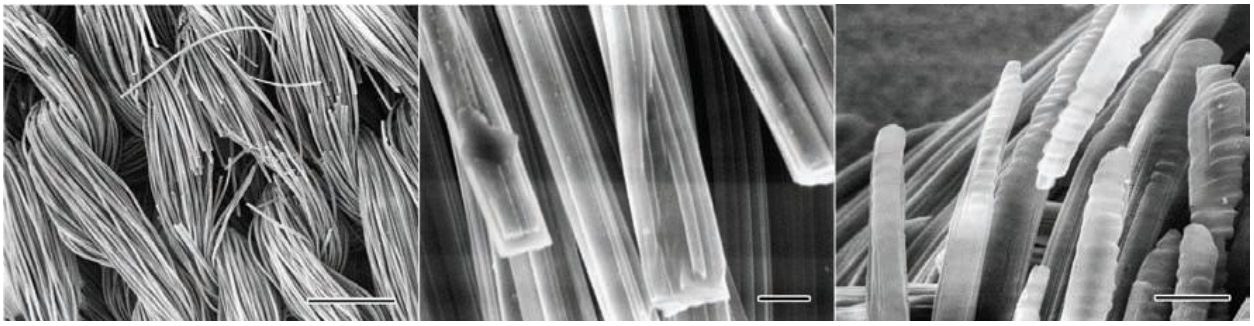

(a) (b) (c)

Figure: SEM micrographs of the damages in the ACC type A after interaction with: (a) 480 pulses, PPD =11.5 MW/cm^2, (b) 480 pulses, PPD=11.5 MW/cm^2, (c) 170 pulses, PPD=40 MW/cm^2

***Journal of Materials Science & Technolgy,* 27 [11] (2011) 979-984.**

Properties of SBA-15/carbon cryogel nanocomposites as a function of synthesis conditions

M. Kokunešoski, B. Matović, B. Babić

Institute of Nuclear Sciences Vinča, P. O. Box 522, 11000 Belgrade, Serbia

Ordered mesoporous silica SBA-15 materials were synthesized by using Pluronic P123 (non-ionic triblock copolymer, $EO_{20}PO_{70}EO_{20}$) as a template, under acidic condition. SBA-15/carbon cryogel composites were obtained by the sol-gel polycondenzation of resorcinol and formaldehyde, in the presence of different amount of SBA-15, followed by freeze drying, and subsequent pyrolysis. These materials were characterized by nitrogen adsorption-desorption measurements, X-ray diffraction and scanning electron microscopy. Samples have high specific surface area (350-520 m^2g^{-1}) developed meso- and microporosity and can be controlled by concentration of starting solution.

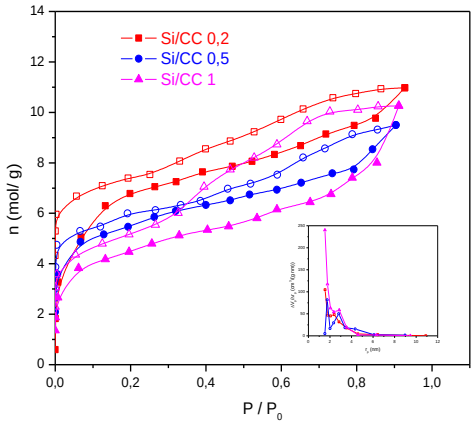

Figure: Nitrogen adsorption-desorption isotherms and BJH-PSD curves (inset) of composites Si/CC x (x = 0.2, 0.5, 1).

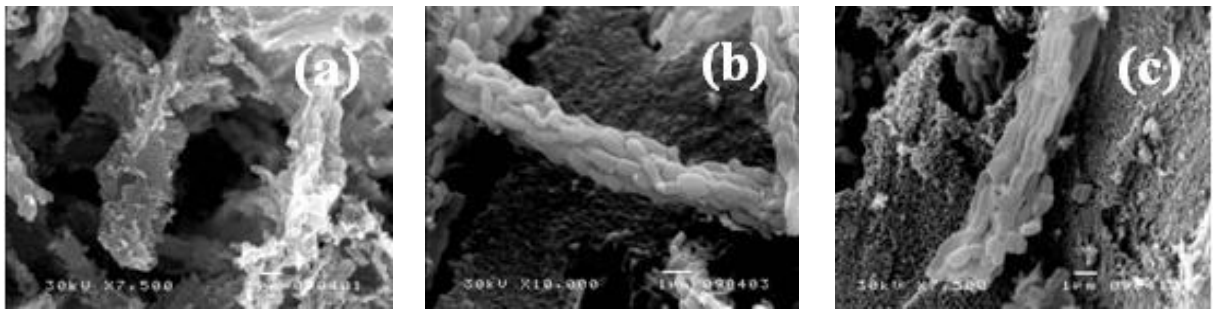

Figure: SEM images of composites Si/CC 0.2 (a), Si/CC 0.5 (b), and Si/CC 1 (c).

***1CSCS-2011*, March 17-18, 2011. Belgrade, Serbia, The Book of Abstracts pp. 41.**

Influence of chemical agents on the surface area and porosity of active carbon hollow fibers

Ljiljana M. Kljajević[1], Vladislava M. Jovanović[2], Sanja I. Stevanović[2], Žarko D. Bogdanov[1], Branka V.Kaluđerović[1]

[1]University of Belgrade, Vinča Institute of Nuclear Sciences, P. O. Box 522, 11001 Belgrade
[2]ICTM – Institute of Electrochemistry, University of Belgrade, P. O. Box 473,11000 Belgrade, Serbia

Active carbon hollow fibers were prepared from regenerated polysulfone hollow fibers by chemical activation using: disodium hydrogen phosphate 2-hydrate, disodium tetraborate 10-hydrate, hydrogen peroxide, and diammonium hydrogen phosphate. After chemical activation fibers were carbonized in an inert atmosphere. The specific surface area and porosity of obtained carbons were studied by nitrogen adsorption–desorption isotherms at 77 K, while the structures were examined with scanning electron microscopy and X-ray diffraction. The activation process increases these adsorption properties of fibers being more pronounced for active carbon fibers obtained with disodium tetraborate 10-hydrate and hydrogen peroxide as activator. The obtained active hollow carbons are microporous with different pore size distribution. Chemical activation with phosphates produces active carbon material with small surface area but with both mesopores and micropores. X-ray diffraction shows that besides turbostratic structure typical for carbon materials, there are some peaks which indicate some intermediate reaction products when sodium salts were used as activating agent. Based on data from the electrochemical measurements the activity and porosity of the active fibers depend strongly on the oxidizing agent applied.

Keywords: carbon hollow fibers; chemical activation; adsorption; cyclic voltammetry.

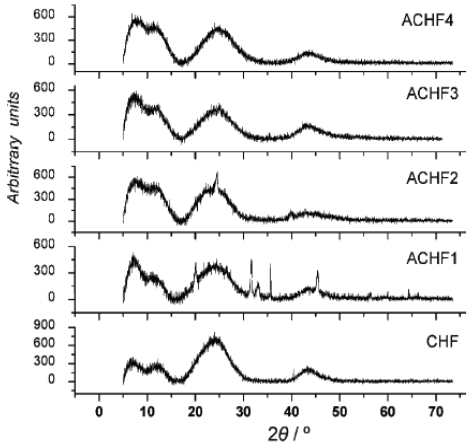

Figure: X-Ray diffraction patterns of the carbon hollow fibers (CHF) and those activated with different agents.

***Journal of Serbian Chemical Society,* 76 (9) (2011) 1283–1294.**

Enviromental protection

Vertical distribution of ^{226}Ra and radiological hazards indices of soil samples

Snežana S. Nenadović[1], Ljiljana M. Kljajević[1], Milos T. Nenadović[2], Mia O. Omerašević[1], Danijela R. Obradović Arsić[3], Milutin A. Ljesšević[3]

[1]Laboratory for Material Science, Institute of Nuclear Science Vinča, University of Belgrade, 522, 11001 Belgrade, Serbia
[2]Laboratory for Atomic Physics, Institute of Nuclear Science Vinča, University of Belgrade, Belgrade, Serbia
[3]Faculty of Geography, University of Belgrade, Belgrade, Serbia

The vertical distribution of ^{226}Ra was investigated in soils from the cultivated and undisturbed areas in Rudovci, municipality Lazarevac, Serbia. There were three profiles, each profile divided on four horizons, what gives 12 soil samples. The specific activity of ^{226}Ra in soil and sediment samples was determined by using the gammaspectrometric method. Analysis of the vertical soil profiles indicated that the activity of ^{226}Ra was not extremely changed with depth. To evaluate the radiological hazards of ^{226}Ra in the samples, the absorbed dose rate, the annual effective dose rate, the radium equivalent activity, and the external hazards index were calculated according to the UNSCEAR 2000 report.

Keywords: ^{226}Ra, Gamma-spectrometric method, Absorbed dose rate, Annual effective dose.

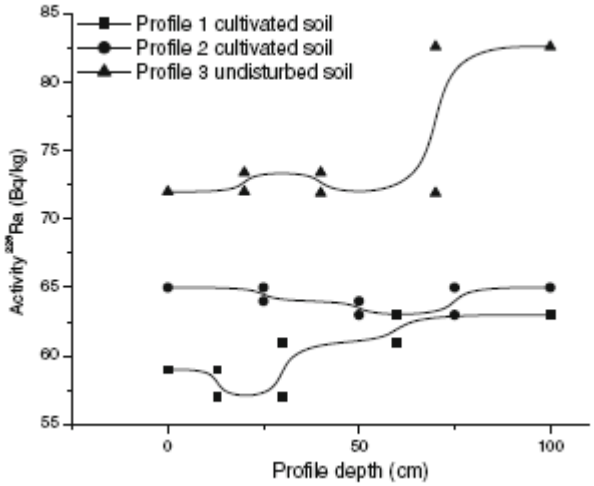

Figure: The vertical depending of ^{226}Ra activity with depth at all measuring sites.

***Journal of Radioanalytical and Nuclear Chemistry*, 290 (2011) 79–84.**

Radiological hazards of ^{137}Cs in cultivated and undisturbed areas

Snežana S Nenadović[1], Miloš T. Nenadović[2], Ivana S. Vukanac[3], Mia O. Omerašević[1], Ljiljana M. Kljajević[1]

[1]Laboratory for Material Science, Vinča Institute of Nuclear Science, University of Belgrade, Belgrade, Serbia
[2]Laboratory for Atomic Physics, Vinča Institute of Nuclear Science, University of Belgrade, Belgrade, Serbia
[3] Laboratory for Nuclear and Plasma Physics, Vinča Institute of Nuclear Science, University of Belgrade, Belgrade, Serbia

The exposure of human beings to ionizing radiation from ^{137}Cs is a continuing and inescapable feature of life on Earth. Artificial radionuclides are widely distributed in various geological formations and ecosystems such as rock, soil, ground water, and food stuffs. In the pres ents study, the dis tribution of ^{137}Cs was mea sured in soil samples collected from different lithological units of the Rudovci, Lazarevac, Serbia. Analysis of the vertical soil profiles indicated that the activity of ^{137}Cs was not extremely changed with depth. The activity concentrations of the ^{137}Cs in measured soil samples ranged from be low minimal detectable concentrations up to 38.1 Bq/kg. In order to evaluate the radiological hazards due to ^{137}Cs in the samples, the absorbed dose rate and the annual effective dose were calculated in accordance with recommendations given in the UNSCEAR 2000 report. The distribution of radionuclides de pends upon the rock composition, chemical and physical proper ties of the soil. The external absorbed gamma dose rates due ^{137}Cs were found to vary from 0 to 1.16 nGy/h.

Keywords: adsorbed dose rate, annual effective dose, ^{137}Cs, radiological hazards

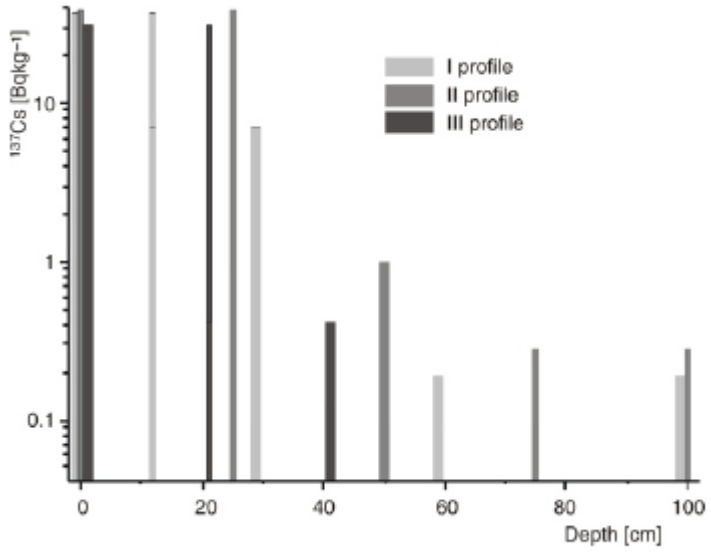

Figure: Vertical distribution of ^{137}Cs at tree examined profiles.

***Nuclear Technol ogy & Radiation Protection*, 26 [2] (2011) 115-118.**

Investigation of Cl^- and SO_4^{2-} anion absorption in natural soils

Snežana Nenadović[1], Miloš Nenadović[2], Ljiljana Kljajević[1], Milutin Lješević[3], Mia Omeragević[1], Branko Matović[1]

[1]Laboratory for Material Science, Institute for Nuclear Science Vinča, University of Belgrade, Belgrade, Serbia
[2]Laboratory for Atomic Physics, Institute for Nuclear Science Vinča, University of Belgrade, Belgrade, Serbia
[3]Faculty of Geography, University of Belgrade, Belgrade, Serbia

In this paper, the results of vertical migration of chloride and sulphate anions in soil are presented. The soil was contaminated with NaCl and $CuSO_4$. Anions migration were monitored during one hydrological year (425 days). The first sample was taken after 150 days and afterwards samples were taken every 50 days. Before the profile contamination physical and chemical analyses of soil have been done. The obtained results show that chloride concentration in soil was in the range from 0.67 mg/kg up to 11.92 mg/kg, while sulphate concentration was in the range from 0.65 mg/kg up to 9.79 mg/kg.

Keywords: natural soil, characterization, anion absorption.

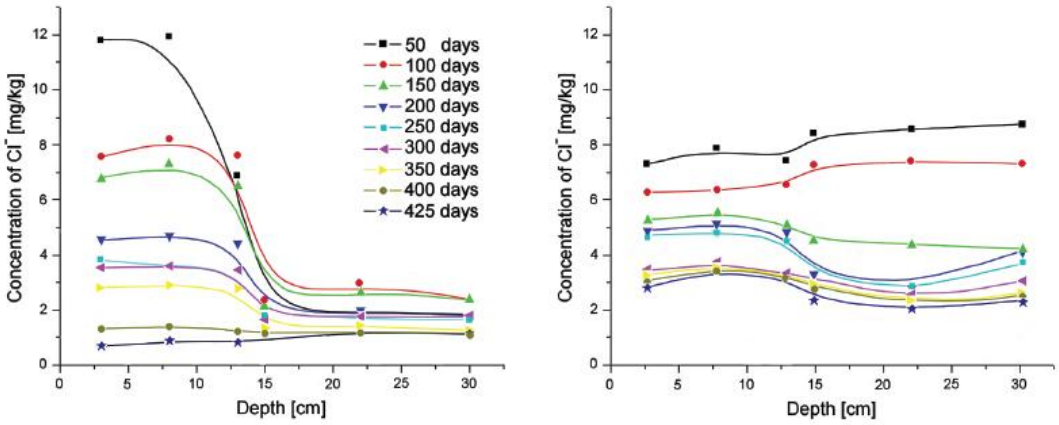

Figure: Anions dispersion in the soil: a) chloride and b) sulphate.

***Processing and Application of Ceramics*, 5 [2] (2011) 85–89.**

Influence of modified kaolin microstructure on its adsorption capacity for Cu(II)

Mia Omerašević[1], Uroš Jovanović[2], Jelena Pantić[1], Tamara Tuvić[2], Vladimir Pavlović[3], Snežana Nenadović[1], Branko Matović[1]

[1]Laboratory for Material Science, Institute of Nuclear Sciences Vinča, University of Belgrade, Belgrade, Serbia
[2]Laboratory of Chemical Dynamics and Permanent Education, Institute of Nuclear Sciences Vinča, University of Belgrade, Belgrade, Serbia
[3]Faculty of Agriculture, University of Belgrade, Belgrade, Serbia

The properties of metakaolin-based geopolymer are influenced by the microstructure and composition of initial kaolin, composition and relative amount of alkali activator used as well as the conditions during the initial period geopolymerization reaction. This study investigated the effect of microstructure changes caused by synthesis on adsorption properties of geopolymer samples. The microstructure of samples has been characterized by X-ray diffraction and scanning electron microscopy. The degree of metal adsorption was evaluated analyzing the Cu(II) contaminated samples by using AAS (Aanalyst 700/Perkin-Elmer). The results show the high degree impact of immobilization efficiency and microstructure on immobilization efficiency.

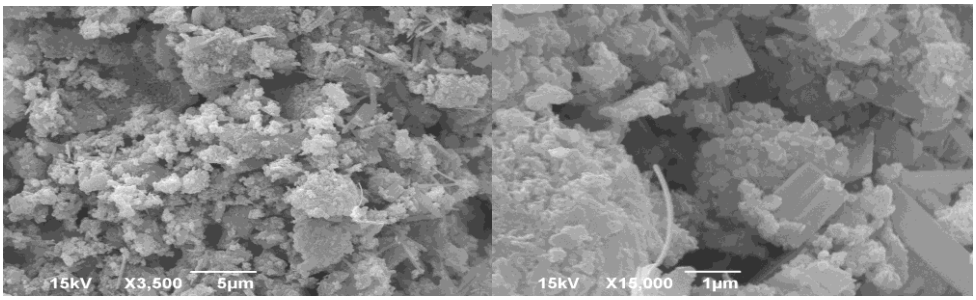

Figure: SEM micrograms of metakaolin based geopolymers.

***Tenth Young Researchers Conference-Materials Science and Engineering*, December 21-23, 2011, pp. 48.**

Investigation of Cl^- and SO_4^{2-} anion absorption in natural soils

Snežana Nenadović[1], Miloš Nenadović[2], Ljiljana Kljajević[1], Milutin Lješević[3], Branko Matović[1]

[1]Laboratory for Material Science, Institute of Nuclear Science Vinča, University of Belgrade, Belgrade, Serbia
[2]Laboratory for Atomic Physics, Institute of Nuclear Science Vinča, University of Belgrade, Belgrade, Serbia
[3]Faculty of Geography, University of Belgrade, Belgrade, Serbia

In this paper, the results of vertical chloride and sulphate anions migration in soil are presented. The soil was contaminated with NaCl and $CuSO_4$. Anions migartion were monitored during one hydrological year (425 days). First sample was taken after 150 days and next following sample was taken after 50 days. Before the profile contamination physical and chemical analisys of soil has been done. The obtained results shows that chloride concentration in soil was in the range from 0,67 $mgkg^{-1}$ up to 11,92 $mgkg^{-1}$, while sulphate concentration was in the range from 0,65 $mgkg^{-1}$ up to 9,79 $mgkg^{-1}$.

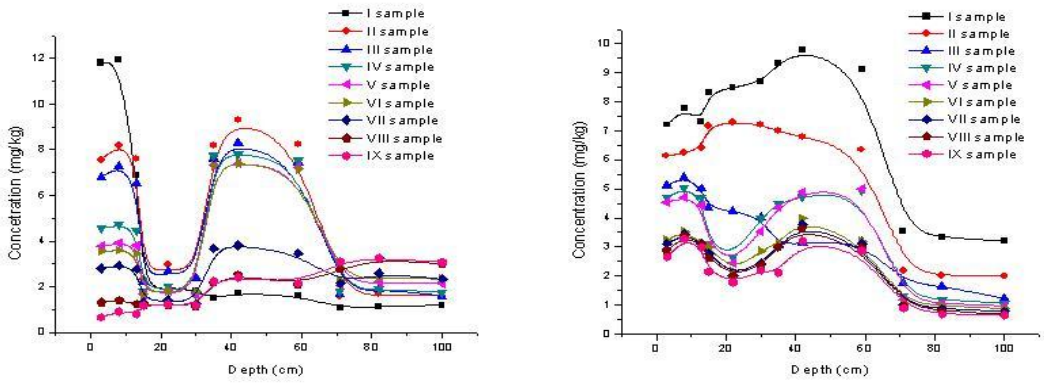

a) b)

Figure: Vertical distribution of Cl^- a) and SO_4^{2-} b) anions in the natural soil of the first profile.

1st Conference of the Serbian Ceramic Society **March 17th-18th 2011, Belgrade, Serbia, Proceedings & Book of abstracts, pp. 49.**

Advanced ceramics

Synthesis and characterization of ceria nanopowders

Branko Matovic[1], Jelena Zagorac[1], Zorana Docevic-Mitrovic[2], Biljana Babic[1], Marko Radovic[2], Snezana Boskovic[1], Zoran Popovic[2]

[1]Institute of Nuclear Sciences, Vinca,
[2]Institute of Physics, Belgrade, Serbia

Nanometric size ceria powder particles with fluorite-type structure were obtained by applying self-propagating room temperature methods. Powder properties such as specific surface area, crystallite and particle size and lattice parameters have been studied. Roentgen diffraction analysis (XRD), BET, SEM, TEM and Raman scattering measurements were used to characterize the samples at room temperature. Also, high temperature X-ray diffraction (up to 800°C) was used to follow grows of crystallites. It was found that average diameter of crystallites is in the range of 3-5 nm. However, these crystallites gradually grow with increasing heat temperature, changing the specific surface area from 105 m2/g to 20 m2/g. Williamson-Hall plots were used to separate the effect of the size and strain in the nanocrystals. The Rietveld refinement was employed for some samples to get the structural information of the synthesized powder. Raman spectra of temperature treated CeO2-y sample was analyzed using phonon confinement model. Best agreement between experimental values and numerical model for the sample heated at 400°C for 2 hours is obtained for the particle size of L0 = 9.5 nm. With further temperature increase, frequency of F2g mode increases and its linewidth decreases. Such a behavior can be explained with particle size increase and agglomeration during the temperature treatment. After the heat treatment at 800°C particle size reaches value larger than 20 nm. Second order Raman mode, which originates from intrinsic oxygen vacancies, disappears with annealing.

Keywords: nanopowder, CeO_2, XRD, raman spectroscopy

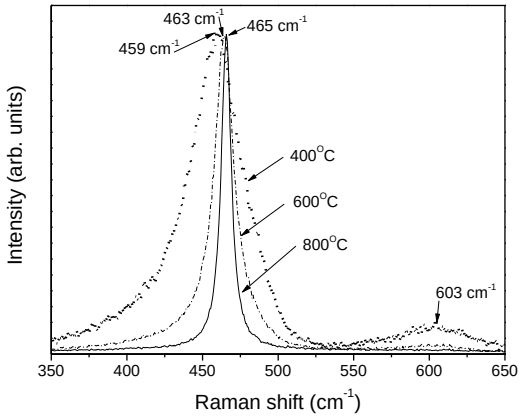

Figure: Room temperature Raman spectra of CeO_{2-y} samples after the heat treatment at different temperature for 15 min.

Proceedings of the *12th Conference of the European Ceramic Society – ECerS XII* Stockholm, Sweden – 2011.

Synthesis and characterization of (Ba,Yb) doped ceria nanopowders

Branko Matović, Jelena Pantić, Jelena Luković, Svetlana Ilić, Nadežda Stanković, Maja Kokunešovski, Miljana Miljević

Materials Science Laboratory, Institute for Nuclear Sciences Vinca, University of Belgrade, P.O. Box 522, Belgrade, Serbia

Nanometric size (Ba, Yb) doped ceria powders with fluorite-type structure were obtained by applying selfpropagating room temperature methods. Tailored composition was: $Ce_{0.95-x}Ba_{0.05}Yb_xO_{2-\delta}$ with fixed amount of Ba − 0.05 and varying Yb content "x" from 0.05 to 0.2. Powder properties such as crystallite and particle size and lattice parameters have been studied. Röntgen diffraction analyses (XRD) were used to characterize the samples at room temperature. Also, high temperature treatment (up to 1550 °C) was used to follow stability of solid solutions. The mean diameters of the nanocrystals are determined from the full width at half maxima (FWHM) of the XRD peaks. It was found that average diameter of crystallites is less than 3 nm. Williamson- Hall plots were used to separate the effect of the size and strain in the nanocrystals.

Keywords: ceria, XRD, solid electrolyte.

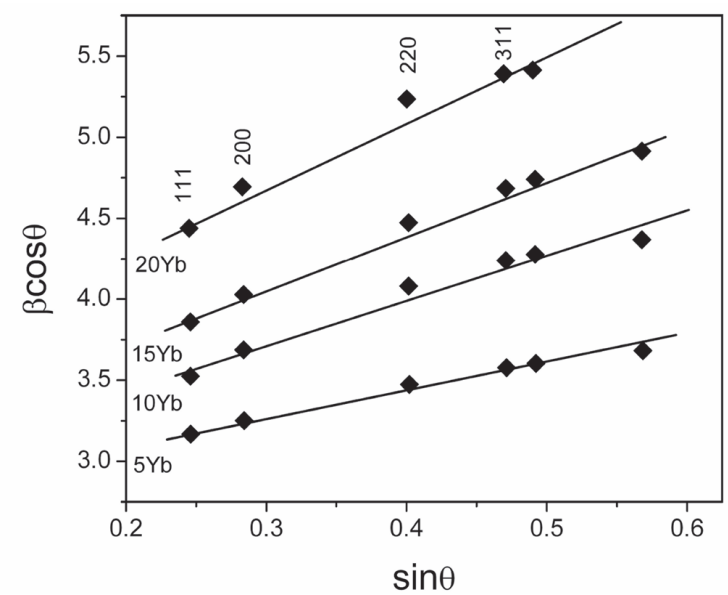

Figure: Williamson-Hall plot of the $Ce_{0.95-x}Ba_{0.05}Yb_xO_{2-\delta}$ powders with different Yb^{3+} content.

***Processing and Application of Ceramics*, 5 [2] (2011) 69–72.**

Synthesis and characterization of Cu- doped ceria nanopowders

B.Z. Matovic[1], S.B. Boskovic[1], M. Rosic[1], B.D. Babic[1], Z.D. Dohcevic-Mitrovic[2], M.B. Radovic[2], Z.V. Popovic[2]

[1]Institute of Nuclear Sciences Vinca, Materials Science Laboratory, Belgrade, Serbia
[2]Institute of Physics, Center for Solid State Physics and New Materials, Belgrade, Serbia

Nanopowdered solid solution $Ce_{1-x}Cu_xO_{2-\delta}$ samples ($0 \leq x \leq 0.15$) were synthesized by self-propagating room temperature synthesis (SPRT). XRD and Raman spectroscopy at room temperature were used to study the vibration properties of these materials as well as the Cu solubility in ceria lattice. Solubility limit of Cu^{2+} in CeO_2 lattice was found to be lower than published in the literature. Results show that obtained powders with low dopant concentration are solid solutions with a fluorite-type crystal structure. However, with Cu content higher than 7.5 %, the phase separation was observed and two oxide phases, CeO_2 and CuO, coexist. All powders were nanometric in size with high specific surface area.

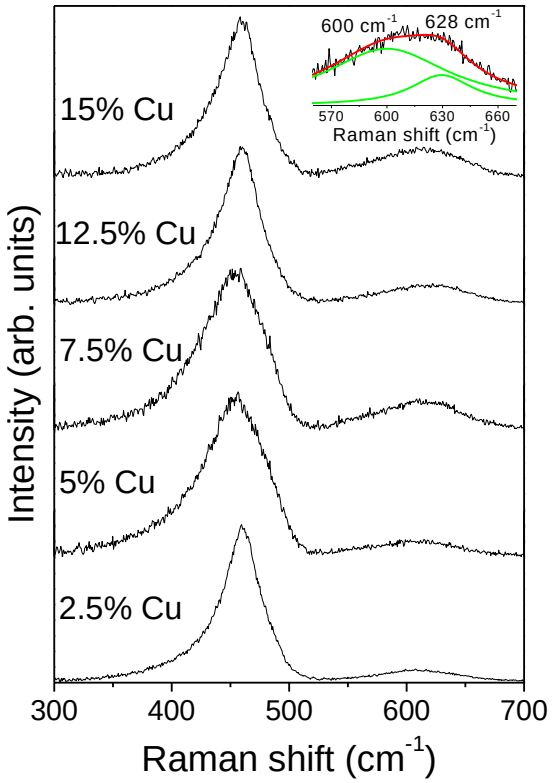

Figure: Room-temperature Raman spectra of $Ce_{1-x}Cu_xO_{2-\delta}$ nanopowders excited by 514 nm radiation from an argon ion laser.

***Ceramics International*, 37 [8] (2011) 3161-3165.**

Simple synthetic route of nanocrystalline boron nitride powder

B. Matovic[1], B. Babic[1], A. Devecerski[1], M. Radovic[2], A. Minovic[1], M. Miljkovic[3], S. Boskovic[1]

[1]Vinča Institute of Nuclear Sciences, Materials Science Lab, P.O. Box 522, 11001, Belgrade, Serbia
[2]Institute of Physics, 11080 Belgrade, Serbia
[3]Centre for Microscopy, Medical faculty Nis, Serbia

Nanocrystalline hexagonal boron nitride powder (h-BN) was synthesized by simple sol-gel polycondenzation of resorcinol and formaldehyde in the presence of boric acid followed by freeze-drying. Pirolysis and subsequent heat treatment of these cryogels resulted in formation of boron nitride powder. Characterization by nitrogen adsorption showed that precomposite cryogels and the BN powders were micro and mesoporous materials with high surface areas. Materials have been analyzed by means of X-ray diffraction, Raman scattering and electron microscopy methods.

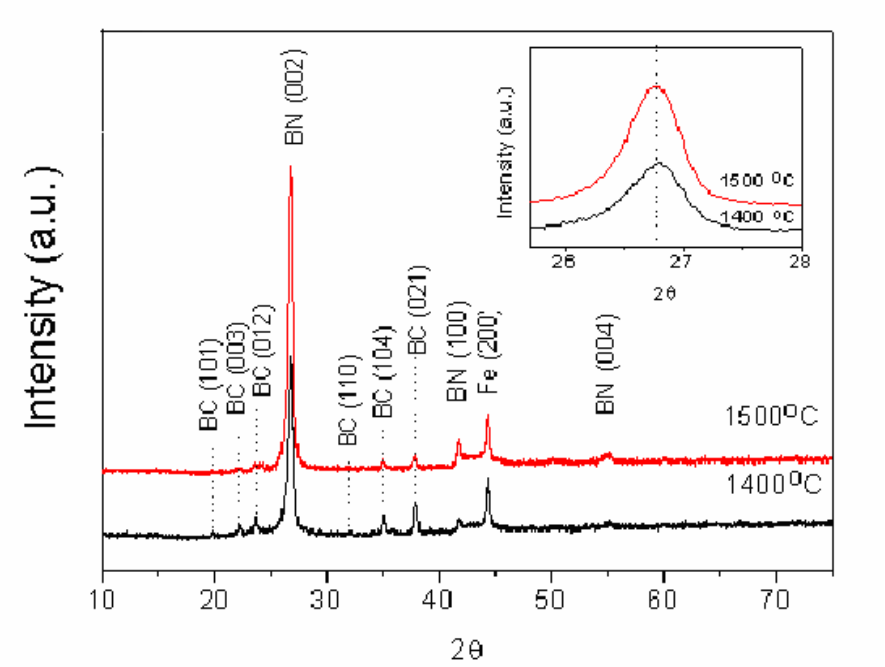

Figure: XRD patterns of BN samples obtained by annealing at 1400 and 1500 °C. BN (boron nitride), BC (boron carbide) and Fe (iron holder).

***Materials Letters*, 65 [2] (2011) 307-309.**

Synthesis, structural and magnetic properties of nanostructured $Ca_{0.9}Gd_{0.1}MnO_3$ obtained by modified glycine nitrate procedure (MGNP)

Milena Rosić[a], Mihovil Logar[b], Aleksandar Devečerski[a], Marija Prekajski[a], Ana Radosavljević-Mihajlović[a], Vladan Kusigerski[c], Vojislav Spasojević[c], Branko Matović[a]

[a]Laboratory for Material Science, Institute of Nuclear Sciences Vinča, University of Belgrade, P.O.Box 522, 11001 Belgrade, Serbia
[b]Faculty of Mining and Geology, University of Belgrade, Đušina 7, 11000Belgrade, Serbia
[c]Condensed Matter Physics Laboratory, Institute of Nuclear Sciences Vinča, University of Belgrade, P.O.Box 522, 11001 Belgrade, Serbia

$Ca_{0.9}Gd_{0.1}MnO_3$ nanopowders with perovskite type crystal structure were synthesized by modified glycine nitrate procedure. Nanopowders were prepared by combining glycine with metal nitrates and/or metal acetates in their appropriate stoichiometric ratios. Modification of the procedure was performed by partial replacement of nitrates by acetates, in order to control the burn-up reaction. Obtained $Ca_{0.9}Gd_{0.1}MnO_3$ powders were calcinated in the temperature interval from 850 ^oC to 950 ^oC for 10 min. Properties such as phase evolution, lattice parameters, chemical composition and magnetic properties were monitored by DTA, X-ray diffraction, SEM/EDS and magnetic measurements. Magnetic measurements performed at the sample with the smallest crystallite size showed that a 10% of Gd^{3+} substituted Ca^{2+} ions changes antiferromagnetic properties of $CaMnO_3$ by the introduction of ferromagnetic interaction due to a double exchange between Mn^{3+} and Mn^{4+} ions. Presence of competing interactions and their randomness lead to a formation of a spin glass state below Neel temperature TN = 110 K. From the high temperature magnetic susceptibility measurements effective magnetic moment of manganese ions is determined which lies between the values for Mn^{3+} and Mn^{4+} ions.

Keywords: Nanostructured materials; Spin glasses; Thermal analysis; Magnetic measurements

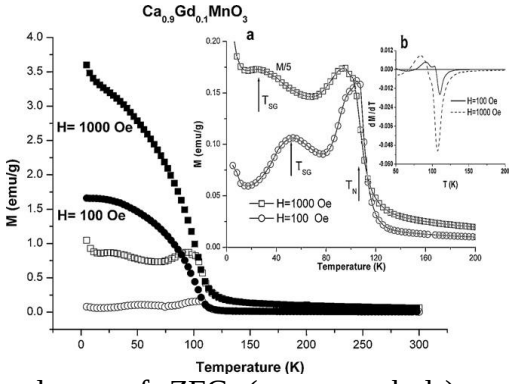

Figure: Temperature dependence of ZFC (open symbols) and FC magnetization (full symbols) of $Gd_{0.1}Ca_{0.9}MnO_3$ in different magnetic fields. Inset a: Details of ZFC magnetization; spin-glass transitions are denoted by arrows; magnetization recorded in 1000 Oe is divided by 5. Inset b: dM/dT derivate vs. T encompassing AF–P transition.

***Ceramics International*, 37 (2011) 1313–1319.**

Synthesis of nanocrystalline tungsten carbide

Jelena Luković[1], N. Stanković[1], M. Prekajski[1], J. Pantić[1], B. Matović[1], M.Kijevčanin[2], B. Babić[1]

[1]Institute of Nuclear Sciences Vinča, University of Belgrade, PO Box 522, 11001 Belgrade, Serbia
[2]Faculty of Technology and Metallurgy, University of Belgrade, Karnegijeva 4, 1100 Belgrade, Serbia

Nano-sized tungsten carbide (WC) was synthesized by thermical treatment of mixture of tungsten powder and carbon under an argon atmosphere. Different reaction condition: temperature, time of heating and C/W ratio were applied. It was found that longer retention time, higher temperature and higher W/C ratio contribute to disappearance of elementary W and production of different WxC mixtures. It was possible to obtain pure WC after eight-hour heat treatment at temperature of 1000 °C with C/W ratio 3. WC powders were characterized by X-ray diffraction, BET method and SEM. Very fine WC particles below 50 nm can be produced. Specific surface area obtained powder is 17 m^2/g.

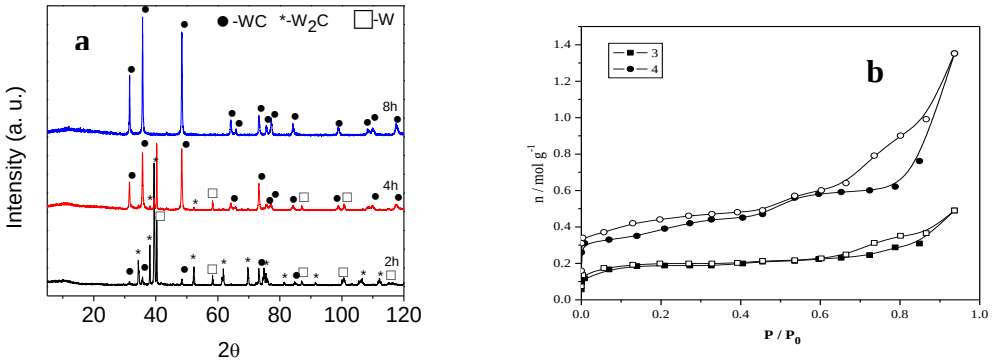

Figures: (a) effect of the retention time on the synthesis at constant temperature (1000 °C) and constant C/W molar ratio 3 (b) nitrogen adsorption isotherms, as the amount of N_2 adsorbed as function of relative pressure for powder obtained at 1000 °C for 8 h and with C/W molar ratio 3 and 4. Solid symbols-adsorption, open symbols-desorption.

***The Ninth Students' Meeting - SM2011*, November 16th-18th 2011, Novi Sad, Serbia, The Book of Abstracts, pp. 26.**

Synthesis and characterization of mullite

Svetlana Ilić, Slavica Zec, Dušan Bučevac, Ana Mihailović - Radosavljević, Biljana Babić, Branko Matović

Materials Science Laboratory, Institute of Nuclear Sciences - Vinča, University of Belgrade, P.O. Box 522, Belgrade, Serbia

Mullite is important material for ceramic applications due to excellent mechanical and thermal properties. In this study, synthesis of mullite ($3Al_2O_3 \cdot 2SiO_2$) powder by sol-gel combustion procedure was investigated. Synthesis was performed from ethanol-water solution of aluminium nitrate, TEOS and glycine as the fuel. The molar ratio of TEOS:Ethanol:Water = 1:20:40 was kept the same during the synthesis while the ratio of glycine:nitrate ions was varied (0.56 and 1). Besides, HNO_3 and NH_4NO_3 were used as the combustion aids. In all reaction mixtures amorphous products were obtained during combustion process and mullite was formed by their complete reaction at 1200 ºC for 4 hours. The phase identification and the characterization of crystal structure were performed by X-ray diffraction. According to the values of the mullite lattice parameters, the chemical composition corresponds to the 3/2 mullite with 62 mol. % of Al_2O_3. The average crystallite size of mullite powders was 40 nm.

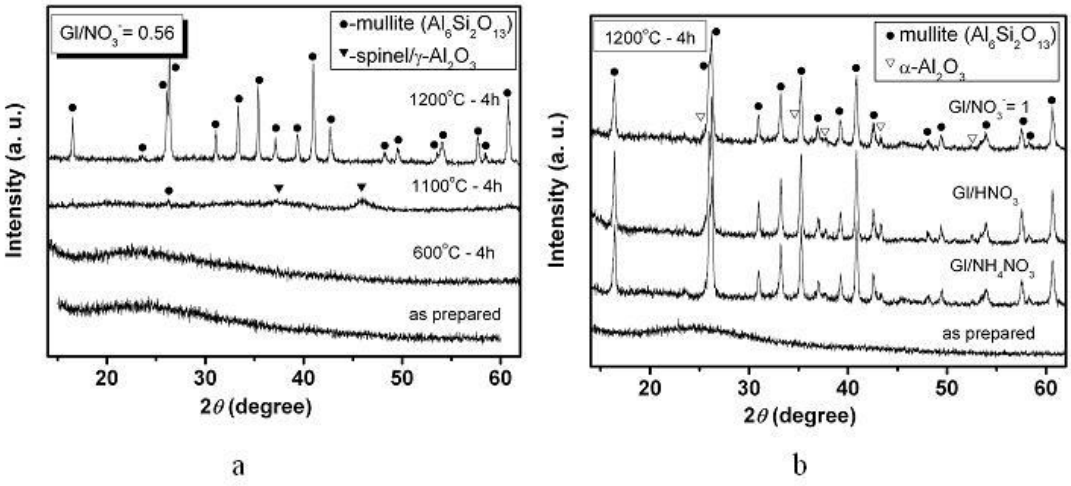

Figures: XRD patterns of (a) synthesized and thermally treated mullite ash and (b) mullite ashes synthesized with combustion aids.

***The 9th Student' Meeting SM-2011 and 2nd ESR COST MP0904 Workshop,* November, 16th-18th 2011, Novi Sad, Serbia, The Book of Abstracts, pp. 66.**

Influence of mechanical activation on sphene ceramic synthesis

Jelena Pantić[1], Marija Prekajski[1], Branko Matović[1], Ana Radosavljević Mihajlović[1],Aleksandar Kremenović[2], Mihovil Logar[2]

[1]Department of material science, INN VINCA, Belgrade, Serbia
[2]Faculty of Mining and Geology, University of Belgrade, Belgrade, Serbia

Sphene ($CaTiSiO_5$), a calcium titanosilicate ceramic has been prepared from a powder mixture of $CaCO_3$, TiO_2 and SiO_2 using vibro-miling for homogenization and activation precursors. The mechanochemical process initially yielded amorphous powders, which on further calcination, crystallized to yield sphene ceramic. The evolution of the phase composition with thermal treatment was investigated by X-ray powder diffraction (XRPD) and thermal analyses (DTA-TGA). Powder morphology and particle size distribution were analyzed by scanning electron microscopy (SEM) and laser diffraction, respectively. Optical dilatometry was used to measure the shrinkage behaviors of green bodies. The Rietveld refinement was employed to get the structural information of the synthesized powder. Densification and microstructure evolution was determined by means of density and scanning electron microscopy (SEM) measurement.

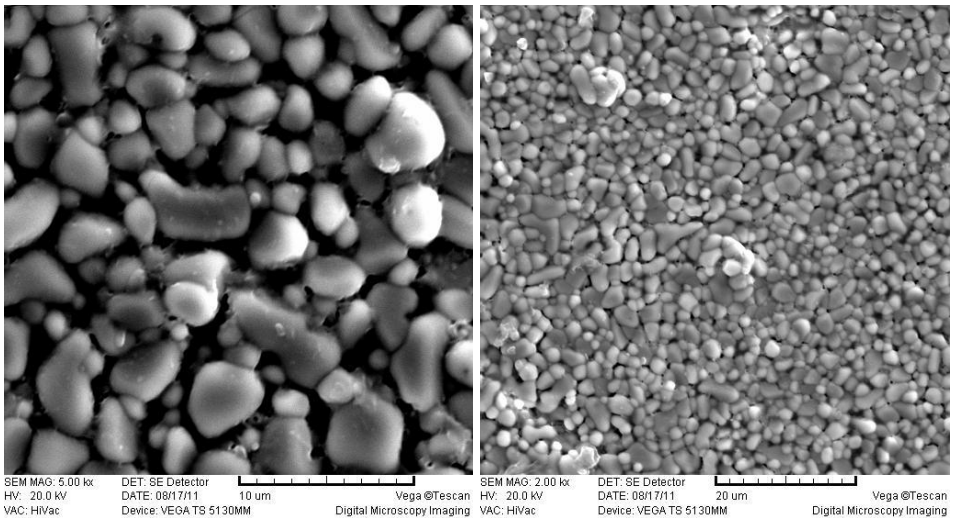

Figure: SEM micrographs at different magnification of sample heated at 1250 °C, with grinding time of 30min.

***VII International Conference on Mechanochemistry and Mechanical Alloying INCOME 2011*, August 31-September 3, 2011, Herceg Novi, Montenegro, book of abstracts, pp. 52.**

Nanocrystalline CeO_2-Bi_2O_3 solid solutions

Prekajski, M.[1], Dohčević-Mitrović, Z.[2], Babić, B.[1], Bučevac, D.[1], Logar, M.[3], Kremenović, A.[1], Matović, B.[1]

[1]Institute of Nuclear Science Vinca, University of Belgrade, 11001 Belgrade, Serbia
[2]Institute of Physics, Pregrevica 118, 11080 Belgrade, Serbia
[3]Faculty of Mining and Geology, Laboratory for Crystallography, University of Belgrade, Djusina 7, 11000 Belgrade, Serbia

A series of nanocrystalline solid solutions CeO_2-Bi_2O_3 were synthesized by applying the method based on self-propagating room temperature reaction (SPRT) between bismuth and cerium nitrates and sodium hydroxide. X-ray powder diffraction (XRPD) and Rietveld's structure refinement method was applied to characterize prepared powder and its microstructure (size-strain). Raman spectral studies conformed that obtained powder is single phase. Differencial termal analysis (DTA) and scaning electron microscopy (SEM) were also employed to characterize optained powders. Sintering of opatained samples was followed by optical dilatometry. Specific surface area of obtained powder was measured by Brunauer-Emmet-Teller (BET) method.

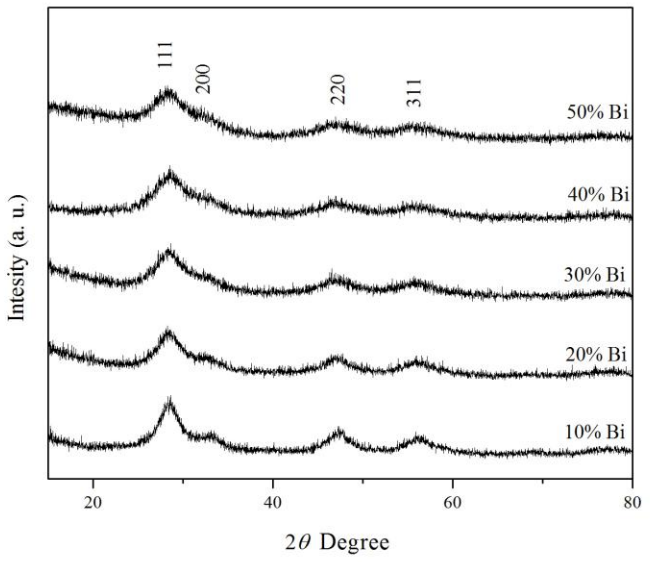

Figure: X-ray diffraction patterns of $Ce_{1-x}Bi_xO_{2-\delta}$ powders (x=0.1, 0.2, 0.3, 0.4 and 0.5)

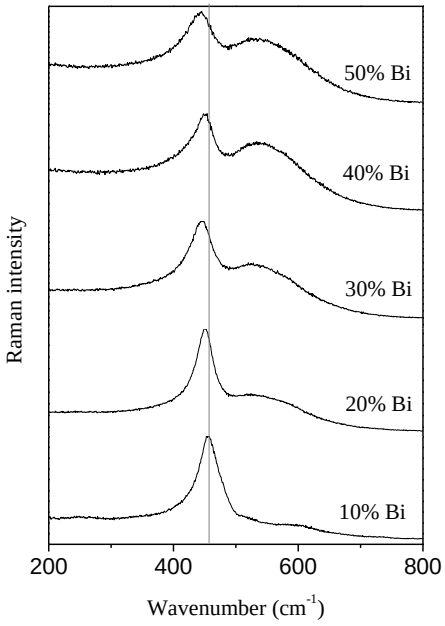

Figure: Raman spectra of bismuth ceriom oxide solid solution

Advanced Research Workshop "Engineering Ceramics 2011" from Materials to Components, Smolenice Castle, Slovakia, May 08 - 12, 2011, The Book of Abstracts pp. 94.

Synthesis and characterization of CeO_2-Bi_2O_3 solid solution

M. Prekajski[a], Z. Dohčević- Mitrović[b], M. Radović[b], B. Babić[a], J. Pantić[a], A. Kremenović[c], B. Matović[a]

[a]Department of material science, INN Vinca, Mihajla Petrovica-Alasa 12-14, POB 522, 11001 Belgrade, Serbia;
[b]Institute of Physics, Pregrevica 118, POB 68, 11080 Belgrade, Serbia;
[c]Faculty of Mining and Geology,University of Belgrade, Djusina 7, 11000 Belgrade, Serbia

Nanocrystalline powders of solid solution CeO_2 - Bi_2O_3 were synthesized by self-propagating room temperature reaction (SPRT) procedure with composition ($Ce_{1-x}Bi_xO_{2-\delta}$ where the x = 0.1 - 1). X-ray diffraction analyses show that for x < 0.50 a solid solution with fluorite structure is formed. Rietveld's structure refinement method was applied to characterize prepared powder and its microstructure (size-strain). The lattice parameters increase according to Vegard's law with increasing of Bi concentration. The average crystal size is about 2 - 3 nm. Spectroscopic ellipsometry and Raman scattering measurements were used to characterize the samples at room temperature. The Raman measurements demonstrated electron molecular vibrational coupling and increase of oxygen vacancy concentration whereas doping provokes a small decrease of optical absorption edge in comparison with pure ceria. Specific surface area of obtained powder was measured by Brunauer-Emmet-Teller (BET) method.

Keywords**:** Self-propagating reaction; X-ray methods; CeO_2; Bi_2O_3;

Table: Refined structural and microstructural parameters for $Ce_{1-x}Bi_xO_{2-\delta}$ samples (x=0.1, 0.2, 0.3, 0.4 and 0.5) and corresponding agreement factors.

Sample	*a* (Å)	Crystallite size (nm)	Strain ($\cdot 10^3$Å)	R_p(%)	χ^2
$Ce_{0.9}Bi_{0.1}O_{2-\delta}$	5.4370(2)	3.60(1)	172.1078	6.10	1.02
$Ce_{0.8}Bi_{0.2}O_{2-\delta}$	5.4470(1)	3.90(6)	214.7329	9.76	1.07
$Ce_{0.7}Bi_{0.3}O_{2-\delta}$	54575(1)	3.92(3)	289.9243	7.66	1.07
$Ce_{0.6}Bi_{0.4}O_{2-\delta}$	5.4640(2)	2.58(1)	350.6067	7.12	1.00
$Ce_{0.5}Bi_{0.5}O_{2-\delta}$	5.4920(2)	3.41(5)	385.0829	9.72	1.24

***XVIII Conference of the Serbian Crystallographic Society*, Andrevlje, Serbia, The Book of Abstracts pp. 30-31.**

Mesoporous CeO_2 nnaopowders with different particle sizes

Z. Dohčević-Mitrović[1], A. Golubović[1], M. Radović[1], V. Fruth[2], A. Kremenović[3], A. Meden[4], B. Babić[5], M. Šćepanović[1], Z. V. Popović[1]

[1]Center for Solid State Physics and New Materials, Institute of Physics, University of Belgrade, Serbia
[2]Institute of Physical Chemistry, Romanian Academy, Romania
[3]Faculty of Mining and Geology, Laboratory for Crystallography, University of Belgrade, Serbia
[4]University of Ljubljana, Faculty of Chemistry and Chemical Technology, Ljubljana, Slovenia
[5]Institute of Nuclear Sciences Vinc˘a, University of Belgrade, Serbia

Ultrafine porous cerium dioxide nanopowders were synthesized by relatively new and cost-effective hydrothermal method varying the main synthesis parameters, temperature of calcination and type of basic solution. Characterization of the as-produced powders was performed by X-ray diffraction (XRD), atomic force microscopy (AFM), Raman scattering and Brunauer-Emmett-Teller (BET) method. This study reveals that difference in synthesis parameters has strong influence on the particle size, surface area, and pore size distribution enabling the more precise control of material properties very important for catalytic and nanosensor applications.

Keywords: Catalysts, Nanosensors, Hydrothermal synthesis, Mesoporous ceria, Structural properties.

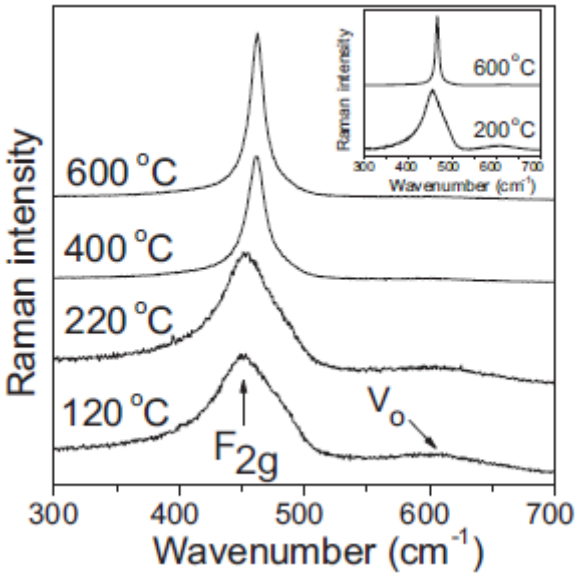

Figure: Room-temperature Raman spectra of the first series of CeO_2 samples. Inset presents the Raman spectra of the second series synthesized from NH_4OH solution.

***Phys. Status Solidi A*, 208 (2011) 1399-1402.**

Raw materials and heritage

Pillared clays as digestive tract MRI contrast agents

Mia Omeragević[1], Draško Vidojević[2], Marko Daković[3], Milos Mojovic[3]

[1] Department of material science, INN Vinca, Serbia
[2]Institute of Oncology and Radiology of Serbia, Pasterova 14, Belgrade, Serbia
[3]Faculty of Physical Chemistry, University of Belgrade, Studentski trg 12-16, Belgrade, Serbia

Gastrointestinal tract MRI generally gives poor results because of the lack of suitable contrast agents. Today's obtainable paramagnetic-based contrasts show side effects like the presence of artifacts arising from clumping, black bowel and diarrhea.
In this MRI study we propose the usage of the pillaring method for paramagnetic metal encapsulation in bentonite, showing that iron-pillared bentonites could be successfully used as MRI contrast agents, altering the longitudinal and transverse relaxation times of fluids in contact with the clay minerals. Relaxation effects of synthesized samples were compared with the clay minerals. Relaxation effects of synthesized samples were compared with the effects of Gd-DTPA contrast and commercial clays such Smecta and green clay.

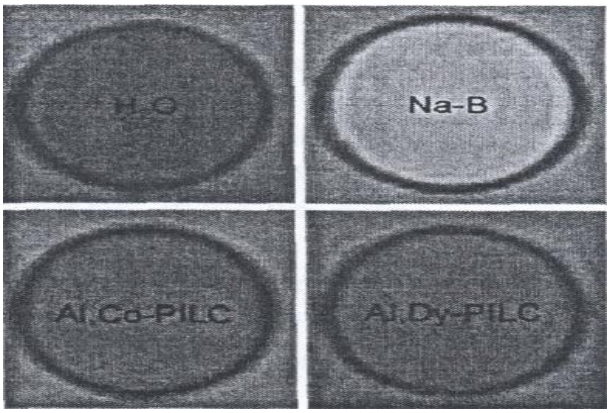

Figure: MRI T1W images of different clay samples

***1st Conference of the Serbian Ceramic Society,* March 17-18, 2011, Belgrade, Serbia, Program & The Book of Abstracts, pp. 53.**

Natural $CaO\text{-}TiO_2\text{-}SiO_2$ based ceramics

Jelena Pantić[1], Volker Kahlenberg[2], Vesna Poharc-Logar[3], Aleksandar Kremenović[3]

[1]Department of Material Science, INS Vinca, University of Belgrade, P. O. Box 522, Belgrade, Serbia
[2]Institut für Mineralogie & Petrographie, Universität Innsbruck, Innrain 52, Austria
[3]Faculty of Mining and Geology, University of Belgrade, Djušina 7, Belgrade, Serbia

Lešnica river deposits consist of a large number of minerals of different grain sizes including sphene. Since it is very difficult to obtain pure monophase titanite by different synthetic routes (sol-gel, coprecipitation, combustion, spray pyrolysis and hydrothermal method), the aim of this work was to study the structure of the sphene from the Lešnica river deposits and possibility of using it as a natural precursor for $CaO\text{-}TiO_2\text{-}SiO_2$ based ceramics. The sphene from Lešnica was analyzed by different methods: tristimulus colorimetry, infrared spectroscopy, electron microprobe and X-ray single crystal diffraction. It was confirmed that Al, Fe, Mn and P are present in the sphene structure and proposed that corresponding structural formula could be:
$(Ca^{2+}_{1.008}Mn^{2+}_{0.002})_{1.010}(Ti^{4+}_{0.901}Fe^{3+}_{0.033}Al^{3+}_{0.060}P^{5+}_{0.001})_{0.995}Si^{4+}_{1.024}O^{2-}_{5}$.

Keywords: sphene, natural precursor, structure analysis.

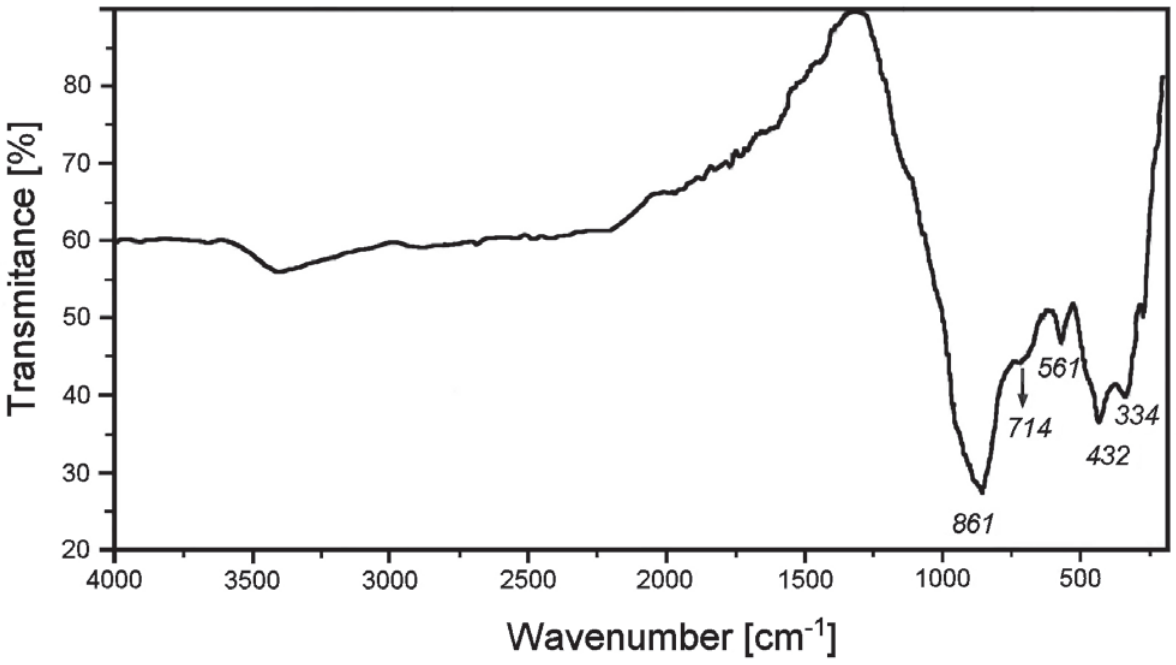

Figure: Infrared spectrum of sphene.

***Processing and Application of Ceramics,* 5 [2] (2011) 79–84.**

Characterization of bentonite clay from "Greda" deposit

Nadežda Stanković[1], Mihovil Logar[2], Jelena Luković[1], Jelena Pantić[1], Miljana Miljević[1], Biljana Babić[1], Ana Radosavljević-Mihajlović[1]

[1]Department of Material Science, Vinča Institute of Nuclear Sciences, University of Belgrade, P.0. Box 522, 11001 Belgrade, Serbia
[2]Faculty of Mining and Geology, University of Belgrade, Djušina 7, 11000 Belgrade, Serbia

Based on mineralogical and technological investigations of the deposit "Greda" important characteristics of bentonite clay were determined. Representative samples of the deposit were characterized with X-ray diffraction, low-temperature nitrogen adsorption, chemical analysis, differential thermal analysis and scanning electron microscopy. It was determined that the main mineral is montmorillonite and in subordinate quantities kaolinite, quartz and pyrite. The chemical composition generally shows high silica and alumina contents in all samples and small quantities of Fe^{3+}, Ca^{2+} and Mg^{2+} cations. Based on technological and mineralogical research, bentonite from this deposit is a high-quality raw material for use in the ceramic industry.

Keywords: bentonite, structural characterization.

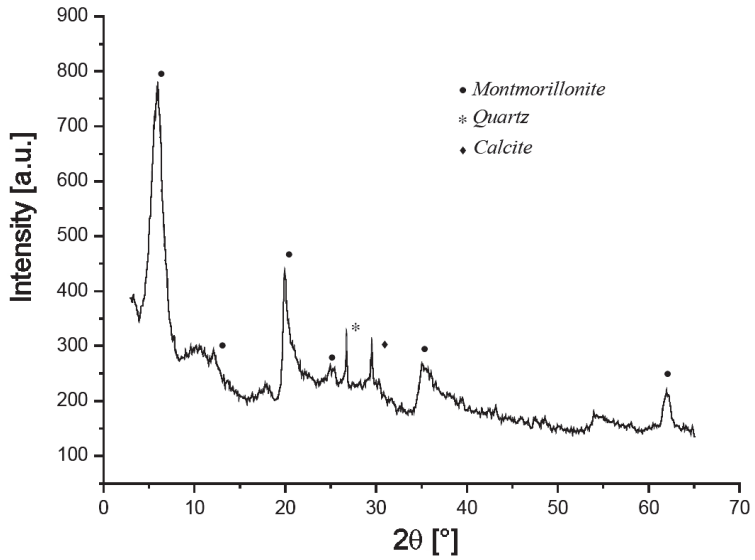

Figure: XRPD diagram of initial raw bentonite from deposit Greda.

***Processing and Application of Ceramics,* 5 [2] (2011) 97–101.**

Structure of sphene monocrystals from Lešnica river deposits on Cer mountain

Jelena Pantic[a], Volker Kahlenberg[b], Vesna Poharc-Logar[c], Aleksandar Kremenovic[c]

[a]Department of Material science, INN Vinca, P. O. Box 522, Belgrade, Serbia
[b]Institut für Mineralogie & Petrographie, Universität Innsbruck, Innrain 52, Innsbruck, Austria
[c]Faculty of mining and Geology, University of Belgrade, Djušina7, Belgrade, Serbia

River drift Lešnica, from which sphene crystals are separated for analysis, consists of a large number of minerals of different grain size. Sphene was found in a fraction of the grain size of 0.25 mm to 0.5 mm in association with garnet, apatite, cassiterite, zircon and other minerals.
Sphene was analyzed by different methods. Density was measured by pycnometer, the color was determined by tristimulus colorimetry, vibrations were analyzed by infrared spectroscopy while chemical composition was analyzed by electron microprobe. In the end crystal structure of sphene was determined by X-ray single crystal diffraction. The structure was refined in space groups *C*2/*c* and the $P2_1/c$, and then transformed into the new space groups *A2/a* and $P2_1/a$. For the graphical representation of the complete structure computer program *ATOMS* was used.
The experimental results are comparable to those of sphene from Grisoms, Switzerland, because of chemical similarities. The distances Ti-O, Si-O Ca-O in space group *A*2/*a* show good agreement with literature data, which is not the case with structure model described in the space group $P2_1/a$ due to lack of displacement of the Ti atom from the geometric center of the Ti octrahedra. On the basis of the statistical indicators of the quality of the refinement (R-value, Goof, residual electron density on differential Fo-Fc map), the structure for this sphene was established in the space group $P2_1/a$.
Structural formula obtained from electron microprobe is taken to be:
$(Ca^{2+}_{1,008}Mn^{2+}_{0,002})_{1,010}\ (Ti^{4+}_{0,901}Fe^{3+}_{0,033}Al^{3+}_{0,060}P^{5+}_{0,001})_{0,995}Si^{4+}_{1,024}O^{2-}_{5}$.

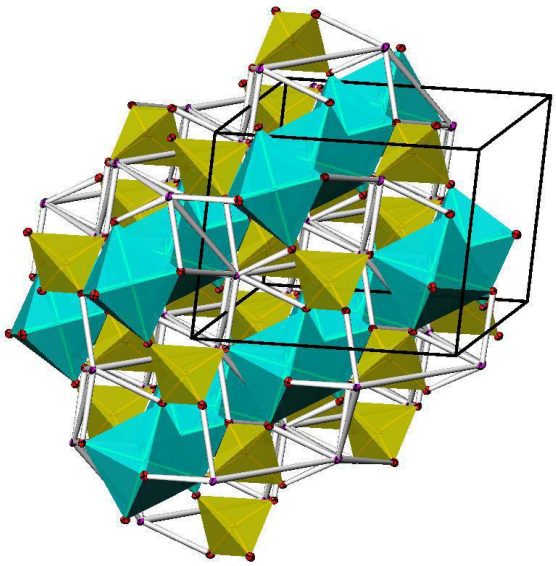

Figure: Unit cell for *sphene2* $P2_1/a$ (ATOMS).

***XVIII Conference of the Serbian Crystallographic Society*, 02-04.06.2011., Andrevlje, Serbia, The Book of Abstracts, pp. 48.**

SiC synthesis using domestic mineral resources

Aleksandar Devečerski[1], Milica Pošarac[1], Adela Egelja[1], Milena Rosić[1], Tatjana Volkov-Husović[2], Branko Matović[1]

[1]Institute for Nuclear Sciences Vinca, University of Belgrade, P.O. Box 522, Belgrade, Serbia
[2]Faculty of Technology and Metallurgy, University of Belgrade, Karnegijeva 4, P.O. Box 3503, Belgrade, Serbia

The possibility of using domestic Mg-silicate (sepiolite, white) as Si source and novolac resin (as carbon source), for synthesis of fine β-SiC powder at relatively low temperatures (1673−1873 K), was demonstrated. Obtained SiC powders consist of fine β-SiC particles and did not retain the fibrous morphology of starting sepiolites. Carbothermal reduction process, which was used in this study, is greatly influenced by catalyst addition ($FeCl_3$, FeSi). In order to obtain pure SiC powders, it is necessary to completely remove all Mg-species, and catalytical influence of Fe is attributed to FeSi important role in reduction of Mg_2SiO_4 and MgO into $Mg_{(g)}$. Formation of SiC whiskers is observed only in samples with Fe introduced in form of iron-silicide (FeSi).

Keywords: SiC; sepiolite; carbothermal reduction; Mg-silicate

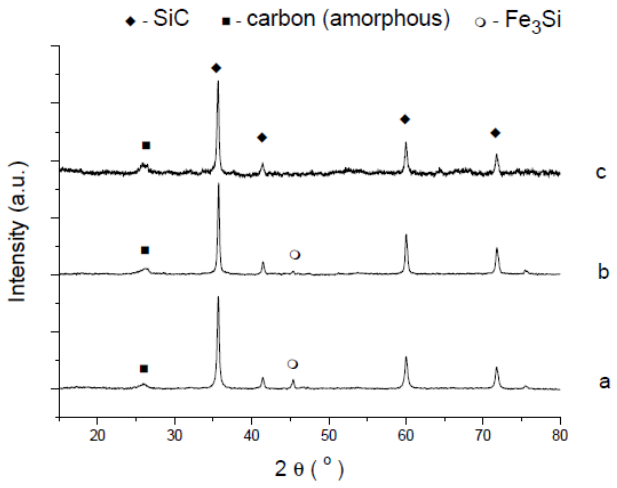

Figure: XRD patterns of samples: a) sepiolite/novolac/FeSi at 1673 K, b) sepiolite/ novolac/Fe at 1773K and c) sepiolite/novolac at 1873K.

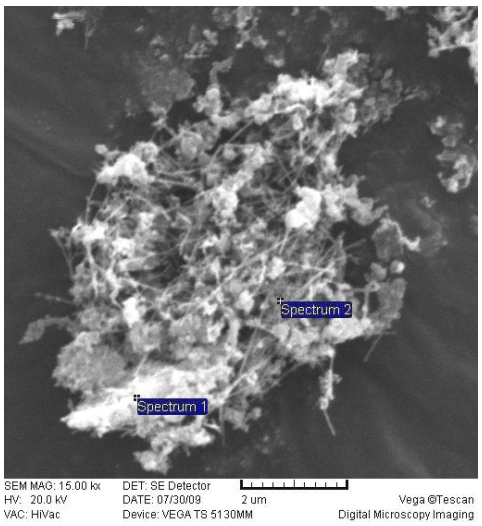

Figure: SEM micrograph of sepiolite/FeSi/novolac sample heat treated at 1673 K.

Table: Phase composition of samples heat-treated at different temperatures

Sample	*1673 K*	*1773 K*	*1873 K*
Sepiolite + novolac	SiC, F, E	SiC, MgO	SiC
Sepiolite + Fe + novolac	SiC, F, E, S	SiC, S	SiC, S
Sepiolite + FeSi + novolac	SiC, S	SiC, S	SiC, S

E-enstatite; F-forsterite; S-suessite

***Processing and Application of Ceramics*, 5 [2] (2011) 63-67.**

Preparation Comparison of structural, textural and thermal characteristics of pure and acid treated bentonites from Aleksinac and Petrovac (Serbia)

Zorica P. Tomić[a], Vesna P. Logar[b], Biljana M. Babić[c], Jelena R. Rogan[d], Petre Makreski[e]

[a]Faculty of Agriculture, Institute of Soil and Melioration, Belgrade University, 11080 Belgrade, Serbia
[b]Faculty of Mining and Geology, Belgrade University, 11000 Belgrade, Serbia
[c]Vinča Institute of Nuclear Sciences, P.O. Box 522, 11000 Belgrade, Serbia
[d]Department of General and Inorganic Chemistry, Faculty of Technology and Metallurgy, University of Belgrade, Karnegijeva 4, 11000 Belgrade, Serbia
[e]Institute of Chemistry, Faculty of Science, SS. Cyril and Methodius University, Arhimedova 5, 1000 Skopje, Macedonia

Bentonite samples collected from vicinity of Petrovac and Aleksinac were treated with different sulfuric acid molarities. Acid attack dissolved the octahedral sheets by interlayer and edge attack. The effects of the H_2SO_4 acid caused an exchange of Al^{3+}, Fe^{3+} and Mg^{2+} with H^+ ions leading to a modification of the smectite crystalline structure. The Mg and Fe substitution in the octahedral sheets promoted the dispersion of corresponding layers and formation of amorphous silicon. The activated bentonites, after the treatment of sulfuric acid, exhibited a lower cation-exchange capacity (CEC) and significant increase of specific surface area from 6 to 387 $m^2\ g^{-1}$ (bentonite from Petrovac) and from 11 to 306 $m^2\ g^{-1}$ (bentonite from Aleksinac). The acid reaction caused a splitting of particles within the octahedral sheet which led to an increase in specific surface area and decrease in CEC in both bentonites.

Keywords: Bentonite, Acid activation, Smectite, Cation exchange capacity, Specific surface area

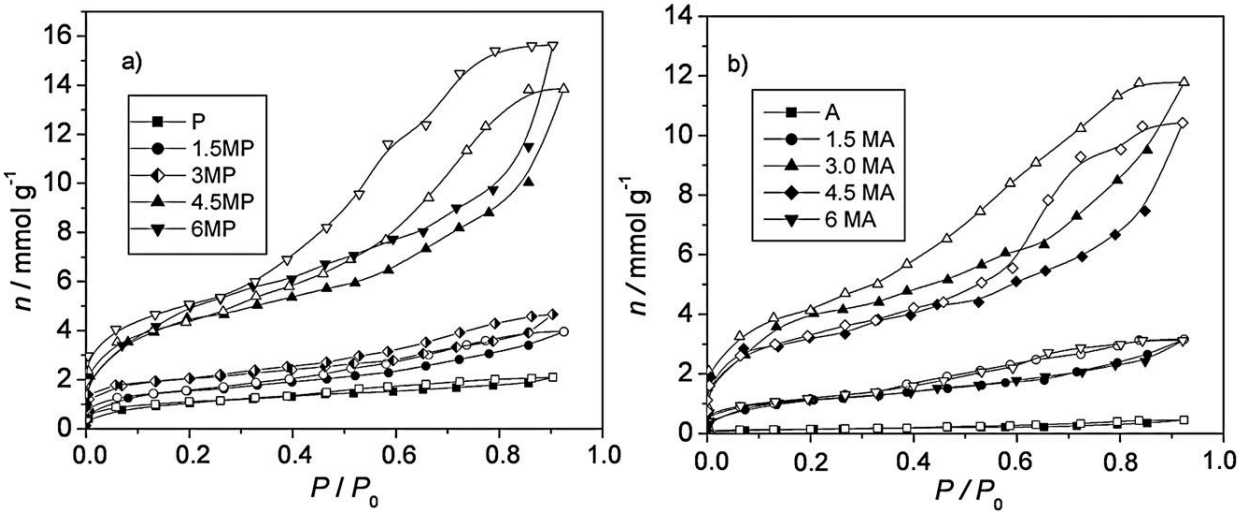

Figure: The adsorption isotherms of nitrogen on the untreated and treated P (a) and A (b) bentonites (solid symbols – adsorption, empty symbols – desorption).

***Spectrochimica Acta Part A*, 82 (2011) 389 – 395.**

Functional ceramics

Nb-TiO_2 supported platinum nanocatalyst for oxigen reduction reaction in alkaline solutions

N.R. Elezović[a], B.M. Babić[b], V. R. Radmilović[c], Lj. M. Vračar[d], N.V. Krstajić[d]

[a]Institute for Multidisciplinary Research, University of Belgrade, Kneza Viseslava 1, Belgrade, Serbia
[b]Vinca Institute of Nuclear Sciences, Belgrade, Serbia
[c]National Center for Electron Microscopy, LBNL University of California, Berkely, USA
[d]Faculty of Technology and Metallurgy, University of Belgrade, Belgrade, Serbia

Platinum based nanocatalyst at home made Nb–TiO_2 support was synthesized and characterized as the catalyst for oxygen reduction reaction in 0.1 mol dm^{-3} NaOH, at 25 °C. Nb doped TiO_2 catalyst support, containing 5% of Nb, has been synthesized by modified acid-catalyzed sol–gel procedure in non-aqueous medium. BET and X-ray diffraction (XRD) techniques were applied for characterization of synthesized supporting material. XRD analysis revealed only presence of anatase TiO_2 phase in synthesized support powder. Existence of any peaks belonging to Nb compounds has not been observed, indicating Nb incorporated into the lattice. Nb–TiO_2 supported Pt nanocatalyst synthesized, using borohydride reduction method, was characterized by TEM and HRTEM techniques. Platinum nanoparticles distribution, over Nb doped TiO_2 support, was quite homogenous. Mean particle size of about 4 nm was found with no pronounced particle agglomeration. Electrochemical techniques: cyclic voltammetry and linear sweep voltammetry at rotating disc electrode were applied in order to study kinetics and estimate catalytic activity of this new catalyst for the oxygen reduction reaction in alkaline solution. Two different Tafel slopes were found: one close to −90 mV dec^{-1} in low current density region and other approximately −200 mV dec^{-1} in high current density region, which is in good accordance with literature results for oxygen reduction at Pt single crystals, as well as Pt nanocatalysts in alkaline solutions. Similar specific catalytic activity (expressed in term of kinetic current density per real surface area) of Nb(5%)–TiO_2/Pt catalyst for oxygen reduction reaction incomparison with the carbon supported platinum (Vulcan/Pt) nanocatalyst, was found.

Keywords: Nb–TiO_2 supportNb–TiO_2/Pt catalyst, Pt nanoparticles, Oxygen reduction reaction, Alkaline solutions.

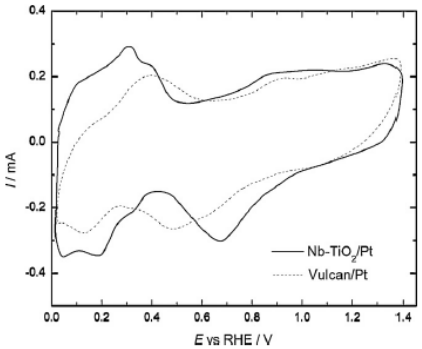

Figure: Cyclic voltammograms (scan rate 100 mV s^{-1}) obtained at Nb–TiO_2/Pt and Vulcan/Pt catalysts, after repetitive cycling – 50 cycles.

***Electrochimica Acta*, 56 (2011) 9020-9026.**

Characterization of sintered magnesite microstructural and XRD analysis

Maria Čebela, Ana Radosavljević Mihajlović, Vesna Maksimović, Branko Matović

Department of material science, INN Vinča, Serbia

Sintered magnesite, the basic raw material for production of refractory materials based on magnesium oxide, is heated at a temperature of 1500-1600 ºC. The samples were investigated through their phase conversions at this temperature range. All the changes were monitored by optical microscope and XRD analyses. Microstructure examination was carried out in the cross section. In order to quantify the grain size and to determine the value of intercept L_3 which is equivalent to the average grain size, line method was used. The results indicate the presence of MgO phase. Bond phase along the grain boundary were observed. Microstructure of sample is shown in the Fig. Polygonal grains are clearly visible.

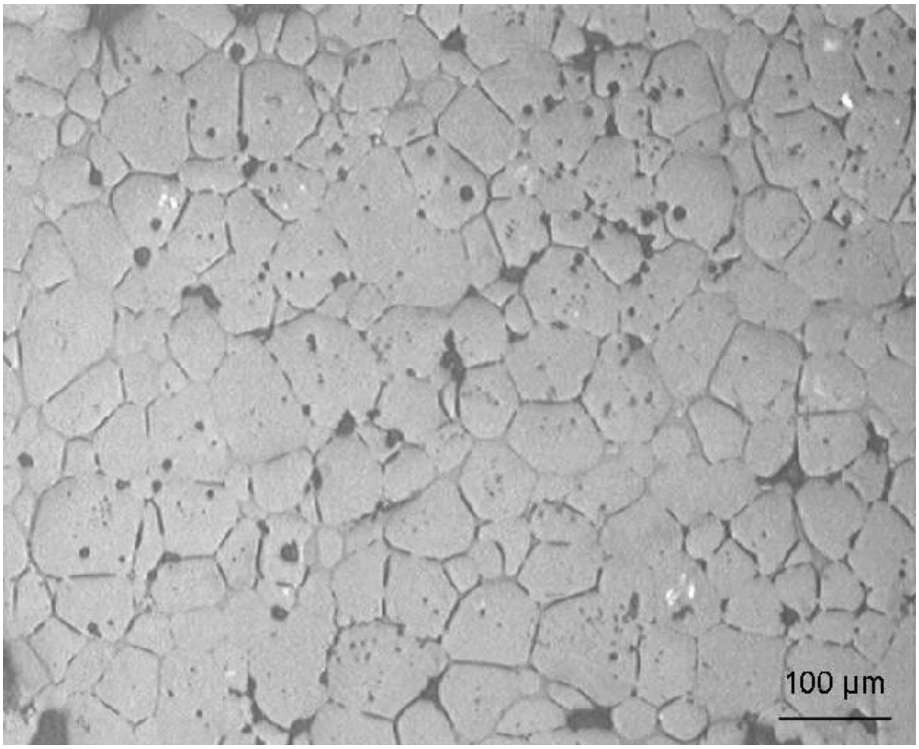

Figure: Microstructure of sample.

***1st Conference of the Serbian Ceramic Society*, March 17-18.2011. The Book of Abstracts, pp. 28.**

Fabrication of ZrC/SiC, ZrO_2/SiC and ZrO_2 powders by carbothermal reduction of $ZrSiO_4$

Ljiljana Kljajević[1], Branko Matović[1], Snežana Nenadović[1], Zvezdana Baščarević[2], Nikola Cvetićanin[3], Aleksandar Devečerski[1]

[1]Department of Material Science, INN Vinča, University of Belgrade, Belgrade, Serbia
[2]Institute for Multidisciplinary Research, Materials Science Dept., Kneza Višeslava 1, University of Belgrade, Belgrade, Serbia
[3]Faculty of Physical Chemistry of Belgrade, University of Belgrade, Belgrade, Serbia

The zirconia/silicon carbide (ZrO_2 /SiC) and ZrO_2 powders are prepared by carbothermal reduction of natural mineral zircon ($ZrSiO_4$). The zircon powder was mixed with activated carbon as a reducing agent and heattreated in a controlled flow atmosphere of Ar. Phase evolution and phase content were followed as a function of temperature (1573–1973 K) and C/ZrSiO4 ratio (C/ZrSiO4 = 1, 4, 5 and 7), by means of ex-situ X-ray diffraction and SEM/EDS analysis. By varying the temperature and C/ZrSiO4 ratio, different powder compositions were obtained (m-ZrO_2; m-ZrO_2/c-ZrO_2; c-ZrO_2; c-ZrO_2/SiC).

Keywords: zirconia, silicon carbide, zirconium carbide, zircon

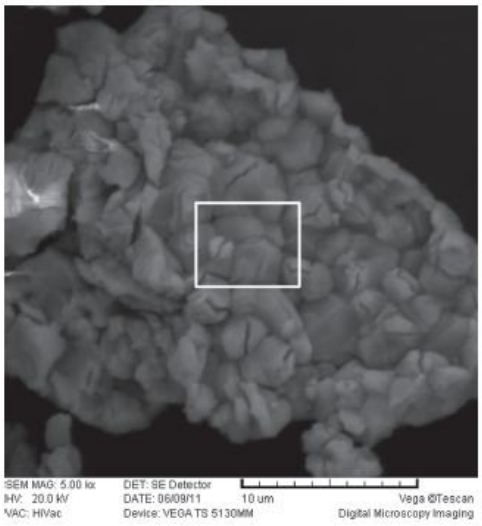

a)

Element	Wt.%	At.%
O	27.69	68.11
Al	0.31	0.43
Si	0.39	0.55
Zr	69.70	30.08
Hf	1.14	0.24
Ti	0.42	0.35
Fe	0.35	0.24

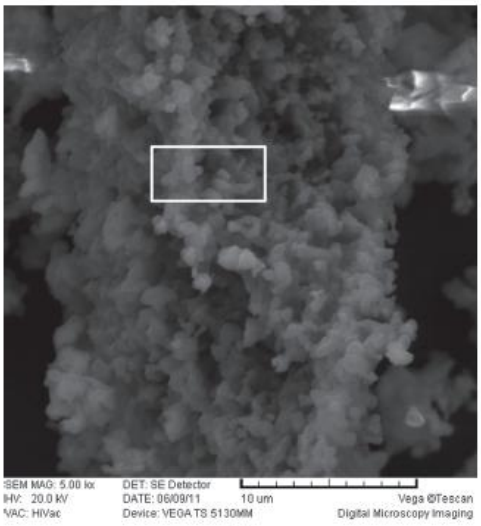

b)

Element	Wt.%	At.%
O	3.07	5.63
Al	1.97	2.14
Si	84.35	87.90
Zr	6.36	2.05
Ti	0.38	0.23
Fe	3.87	2.05

Figure: SEM/EDS analysis of sample with C/$ZrSiO_4$ ratio = 7:1.

***Processing and Application of Ceramics*, 5 [2] (2011) 103–112.**

Fabrication ZrO_2 and ZrO_2/SiC by carbothermal-reduction reactions of $ZrSiO_4$

Ljiljana Kljajević[1], Branko Matović[1], Snežana Nenadović[1], Nikola Cvetićanin[2], Aleksandar Devečerski[1]

[1]Department of material science, INN Vinča, University of Belgrade, Belgrade, Serbia
[2]Faculty of physical chemistry of Belgrade, University of Belgrade, Belgrade, Serbia

The synthesis of zirconia/silicon carbide (ZrO_2/SiC) and ZrO_2 powders are obtained by carbothermal reduction of natural mineral zircon ($ZrSiO_4$). The influence of carbon to $ZrSiO_4$ ratio is investigated for a three range of compositions ($C/ZrSiO_4$ = 3, 5 and 7) and temperatures (1473–1973 K). The zircon powder was mixed with activated carbon as a reducing agent and heat treated in a controlled flow atmosphere of Ar. Phase evaluation and phase content were followed as a function of temperature and $C/ZrSiO_4$ ratio. The obtained powders were characterized by means of ex-situ X-ray diffraction and SEM/EDS investigation.

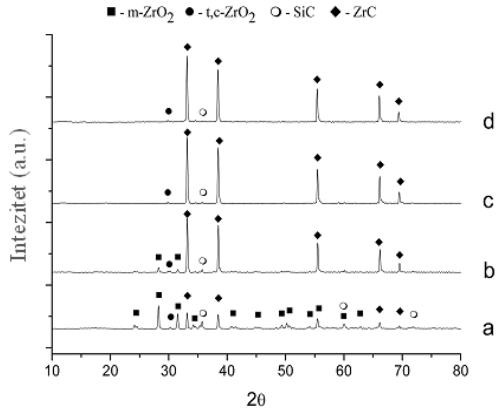

a)

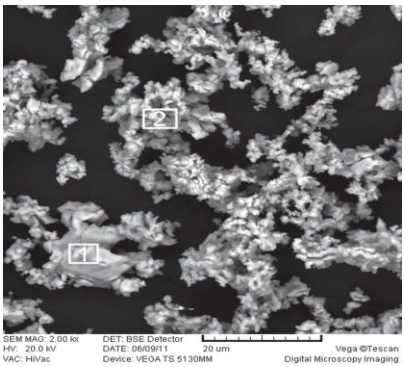

b)

Element	Maseni %	Atomski %
O	32,43	72,97
Al	0,30	0,39
Zr	65,41	25,77
Hf	0,86	0,18
Ti	0,38	0,29
Fe	0,62	0,40

c)

Figure: XRD a) and SEM/EDS b), c) analysis of sample with $C/ZrSiO_4$ ratio = 5:1.

1st Conference of the Serbian Ceramic Society **March 17th-18th 2011, Belgrade, Serbia, Proceedings & Book of abstracts, pp. 41.**

Preparation of ZrO_2 and ZrO_2/SiC powders by carbothermal reduction of $ZrSiO_4$

Lj. Kljajević, B. Matović, A. Radosavljević-Mihajlović, M. Rosić, S. Bosković, A. Devečerski

Materials Science Lab, Vinča Institute of Nuclear Sciences, University of Belgrade, P.O. Box 522, 11001, Belgrade, Serbia

This paper is dealing with the synthesis of zirconia/silicon carbide (ZrO_2/SiC) and ZrO_2 powders obtained by carbothermal reduction of natural mineral zircon ($ZrSiO_4$). For the first time, the influence of carbon to $ZrSiO_4$ ratio is thoroughly investigated for a wide range of compositions ($C/ZrSiO_4$ = 1–8) and temperatures (1473–1973 K). The zircon powder was mixed with activated carbon as a reducing agent and heat treated in a controlled flow atmosphere of Ar. Periclase (MgO) was added in order to facilitate the formation of high temperature form of zirconia as well as to examine the possible catalytic effect of MgO on the overall reaction. Phase evaluation and phase content were followed as a function of temperature, $C/ZrSiO_4$ ratio and different quantity of introduced MgO. The obtained powders were characterized by means of ex-situ X-ray diffraction and SEM/EDS investigation. It was found that, depending on $C/ZrSiO_4$ ratio, it is possible to produce either a m-ZrO_2, c-ZrO_2 or ZrO_2/SiC powders by using zircon as precursor.

Keywords: Ceramics, Gas–solid reactions, Solid state reactions, Microstructure, X-ray diffraction, Scanning electron microscopy

Table. Phase composition and color of the samples.

	1673 K	Decarb.	1773 K	Decarb.	1873 K	Decarb.	1973 K	Decarb.
1:1	$ZrSiO_4$ (100) m-ZrO_2 (29) Dark-grey	$ZrSiO_4$ (100) m-ZrO_2 (24) Light-grey	$ZrSiO_4$ (100) m-ZrO_2 (44) Dark-grey	$ZrSiO_4$ (100) m-ZrO_2 (45) Light-grey	m-ZrO_2 (100) Dark-grey	m-ZrO_2 (100) Light-grey	m-ZrO_2 (100) Dark-grey	m-ZrO_2 (100) Cream
2:1	m-ZrO_2 (100) $ZrSiO_4$ (85) Dark-grey	$ZrSiO_4$ (100) m-ZrO_2 (83) Light-grey	m-ZrO_2 (100) $ZrSiO_4$ (14) Dark-grey	m-ZrO_2 (100) $ZrSiO_4$ (17) Light-grey	m-ZrO_2 (100) ZrC (36) Black	m-ZrO_2 (100) c-ZrO_2 (9) Light-grey	m-ZrO_2 (100) ZrC (54) Black	m-ZrO_2 (100) c-ZrO_2 (11) Cream
3:1	m-ZrO_2 (100) $ZrSiO_4$ (35) SiC (u) Dark-grey	$ZrSiO_4$ (100) m-ZrO_2 (18) SiC (u) Light-grey	m-ZrO_2 (100) ZrC (12) SiC (12) c-ZrO_2 (t) Dark-grey	m-ZrO_2 (100) SiC (12) c-ZrO_2 (4) Light-grey	ZrC (100) m-ZrO_2 (51) c-ZrO_2 (7) Black	m-ZrO_2 (100) c-ZrO_2 (31) Light-grey	ZrC (100) m-ZrO_2 (18) c-ZrO_2 (t) Black	m-ZrO_2 (100) c-ZrO_2 (56) Cream
4:1	m-ZrO_2 (100) SiC (21) c-ZrO_2 (5) ZrC (4) Dark-grey	m-ZrO_2 (100) SiC (20) Light-grey	m-ZrO_2 (100) ZrC (54) SiC (23) c-ZrO_2 (4) Dark-grey	m-ZrO_2 (100) SiC (20) c-ZrO_2 (10) Light-grey	ZrC (100) m-ZrO_2 (14) c-ZrO_2 (5) Black	c-ZrO_2 (100) m-ZrO_2 (87) Light-grey	ZrC (100) m-ZrO_2 (4) c-ZrO_2 (t) Black	c-ZrO_2 (100) m-ZrO_2 (43) Cream
5:1	m-ZrO_2 (100) ZrC (71) SiC (32) c-ZrO_2 (7) Black	m-ZrO_2 (100) SiC (26) c-ZrO_2 (14) Light-grey	ZrC (100) m-ZrO_2 (9) SiC (6) c-ZrO_2 (t) Black	m-ZrO_2 (100) c-ZrO_2 (80) SiC (43) Light-grey	ZrC (100) SiC (t) c-ZrO_2 (t) Black	c-ZrO_2 (100) SiC (18) Light-grey	ZrC (100) SiC (t) c-ZrO_2 (t) Black	c-ZrO_2 (100) SiC (u) Light-grey
6:1	ZrC (100) m-ZrO_2 (53) SiC (29) c-ZrO_2 (12) Black	m-ZrO_2 (100) SiC (38) c-ZrO_2 (33) Light-grey	ZrC (100) SiC (9) c-ZrO_2 (t) Black	c-ZrO_2 (100) SiC (56) m-ZrO_2 (32) Light-grey	ZrC (100) SiC (6) c-ZrO_2 (t) Black	c-ZrO_2 (100) SiC (41) Light-grey	ZrC (100) SiC (8) c-ZrO_2 (t) Black	c-ZrO_2 (100) SiC (43) Light-grey
7:1	ZrC (100) m-ZrO_2 (21) SiC (29) c-ZrO_2 (5) Black	m-ZrO_2 (100) SiC (96) c-ZrO_2 (90) Light-grey	ZrC (100) SiC (15) c-ZrO_2 (6) Black	SiC (100) c-ZrO_2 (81) Light-grey	ZrC (100) SiC (18) c-ZrO_2 (t) Black	c-ZrO_2 (100) SiC (84) Light-grey	ZrC (100) SiC (22) c-ZrO_2 (t) Black	c-ZrO_2 (100) SiC (87) Light-grey
8:1	ZrC (100) m-ZrO_2 (44) SiC (27) c-ZrO_2 (9) Black	m-ZrO_2 (100) SiC (46) c-ZrO_2 (41) Light-grey	ZrC (100) SiC (13) c-ZrO_2 (t) Black	c-ZrO_2 (100) SiC (69) Light-grey	ZrC (100) SiC (13) c-ZrO_2 (t) Black	c-ZrO_2 (100) SiC (68) Light-grey	ZrC (100) SiC (8) c-ZrO_2 (t) Black	c-ZrO_2 (100) SiC (38) Light-grey

Decarb. – after decarburization process (873 K, 2 h, air); t – traces; u – impossible to determine due to the overlapping;

***Journal of Alloys and Compounds*, 509 (2011) 2203–2215.**

A novel platinum-based nanocatalyst at a niobia-doped titania support for the hydrogen oxudation reaction

Nevenka R. Elezović[1], Biljana M. Babić[2], Velimir Radmilović[3], Ljiljana M. Gajić-Krstajić[4], Nedeljko V. Krstajić[5], Ljliljana Vračar[5]

[1]Institute for Multidisciplinary Research, University of Belgrade, Kneza Višeslava 1, 11030 Belgrade,
[2]Vinča Institute of Nuclear Sciences, P. O. Box 522, 11001 Belgrade, Serbia,
[3]National Center for Electron Microscopy, LBNL University of California, Cyclotron Road CA 94720 - Berkeley, USA
[4]Institute of Technical Sciences-SASA, Knez Mihailova 35, Belgrade
[5]Faculty of Technology and Metallurgy, University of Belgrade, Karnegijeva 4, 11000 Belgrade, Serbia

The kinetics of the hydrogen oxidation reaction (HOR) was studied at Pt nanoparticles supported on niobia-doped titania (Pt/N–T). The catalyst support, with the composition of $0.05NbO_{2.5-\delta}$–$0.995TiO_2$ ($0 < \delta < 1$), was synthesized by a modified sol–gel procedure and characterized by the BET and X-ray diffraction (XRD) techniques. The specific surface area of the support was found to be 70 m^2 g^{-1}. The XRD analysis revealed the presence of the anatase TiO_2 phase in the support powder. No peaks indicating the existence of Nb-compounds were detected. Pt/N–T nanocatalyst was synthesized by the borohydride reduction method. Transmission electron microscopy revealed a quite homogenous distribution of the Pt nanoparticles over the support, with a mean particle size of about 3 nm. The electrochemical active surface area of Pt of 42±4 m^2 g^{-1} was determined by the cyclic voltammetry technique. The kinetics of the HOR was investigated by linear sweep voltammetry at a rotating discelectrode in 0.5 mol dm^{-3} $HClO_4$ solution. The determined value of the Tafel slope of 35 mV dec^{-1} and an exchange current density of 0.45 mA cm^{-2} per real surface area of the Pt are in good accordance with those already reported in the literature for the HOR at polycrystalline Pt and Pt nanocatalysts in acid solutions. This new catalyst exhibited better activity for the HOR in comparison with Pt nanocatalyst supported on Vulcan® XC-72R high area carbon.

Keywords: Niobia-doped titania support, Pt nanocatalyst, Hydrogen oxidation reaction, Fuel cell

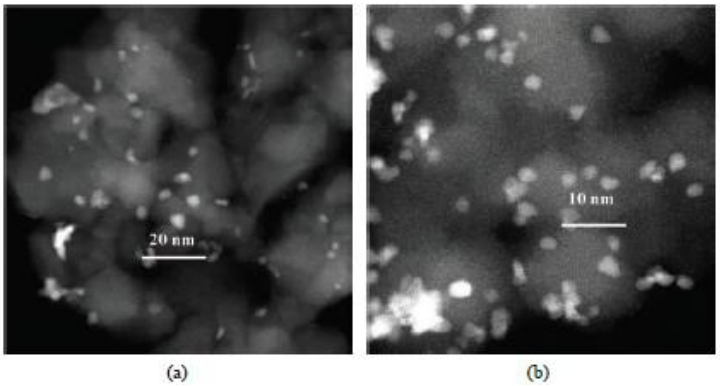

Figure: TEM micrographs of the Pt/N–T nanocatalyst: a) low magnification image showing a homogeneous distribution of Pt particles on the catalyst support; b) high resolution dark field image of the catalyst, showing no pronounced agglomeration of the particles.

***Journal of the Serbian Chemical Society*, 76 (2011) 1139-1152.**

Ceramic composites

Effect of post-sintering heat treatment on mechanical properties and microstructure of SiC-TiB_2 composites

Dusan Bucevac[1,2], Branko Matovic[2], Biljana Babic[2], Vladimir Krstic[1]

[1]Department of Mechanical and Materials Engineering, Queen's University, Kingston, Ontario K7L 3N6 Canada
[2]Institute of Nuclear Sciences Vinca, University of Belgrade, P.O. Box 522, Belgrade 11001, Serbia

Dense SiC-TiB_2 composites with 24 vol% TiB_2 were fabricated by pressureless sintering at 1940 ^oC in the presence of liquid forming additives of Al_2O_3 and Y_2O_3. TiB_2 was formed by an *in-situ* reaction between TiO_2, B_4C and C. The effect of temperature of post-sintering heat treatment on microstructure and mechanical properties of SiC-TiB_2 composite was presented. Heat treatment at 1970 ^oC considerably improved the strength and fracture toughness of the sintered samples while maintaining high density. The elongation of α-SiC grains during the heat treatment was found to be responsible for an increase in fracture toughness. The presence of liquid phase assisted the elongation of grains which in turn activated crack bridging and crack deflection toughening mechanisms. Maximum strength of 540 MPa was found to be the result of improved fracture toughness. Heat treatment above 1970 ^oC led to a deterioration of mechanical properties.

Keywords: SiC ceramics, sintering, heat treatment, mechanical properties, microstructure

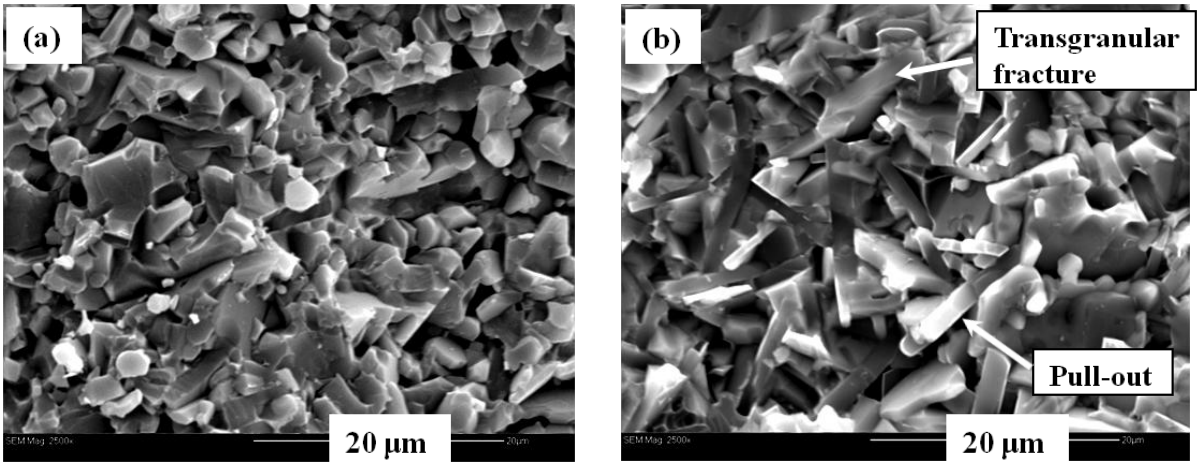

Figure: SEM micrographs of fracture surfaces of samples with 24 vol% TiB_2 (a) sintered sample and (b) sample post-sintering heat-treated at 1970 ◦C.

***Materials Science and Engineering A*, 528 (2011) 2034–2041.**

Pressureless Sintering of Internally Synthesized SiC-TiB_2 Composites with Improved Fracture Strength

Dusan Bucevac[1,2], Branko Matovic[2], Snezana Boskovic[2], Slavica Zec[2], Vladimir Krstic[1]

[1]Department of Mechanical and Materials Engineering, Queen's University, Kingston, Ontario K7L 3N6 Canada
[2]Institute of Nuclear Sciences Vinca, University of Belgrade, P.O. Box 522, Belgrade 11001, Serbia

SiC-TiB_2 particulate composites were fabricated by converting TiO_2 to TiB_2 through the reaction between TiO_2, B_4C and C. The presence of initially very fine, *in-situ* created, TiB_2 particles increased driving force for sintering and enabled fabrication of a dense composite utilizing pressureless sintering and the liquid phase created between Al_2O_3 and Y_2O_3 additives. The effect of volume fraction of the *in-situ* formed TiB_2 on density, microstructure and flexural strength was discussed. It was found that the presence of TiB_2 particles suppressed the growth of SiC grains and enhanced fracture strength. The fracture strength of samples containing 12 vol% TiB_2 was more than 30% higher than that of the monolithic SiC. The effect of SiC grain size on fracture strength was also analyzed.

Keywords*:* silicon carbide, ceramics, sintering, mechanical properties, optical microscopy

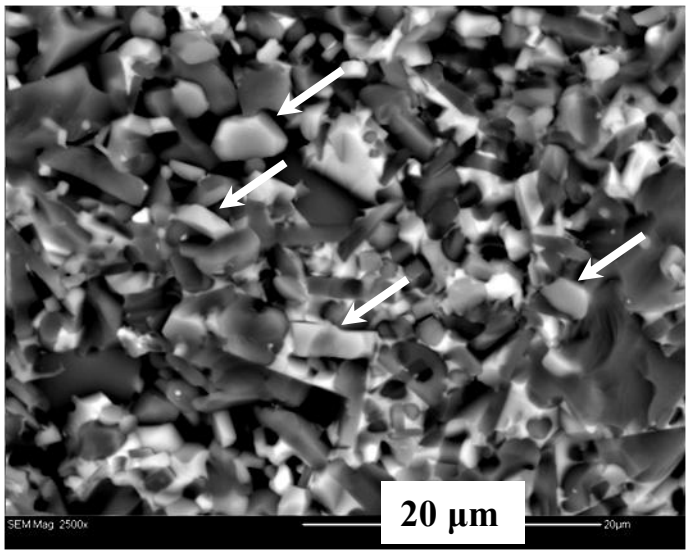

Figure: SEM micrograph of fracture surface of sample with 24 vol% TiB_2 (back scattering electrons) showing crack deflection (the arrows indicate TiB_2 particles).

***Journal of Alloys and Compounds,* 509 (2011) 990–996.**

Influence of TiB_2 content on mechanical properties of SiC-TiB_2 composites

Dusan Bucevac[1], Marija Prekajski[1], Branko Matovic[1], Vladimir Krstic[2]

[1]Institute of Nuclear Sciences Vinca, University of Belgrade, P.O. Box 522, Belgrade 11001, Serbia
[2]Department of Mechanical and Materials Engineering, Queen's University, Kingston, Ontario K7L 3N6 Canada

Microstructure and mechanical properties (fracture toughness, flexural strength and hardness) of SiC-TiB_2 composite were studied. Pressureless sintering experiments were carried out on samples containing 0 to 50 vol% of TiB_2 created by *in-situ* reaction between TiO_2, B_4C and carbon. Al_2O_3 and Y_2O_3 were used as sintering additives to create liquid phase and promote densification at sintering temperature of 1940 ^oC. The sintered samples were subsequently heat treated at 1970 ^oC. It was found that the presence of TiB_2 suppresses SiC grain growth and prevents crack propagation which increases both strength and fracture toughness of sintered SiC-TiB_2 composite. The subsequent heat treatment of sintered samples promoted the elongation of SiC matrix and further improved mechanical properties of the composite. The best mechanical properties were measured in heat-treated samples containing 12-24 vol% TiB_2. The maximum flexural strength of ~600 MPa was obtained in samples with 12 vol% TiB_2 whereas the maximum fracture toughness of 6.6 $MPa \cdot m^{1/2}$ was obtained in samples with 24 vol% TiB_2. Typical microstructures of samples with the mentioned volume fractions of TiB_2 consist of TiB_2 particles (<5 μm) uniformly dispersed in a matrix of elongated SiC plates. The relations between microstructure and mechanical properties were discussed.

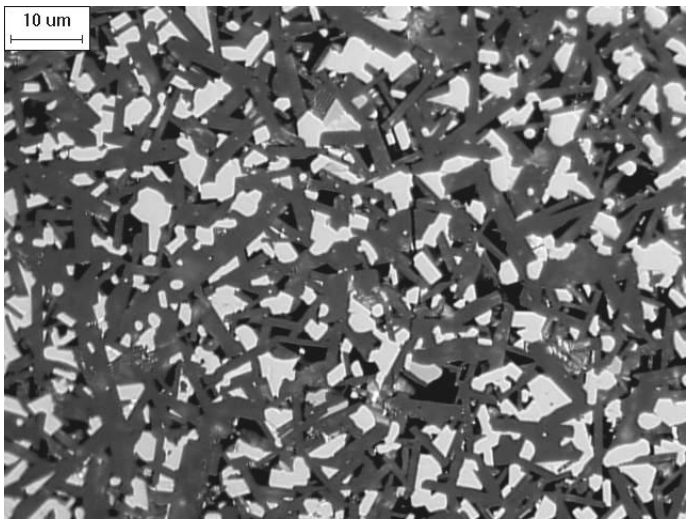

Figure: Optical micrograph of SiC containing 24 vol% TiB_2, sintered at 1940 ^oC and heat-treated at 1970 ^oC.

***Engineering Ceramics 2011: From Materials to Components*, May, 8th-12th 2011, Smolenice castle, Slovakia, Book of abstracts, pp. 62.**

Effect of heat treatment on mechanical properties of SiC-TiB_2 composites

Dusan Bucevac, Biljana Babic, Snezana Boskovic

Institute of Nuclear Sciences Vinca, University of Belgrade, P.O. Box 522, Belgrade 11001, Serbia

Dense SiC-TiB_2 composites with 24 vol% TiB_2 were fabricated by pressureless sintering at 1940 ^oC in the presence of liquid forming additives of Al_2O_3 and Y_2O_3. The effect of post-sintering heat treatment on microstructure and mechanical properties of SiC-TiB_2 composite was presented. Heat treatment at 1970 ^oC considerably improved the strength and fracture toughness of the sintered samples while maintaining high density. The elongation of α-SiC grains during the heat treatment was found to be responsible for an increase in fracture toughness. The presence of liquid phase assisted the elongation of grains which in turn activated crack bridging and crack deflection toughening mechanisms. Maximum strength of 540 MPa was found to be result of improved fracture toughness.

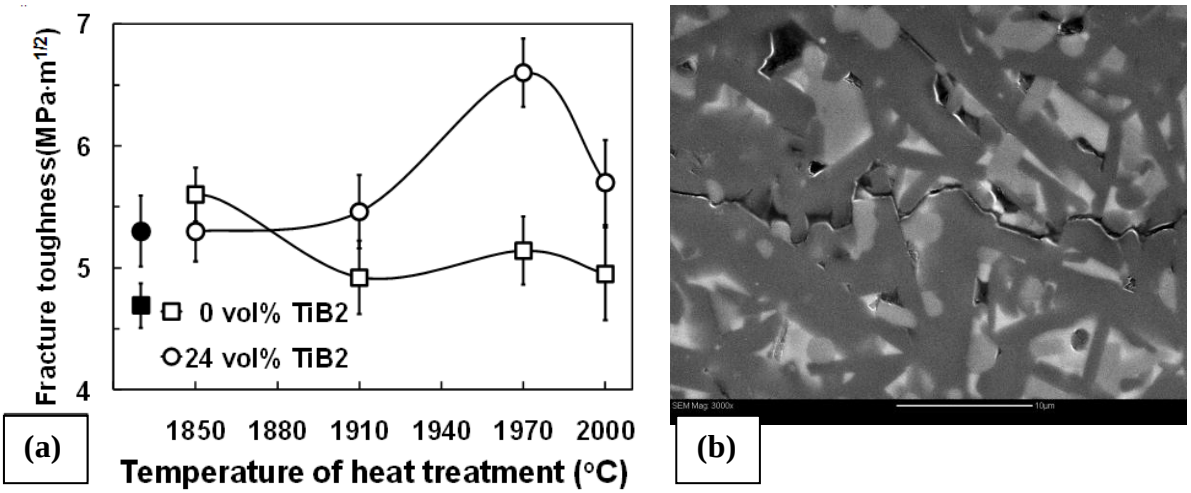

Figure: (a) Effect of temperature of post-sintering heat treatment on fracture toughness of the samples sintered at 1940 ^oC with 0 vol% and 24 vol% TiB_2. The black markers (■,●) denote sintered samples, (b) resistance of elongated SiC grains to crack propagation.

***1st Conference of the Serbian Ceramic Society*, March 17th-18th 2011, Belgrade, Serbia, Program and The Book of Abstracts, pp. 27.**

Synthesis and characterization of ceramic composite materials based on silicon-carbide and cordierite materials

M. Posarac*, M. Dimitrijevic**, J. Majstorovic***, T. Volkov-Husovic**, A. Devecerski*, B. Matovic*

*Institute of Nuclear Sciences Vinca, University of Belgrade, PO Box 522, 11001 Belgrade, Serbia
**Faculty of Technology and Metallurgy, University of Belgrade, Karnegijeva 4, POB 3503, Belgrade, Serbia
***Faculty of Mining and Geology, University of Belgrade, Belgrade, Serbia

SiC ceramics is widely used because of its high hardness value, high thermal stability, good thermal conductivity and good thermal shock resistance. Cordierite are promising material because of his excellent properties, e.g., low dielectric constant, high resistivity, elevated chemical and thermal stability, and low thermal expansion coefficient. Composite materials based on SiC and cordierite materials offers combination of properties that are desirable for high-temperature structural applications. Cordierite was synthesised from spinel, quartz and alumina and used as starting material for SiC/cordierite composite ceramics with weight ratio 70:30. Thermal stability of composite materials was investigated by water quench method. Microstructural investigation of samples after quenching was conducted by SEM and phase analysis was done by XRD.

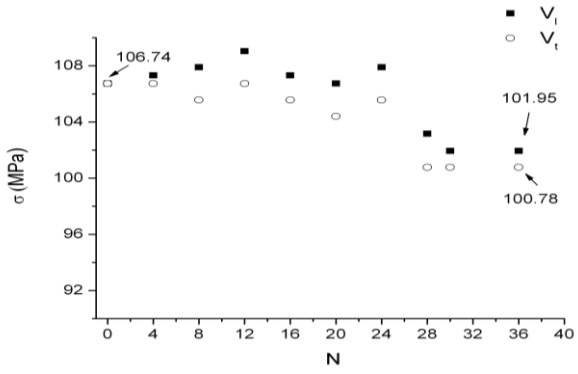

Figure: Strength degradation versus number of quench experiments.

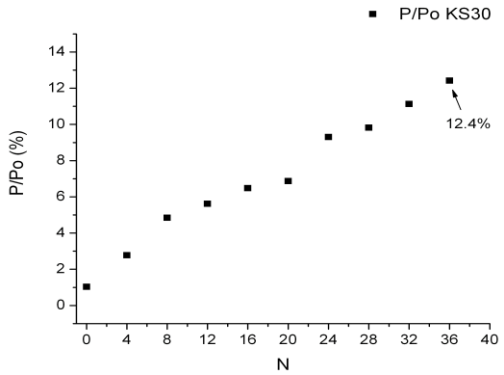

Figure: Damaged surface level (P/P_o) versus number of quench experiments (N).

The First Conference of The Serbian Ceramic Society, **2011., Belgrade, Serbia, Proceedings & Book of abstracts.**

Influence of Microstructure on Mechanical Properties of Porous SiC/Cordierite Composite Materials

M. Dimitrijevic[a], Radmila Jancic Heinemann[a], Tatjana Volkov Husovic[a], Milica Posarac[b], Jelena Majstorovic[c]

[a]Faculty of Technology and Metallurgy, University of Belgrade, Serbia
[b]Institute of Nuclear Sciences Vinca, University of Belgrade, P.O.Box. 522, 11001 Belgrade, Serbia
[c]Faculty of Mining and Geology, University of Belgrade, Serbia

Thermal stability of the alumina based samples were measured using the water immersion test.Mechanical characteristics such as strength, dynamic modulus of elasticity resulting from resonancefrequency measurements were considered. Image analysis was used to measure the fiber lengthsdistribution, homogeneity of fiber distribution in the matrix and finally the measurement andcharacterization of surface degradation of specimens during thermal stability testing. The morphology of resulting surface destruction was analyzed using mathematical morphology tools.

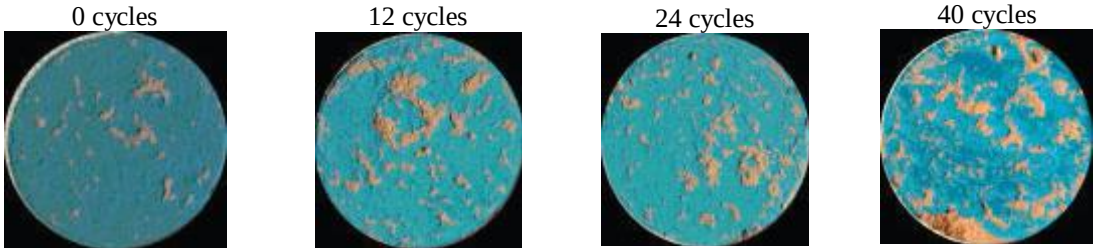

Figure: Samples without fibres before and during testing.

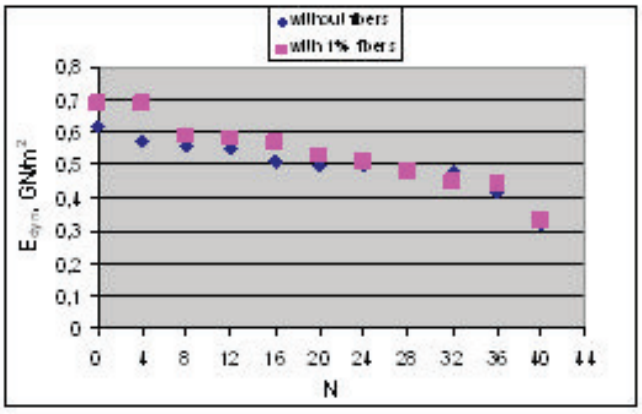

Figure: Values of Dynamic Young's modulus of elasticity vs. number of quenching experiments.

***11th International Conference on the Mechanical Behavior of Materials (ICM11),* Procedia Engineering, 10 (2011) 2153–2157.**

Doctoral dissertations

Šaponjić B. Aleksandra

SYNTHESIS AND CHARACTERISTICS OF Si-NON OXOXIDE COMPOUNDS OBTAINED BY THE CAROTHERMAL REDUCTION OF DIATOMACEOUS EARTH

The possibility of using natural inorganic precursors for the synthesis of silicon carbides and nitrides, and their composites, is investigated. The starting material was diatomaceous earth as a source of S_iO_2 and three different carbon sources: sacharosis, carbon cryogel, and active coal. For this purpose, on one side, a study is performed of the influence of different molar ratios C/S_iO_2 on the process of carbothermal reductions and nitrifications during the synthesis of non-oxidizing nano-particle powders based on silicon nitride. On the other side, the influence of each individual carbon source on the process of carbothermal reductions and nitrifications and properties of the obtained powders in the course of synthesis of composite powders based on silicon nitride and silicon carbide is also performed.

Parameters of the chemical reaction gas-solid (temperature, time, structure, and contents of the reduction substance) have been defined. In the course of synthesis of inorganic powders of silicon carbides and nitrides, different synthesis methods requiring the expensive initial components, high temperatures, and high pressures are applied. In this work, however, the considerably more economical method of carbothermal reduction is applied. The carbothermal reduction is a not fully investigated process. The process itself allows obtaining the mentioned non-oxide compounds from very cheap natural raw materials at a relatively low temperature. The significance of these investigations is obtaining new information concerning the process itself together with systems Si-N, Si-C, and Si-C-N.

According to the available published data, this is the first use in this country of the method of carbothermal reduction and nitrification, applied in this work for obtaining nano-particle powders based on Si_4N_4 and SiC. Also, this is the first production in this country of carbon cryogel which used as a source of carbon in the synthesis of the composite nano-particle powders. During the synthesis of these powders, special attention is paid to the preparation of the starting mixtures in order to achieve a homogenous distribution of initial components in the produced samples.

The results show that diatomay earth, owing to its genesis and a submicron size of particles, can be very successfully used as a natural source of SiO_2 for the purpose of synthesizing ceramic powders.

Active coal turned out to be the most efficient reduction reagent in so far as the speed of the carbothermal reduction and nitrification is concerned. However, the results of roentgen diffraction (XRD) and infrared spectroscopy showed that sacharosis was the best source for the synthesis of non-oxide composite powders based on silicon nitride and silicon carbide since the application of this reduction reagent at 1450^oC results in the best yield of powders. Carbon cryogel showed inefficient in so far as the speed of the carbothermal reduction process and powder yield were concerned compared to sacharosis and active coal. However, application of this source of carbon results in the nano-particle powders having specific, needle-like, shapes of particles which may successfully be used as a reinforcing phase in the synthesis of a special purpose self-reinforced ceramics for different industrial applications.

Key words: carbothermal reduction, diatomay earth, nitrification, $S_{i4}N_4$, S_iC, $S_{i4}N_4/S_iC$, nano-particle powders

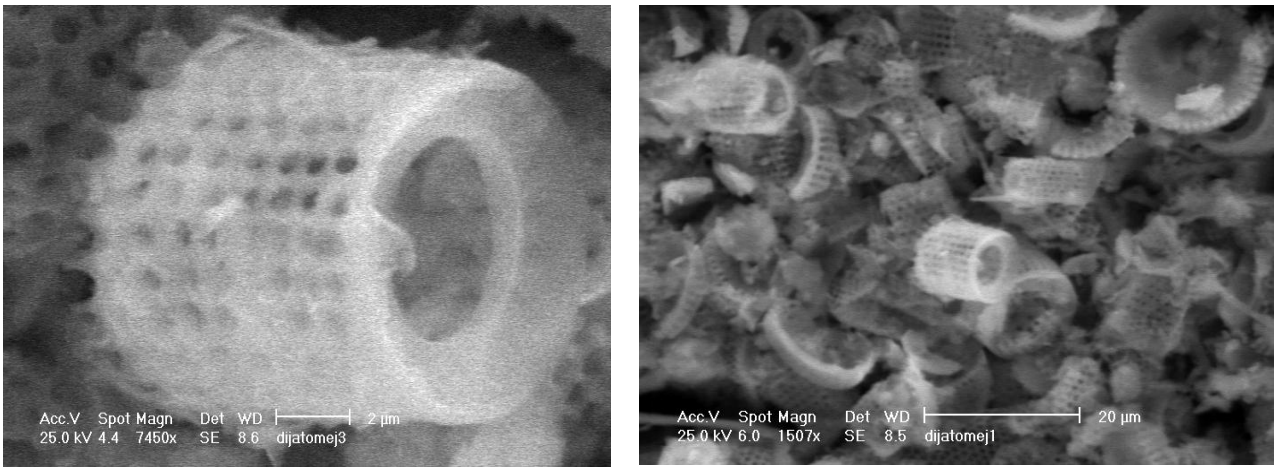

a) **b)**

Figure: SEM micrographs diatoms (frustules) and powder (Matović et al 2006; Matović et al. 2007).

Maja Kokunešoski

SYNTHESIS AND CHARACTERIZATION OF MESOPOROUS SILICATE CARBON MATERIALS AND THEIR APPLICATION IN ADSORPTION ORGANIC POLLUTANTS

Mesoporous templates, SBA-15/80 and SBA-15/100, are synthesized in acid environment, by applying the surfactant Pluronic P123 and tetraethoxysilane as the source of silica. From nitrogen adsorption and desorption isotherms it was determined that they have large specific surface areas (640 and 710 m^2/g) with especially developed mesoporosity with present microporosity whose ratio as well as structural characteristics of these materials depend on the temperature and time of execution of certain phases of their synthesis. X-ray difractional analysis (XRD) confirmed their amorphous structure; scanning electron microscopy (SEM) demonstrated that they have more areas made of elongated relatively even grains, size of 1 μm as well as elongated grain agglomerates, and atomic force microscopy that particle SBA-15/80 is agglomerate, and SBA-15/100 is a compact particle, of spherical form. By thermo-gravimetric analysis it was demonstrated that the loss of mass of these materials at 212 ^oC and 450 ^oC is equivalent to desorption and disintegration of $P_{123.}$ Presence of P_{123} in these materials after their calcination was also confirmed by Fourier-transformed infrared spectroscopy. At SBA-15/80 the point of zero charge is $pH_{PZC} = 5,2 \pm 0,2$, and isoelectric point $pH_{IEP} = 2,3 \pm 0,1$. Rinsing of the samples in diluted HNO_3 moved pH_{IEP} to higher values of $pH_{IEP} = 3,0 \pm 0,2$ while pH_{PZC} remained unchanged which points to slight presence of impurities in the template. By applying the template, composites on the kryogel base have been synthesised (Si80/CCx, Si100/CCx) and saccharose (Si80/saccharose, Si100/ saccharose) and carbon replica CC80/x, CC100/x, C80/ saccharose and C100/saccharose. Share of silica from 0,2 to 1 was marked with x. Replicas ($S_p \leq 771$ m^2/g) have greater specific surface areas from the composites ($S_p \leq 519$ m^2/g). XRD analyses of composites and replicas has pointed to their weakly defined structure and SEM to similarity between SBA-15, composites and replicas which is also a confirmation that there is a successful transfer of the template structure to the composite and then to the carbon replica.
Possibilities of application of composites and replicas are defined on the basis of nitrogen and phenol adsorption isotherms done at 25 ^oC. With the increase in content of kryogel the quantity of adsorbed nitrogen grew both in composites and replicas. Although the porosity of replica C100/saccharose is smaller than that of CC80/0.75 i CC100/1 it is interesting to note that replica C100/saccharose adsorbs smaler quantities of nitrogen than CC80/0,75 i CC100/1. Based on analysis of the data we may conclude that possibly the best adsorbent of nitrogen of all the tested synthesised materials, is a carbon replica CC80/0,75. According to the amount of adsorbed phenol from aqueous solutions, we can deduct that carbon replica C80/saccharose is a good adsorber of phenol. This replica is a better adsorbent of phenol than the two other investigated carbon replicas, CC80/0.75 and CC100/1. Compared to them it adsorbs slightly higher amounts of this organic pollutants.

Keywords: Porosity, Mesoporous silica, Microporosity, Specific surface, Amorphous materials, Nanomaterial, Nanostructures, Nanocomposites, Carbon replica, Surface properties

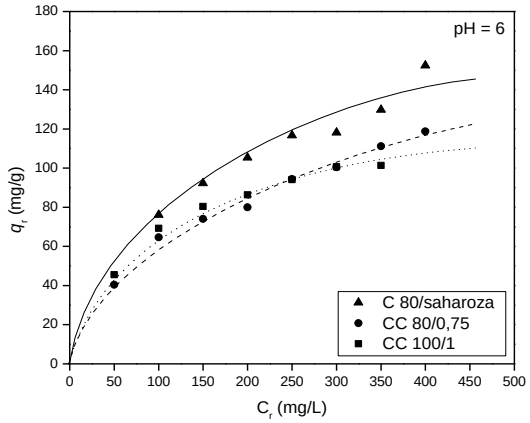

Figure: Phenol adsorption isotherms for C80/saharoza, CC 80/0.75 and CC 100/1.

Material science laboratory – Domestic collaborations

IHIS Research and Development Center, Belgrade, Serbia

-Bobić, B

School of Dental Medicine, University of Belgrade, Belgrade, Serbia

-Čairović, A

Department of General and Inorganic Chemistry, Faculty of Technology and Metallurgy, University of Belgrade, Belgrade, Serbia

-Rogan, R.J

Faculty of Agriculture, Institute of Soil and Melioration, Belgrade University, Belgrade, Serbia

- Tomić, P.Z

ICTM - Institute of Electrochemistry, University of Belgrade, Belgrade

-Nikolić, N.D
-Jovanović, V.M
-Pavlović, Lj.J
-Pavlović, M.G
-Stevanović S.I.
-Panić, V

Faculty of Technology and Metallurgy, University of Belgrade, Belgrade

-Aćimović-Pavlović, Z
-Bajat, J
-Cvijović, Z
-Dimitrijević, M
-Jančić-Heinemann, R
-Kijevčanin, M
-Krstajić, N.V
-Popov, K.I
-Raić, K
-Rakin, M.B
-Volkov-Husović, T
-Vračar, Lj.M

Faculty of Metallurgy and Technology, University of Montenegro, Podgorica, Montenegro

-Vratnica, M.

Faculty of Mining and Geology, University of Belgrade, Belgrade

-Kremenović, A
-Majstorovic, J
-Logar, M
-Poharc-Logar, V
-Rosić, A

Institute for Multidisciplinary Research, University of Belgrade, Belgrade

-Baščarević, Z
-Branković, G
-Elezović, N.R
-Jović, B.M
-Jović, V.D
-Lačnjevac, U.Č.

University of Belgrade, Faculty of Mechanical Engineering, Belgrade

-Veljić, M
-Marković, D
-Simonović, V

Tribology Laboratory, Faculty of Mechanical Engineering, University of Belgrade, Belgrade

-Vencl, A

Faculty of Agriculture, University of Belgrade, Belgrade

-Pavlović, V

Institute of Technical Sciences of SASA (Serbian Academy of Sciences and Arts), Belgrade

-Gajić-Krstajić, Lj

Faculty of Physical Chemistry, University of Belgrade, Belgrade

-Cvjetićanin, N
-Daković, M
-Mojović, M

Institute of Physics, Belgrade, Belgrade

-Dohčević-Mitrović, Z
-Golubović, A
-Popović, Z.V
-Radović, M
-Šćepanović, M

University of Belgrade, Faculty of Geography, Belgrade

-Lješević, M.A
-Obradović Arsić, D.R

Center of Electron Microscopy, Medical Faculty, University of Niš

-Miljković, M

Tribology Center, Faculty of Engineering, University of Kragujevac, Kragujevac

-Babić, M.
-Mitrović, S
-Živić, F

Faculty of Technical Sciences, University of Novi Sad, Novi Sad

-Gerić, K

Institute of Oncology and Radiology of Serbia, Belgrade, Serbia

-Vidojević, D

Faculty of Technology Zvornik, University of Eastern Sarajevo, Zvornik, Republic of Srpska

-Tomić, M

Plasma Jet Co, Belgrade, Serbia

-Marković, P

Institute of Nuclear Sciences, Vinča, University of Belgrade, Serbia

Laboratory of Physics (010)

-Jovanović, Z

Laboratory for Nuclear and Plasma Physics (011)

-Cekić, B. Dj
-Koteski, V.J
-Ivanović, N
-Novaković, N
-Paškaš Mamula, B
-Vukanac, I
-Ćirić, K.D

Laboratory GAMMA (030)

-Jokanović, V

Laboratory of Theoretical and Condensed Matter Physics (020)

-Kusigerski, V
-Spasojević, V

Laboratory for Atomic Physics (040)

-Bogdanov, Ž.D
-Nenadović, M.T

Laboratory of Physical Chemistry (050)

-Radak, B.B
-Stoiljković, M.M
-Trtica, M.S
-Stojić, D.Lj

Laboratory for Chemical Dynamics and Permanent Education (060)

-Jovanović, U
-Milonjić, S.K
-Tuvić, T

Material science laboratory – International collaborations

Department of Engineering, University of Liverpool, Liverpool L69 3GH, UK

-Perrie, W
-Watkins, K

ENEA, UTTMAT Research Centre of Casaccia, Rome, Italy

-Aurora, A
-Montone, A

Institute of Physical Chemistry, Romanian Academy, Bucharest, Romania

- Fruth, V

University of Ljubljana, Faculty of Chemistry and Chemical Technology, Ljubljana, Slovenia

-Meden, A

Institut für Mineralogie & Petrographie, Universität Innsbruck, Innrain 52, Austria

-Volker Kahlenberg, V

Institute of Chemistry, Faculty of Science, SS. Cyril and Methodius University, Skopje, Macedonia

-Makreski, P

National Center for Electron Microscopy, LBNL University of California, Berkely, USA

-Radmilović, V.R

Department of Mechanical and Materials Engineering, Queen's University, Kingston, Ontario, Canada

-Krstić, V